UNIVERSITY OF CALIFORNIA
IRVINE

Developing a high resolution coupled hydrologic-hydraulic model (HiResFlood-UCI) for flood modeling

DISSERTATION

submitted in partial satisfaction of the requirements
for the degree of

DOCTOR OF PHILOSOPHY

In Civil Engineering

By

Phu Dinh Nguyen

Dissertation Committee:
Distinguished Professor Soroosh Sorooshian, Chair
Professor Kuolin Hsu
Professor Amir AghaKouchak
Professor Brett Sanders

2014

DEDICATION

To

My parents,

Vi, my wonderful wife,

Ryan, my son,

My sisters and brothers,

My friends

Without your constant support, encouragement and love, this dissertation would not have been possible

TABLE OF CONTENTS

LIST OF FIGURES

Page

LIST OF TABLES

Page

ACKOWLEDGEMENTS

I came to UC Irvine in September 2010 with my wife, who was seven months pregnant with my son Ryan. My life and study would be too difficult if I were not blessed with great help and support from my great advisors, wonderful family, and amazing friends. My thanks go to those who provided me advice and support during my PhD program.

First of all, I would like to express my deepest gratitude and respect to my primary advisor, Professor Soroosh Sorooshian. He has been not only my academic advisor but also my life's guide throughout the years at UCI.

I would also like to thank my co-advisors, Professor Kuolin Hsu and Professor Amir AghaKouchak, for their invaluable advice on my research. My special thanks go to Dr. Xiaogang Gao and Dr. Jialun Li for the advice and comments on my research.

I am grateful to Professor Brett Sanders for unconditionally providing his model BreZo with guidance used in my research. He also provided invaluable advice on my dissertation as a PhD committee member. I would like to thank Dr. Jochen Schubert and Dr. Byunhyun Kim at the Computational Hydraulic Group at UCI for their great advice on hydraulic modeling with BreZo.

I would like to thank Dr. Michael Smith and Dr. Victor Koren at National Weather Service for the advice on hydrologic modeling with HL-RDHM model.

My special thanks go to Mr. Dan Braithwaite, IT Manager at CHRS. He has provided me guidance on coding and software with his patience. I would also like to thank Mrs. Diane Hohnbaum, Administrative Assistant at CHRS, for her kindness and support throughout my years at CHRS.

I would also like to thank my dear colleagues and friends at CHRS for their friendship and support: Nasrin, Rebecca, Ali Z, Alex, Joey, Jingjing, Hamed, Scott, Hao, Andrea, Sepideh, Tiantian, Negar and Yumeng. I would extend my special thanks to Scott for his friendship and support since I came to UCI. I wish to extend my gratitude to Andrea for our meaningful friendship and collaboration in research.

My little family was my motivation to move forward during these years. I thank my wife, Vi, for her care, kindness and support. My son Ryan is the most enjoyable part of my life.

Finally, I thank my parents, brothers, and sisters for their love and support. This dissertation is dedicated to them.

Financial support was provided by the Center for Hydrometeorology & Remote Sensing (CHRS) at UC Irvine, the Vietnamese International Education Development (VIED) program, the NOAA Office of Hydrologic Development (OHD) National Weather Service (NWS) Student Research Fellowship, the UC Irvine Chancellor Club for Excellence Fellowship, the Cooperative Institute for Climate and Satellites (CICS), and the Army Research Office (Award W911NF-11-1-0422). I would like to acknowledge high-performance computing support from Yellowstone

(ark:/85065/d7wd3xhc) provided by NCAR's Computational and Information Systems Laboratory, sponsored by the National Science Foundation.

CURRICULUM VITAE

Phu Nguyen

EDUCATION

Ph.D. **Water Resources Management**, at Center for Hydrometeorology and Remote Sensing (CHRS), University of California, Irvine, 2014.

Thesis: *Developing a high resolution coupled hydrologic-hydraulic model (HiResFlood-UCI) for flood modeling*.

Directed by Distinguished Professor Soroosh Sorooshian, Professor Kuolin Hsu, and Professor Amir AghaKouchak.

M.S. **Applied Science** (Water Resources Management), University of Melbourne, Australia, December 2008.

Thesis: *Using a numerical model to assessing the relationship of an arid zone unconfined groundwater table with the deeper artesian aquifer in the Great Artesian Basin, Australia*.

Directed by Dr. Justin Costelloe and Professor Andrew Western.

B.S. **Civil Engineering** (Hydraulics – Water supply & Drainage), Bach Khoa University – Hochiminh City, Vietnam, 2003.

Thesis: *Calculating and Designing the construction of Eakao Reservoir in Daklak, Vietnam*.

Directed by A. Professor Huynh Thanh Son.

RESEARCH INTERESTS

Surface hydrology, subsurface hydrology, hydroclimate modeling, application of remote sensing in hydrology, rainfall-runoff modeling, flood/flash flood/drought forecasting and control, parameter estimation, watershed management, natural hazards early warning systems, extreme precipitation events, decision making, system optimization, application of GIS in natural resources management, parallel computing, and crowdsourcing in weather observation and natural hazard management.

RESEARCH EXPERIENCES

- **September 2010 - 2014**: Graduate Student Researcher, Center for Hydrometeorology and Remote Sensing (CHRS), University of California, Irvine, California, USA.

- **June 2008**: Field technician, Australian National Water Commission "Ecological Outcomes of Flow Regimes":

- River Surveying in Lachlan and Macquarie Basin, New South Wales, Australia

- **June – July 2007**: Volunteer, ARC Linkage Project "Quantifying near-surface diffuse discharge from the southwest Great Artesian Basin, Australia":

- Research on groundwater, geology and meteorology.

- **October 2003 – March 2006**: Technician, International Rice Research Institute (IRRI) Program "Managing Water and land resources for sustainable livelihoods at the interface between fresh and saline water environments in Vietnam and Bangladesh" (CP10):

- Monthly monitoring the water quality in Camau Peninsula, Mekong Delta, Vietnam.

- **June 2003 – March 2006**: Technician, World Bank Program "Education Capacity Enhancement Project".

- **2003 – 2010**: Lecturer, Water Management Department, Nong Lam University, Hochiminh City, Vietnam.

AWARDS

- Chancellor's Club for Excellence Fellowship Award 2014 by **Chancellor** of University of California, Irvine.

- Travel grant to AGU Meeting 2013 by **Associated Graduate Students** (AGS) – University of California, Irvine.

- Graduate student travel grant for the NEMS/GFS 2013 Summer Modeling School on the NOAA operational Global Forecast System at the NCEP Environmental Modeling Center, Maryland in July 2013, supported by **NOAA**.

- National Fellowship Incentive Program Award 2013 by **the Henry Samueli School of Engineering**, University of California, Irvine.

- Graduate Student Scholarship to attend the Studies of Precipitation, flooding, and Rainfall Extremes Across Disciplines (SPREAD) workshop in Fort Collins, Colorado in 2013 & 2014 by **Colorado State University** through the sponsorship of the National Science Foundation (NSF).

- Graduate Student Scholarship to attend the Community Surface Dynamics Modeling System (CSDMS) Meeting 2013 in Boulder, Colorado, USA in March 2013 by **University of Colorado**, **Boulder** through the sponsorship of the National Science Foundation (NSF).

- Graduate Student Research and Travel Grant 2012 by **the Henry Samueli School of Engineering**, University of California, Irvine.

- Outstanding Student Paper Award 2012 by **American Geophysical Union** (AGU).

- Student Research Fellowship 2012-2014 by **National Weather Service, NOAA**.

- Full scholarship for Climate Sciences Inaugural Summer School at CalTech, Pasadena, California, August 2011 by **NASA**.
- Vietnam International Education Development Fellowship for PhD program (UC Irvine, 2010 - 2014) by **Vietnamese Government**.
- Australian Development Scholarship for Master of Applied Sciences program (University of Melbourne, 2007 - 2008) by **Australian Government**.
- **Bac Lieu Province People's Committee**'s award for the contributions to the International Conference on Effective Land-Water Interface Management for Solving Agriculture-Fishery-Aquaculture Conflicts in Coastal Zones 1-3 March 2005.
- **Gia Lai Province People's Committee**'s award for Green Summer Campaign 2003.

PUBLICATIONS

Journals

Nguyen, P., A. Thorstensen, S. Sorooshian, K. Hsu, and A. AghaKouchak. Flood forecasting and inundation mapping using HiResFlood-UCI and near real-time satellite precipitation data: the 2008 Iowa flood. Journal of Hydrometeorology. 2014. Under review.

Nguyen, P., A. Thorstensen, S. Sorooshian, K. Hsu, A. AghaKouchak, B. Sanders, V. Koren, Z. Cui, and Michael Smith. A high resolution coupled hydrologic-hydraulic model (HiResFlood-UCI) for flash flood modeling. Journal of Hydrology. 2014. Under review.

Nguyen, P., S. Sellars, A. Thorstensen, Y. Tao, H. Ashouri, D. Braithwaite, K. Hsu and S. Sorooshian. 2014. Satellite Track Precipitation of Super Typhoon Haiyan. *AGU EOS,* **95** (16), 133&135.

Phong, N.D., T.P. Tuong, **N.D. Phu**, N.D. Nang, C.T. Hoanh. 2013. Quantifying Source and Dynamics of Acidic Pollution in a Coastal Acid Sulphate Soil Area. *Water Air Soil Pollut* 224:1765. DOI 10.1007/s11270-013-1765-0.

Sellars, S., **P. Nguyen**, W. Chu, X. Gao and S. Sorooshian. 2013. Computational Earth Science: Big Data Transformed Into Insight. *AGU EOS,* **94** (32), 277-278.

Kuolin Hsu, Scott Sellars, **Phu Nguyen**, Dan Braithwaite and Wei Chu. 2013. G-WADI PERSIANN-CCS GeoServer for extreme precipitation event monitoring. *Sciences in Cold and Arid Regions,* **5** (1), 0006-0015.

Book Chapter

Sorooshian, S., **P. Nguyen**, S. Sellars, D. Braithwaite, A. AghaKouchak, and K. Hsu. 2014. Satellite-based remote sensing estimation of precipitation for early warning systems, Extreme Natural Hazards, Disaster Risks and Societal Implications, A. Ismail-

Zadeh, J.U. Fucugauchi, A. Kijko, K. Takeuchi, and I. Zaliapin, Cambridge University Press, 99-111.

Conference presentations, papers and posters

Nguyen, P., A. Thorstensen, K. Hsu, A. AghaKouchak, B. Sanders, and S. Sorooshian. 2014. Simulation of the 2008 Iowa Flood using HiResFlood-UCI model with remote sensing data. Poster session presented at the annual meeting of the American Geophysical Union; 2014 Dec 15-19; San Francisco, California, USA.

Nguyen, P., P. Huynh, D. Braithwaite, K. Hsu, and S. Sorooshian. Monitoring Global Precipitation through UCI CHRS's RainMapper App on Mobile Devices. Poster session presented at the annual meeting of the American Geophysical Union; 2014 Dec 15-19; San Francisco, California, USA.

Nguyen, P., A. Thorstensen, K. Hsu, A. AghaKouchak, B. Sanders and S. Sorooshian. Developing a Global High-Resolution Flash Flood Forecasting System Using Multiple Sources of Precipitation Data. Oral presentation at 2014 AGS Symposium; 2014 April 18; University of California, Irvine, California, USA.

Nguyen, P., K. Hsu, A. AghaKouchak, B. Sanders and S. Sorooshian. Evaluating the Performance of a Coupled Distributed Hydrologic – Hydraulic Model for Flash Flood Modeling Using Multiple Precipitation Data Sources. Poster section presented at the annual meeting of the American Geophysical Union; 2013 Dec 9-12; San Francisco, California, USA.

Thorstensen, A., **P. Nguyen**, K. Hsu, S. Sorooshian and W. Krajewski. Comparison of Multiple Precipitation Products over a Densely Gauged Basin through Distributed Hydrologic Modeling. Poster session presented at the annual meeting of the American Geophysical Union; 2013 Dec 9-12; San Francisco, California, USA.

Sorooshian, S., **P. Nguyen**. Role of advanced Observational, Information and GIS tools in assessing hydroclimate change and variability effects on urban areas. Oral presentation at the American Public Works Association (APWA) 15th Annual GIS Conference: GIS Role in Government Agencies. Sep 5, 2013. Cypress, California, USA.

Nguyen, P., S. Sorooshian, K. Hsu and A. AghaKouchak. ArcGIS for a coupled hydrologic - hydraulic model. Oral presentation at the ESRI International User Conference; July 2013. San Diego, California, USA.

Sellars, S., **Nguyen, P**., Chu, W., Gao, X. and Sorooshian, S. A New Global Precipitation Event Database: Big Data Approach to Knowledge Discovery In Remotely Sensed Precipitation Datasets. Poster section presented at Interface 2013 workshop; April 2013. Chapman University, Orange County, California, USA.

Nguyen, P., S. Sorooshian, K. Hsu, A. AghaKouchak and B. Sanders. Modeling the Upper Little Missouri River flash flood 2010 using a coupled distributed hydrologic-

hydraulic model. Poster section presented at CSDMS Meeting 2013; March 2013. University of Colorado, Boulder, USA.

Nguyen, P., S. Sorooshian, K. Hsu, A. AghaKouchak and B. Sanders. A Coupled Distributed Hydrologic and Hydraulic Model for Flash Flood Modeling. Oral presentation at the First IUGG GRC Conference on Extreme Natural Hazards and Their Impacts; 2012 December 8-11. Chapman University, Orange County, California, USA.

Nguyen, P., S. Sorooshian, K. Hsu, A. AghaKouchak, B. Sanders, M. Smith and V. Koren. Improving flash flood forecasting through coupling of a distributed hydrologic rainfall-runoff model (HL-RDHM) with a hydraulic model (BreZo). Poster session presented at the annual meeting of the American Geophysical Union; 2012 Dec 3-7; San Francisco, California, USA.

Nguyen, P., S. Sellars, K. Hsu, D. Braithwaite, S. Sorooshian, T. Le. Precipitation estimation using remote sensing technology. Proceeding of Conference on Agriculture; 2012 Dec 20. Nong Lam University, Hochiminh City, Vietnam.

Nguyen, P., S. Sellars, K. Hsu, D. Braithwaite, W. Chu, S. Sorooshian, L. Nguyen. The near real-time global precipitation G-WADI PERSIANN-CCS GeoServer. Proceeding of Conference on GIS Applications 2012; 2012 Oct 29-30. Hochiminh City, Vietnam.

Contributed conference presentations, posters and papers

Thorstensen, A., **P. Nguyen**, K. Hsu, R. Zamora, and S. Sorooshian. Data Assimilation of Soil Moisture in a Distributed Hydrologic Model: A case study over the Russian River Basin. Oral presentation at the annual meeting of the American Meteorological Society; 2015 Jan 4-8; Phoenix, Arizona, USA.

Thorstensen, A., **P. Nguyen**, K. Hsu, and S. Sorooshian. Calibration of a Hydrologic Model via Densely Distributed Soil Moisture Observations. Poster session presented at the annual meeting of the American Geophysical Union; 2014 Dec 15-19; San Francisco, California, USA.

Ashouri, H., **P. Nguyen**, A. Thorstensen, K. Hsu, and S. Sorooshian. Long-Term Rainfall-Runoff Modeling Using High-Resolution Satellite-based Precipitation Products. Poster session presented at the annual meeting of the American Geophysical Union; 2014 Dec 15-19; San Francisco, California, USA.

To, H., **P. Nguyen**, C. Shahabi, and S. Sorooshian. iRain: A Spatial Crowdsourcing App for Real-time Rainfall Observation. Poster session presented at Environmental Sustainability Research Network; 2014 May, University of Southern California, Los Angeles, California, USA.

Sellars, S., **P. Nguyen**, W. Chu, X. Gao, K. Hsu and S. Sorooshian. The Application of Object-Oriented Data Analysis for Developing a Higher Dimensional Knowledge Discovery Dataset: Regional Hydroclimatology of Western U.S Atmospheric Rivers.

Poster session presented at the Third workshop on Understanding Climate Change from Data; 2013 Aug; Northwestern University, Evanston, Illinois.

Sellars, S., **P. Nguyen**, W. Chu, X. Gao and S. Sorooshian. A New Global Precipitation Event Database: Applications of Object-Oriented Connectivity Algorithm Applied to Remotely Sensed Precipitation Data. Poster session presented at the annual meeting of the American Geophysical Union; 2012 Dec 3-7; San Francisco, California, USA.

Sellars, S., **P. Nguyen**, W. Chu, X. Gao and S. Sorooshian. The Application of Object Based Methods and Machine Learning to remote Sensing Precipitation Data. Poster session presented at the University of Minnesota: Workshop on Understanding Climate Change from Data; 2012 Aug 6-7; Minneapolis, Minnesota, USA.

Phong ND, Nang ND, Hoanh CT, Tuong TP, Ngoc NV, **Phu ND**, An LT, Phuong NV, Malano H and Weaver T. 2008. Loading amount, temporal and spatial distribution of acid pollution in coastal zones: A Study Case of Ca Mau peninsula, Vietnam. International Conference Delta 2007: Managing the coastal Land-water interface in tropical delta systems.

Database

Sellars, S., **P. Nguyen**, W. Chu, X. Gao, K. Hsu, and S. Sorooshian, 2013: A New Near Global Precipitation Database: An Objected Oriented Approach [Data set]. Irvine, CA: Center for Hydrometeorology and Remote Sensing, University of California, Irvine. Available online: ftp://persiann.eng.uci.edu/pub/ssellars/voxel_data/

App Development

RainMapper – access to real-time global high-resolution satellite precipitation products from the UCI CHRS's PERSIANN-CCS. Available on App Store and Google Play.

iRain – the first global crowdsourcing rainfall observation system (http://irain.eng.uci.edu). Available on App Store and Google Play.

Tutorials

G-WADI GeoServer Tutorial (Vietnamese version) – Spring 2012. Available at: http://persiann.eng.uci.edu/gwadi_tutorial_videos.html

CONFERENCE ATTENDANCE WITHOUT PRESENTATIONS

- ESRI User Conference 2014, July 14-18, 2014, San Diego, California, USA.
- Studies of Precipitation, flooding, and Rainfall Extremes Across Disciplines (SPREAD) workshop, July 23-25, 2014, NCAR, Colorado State University, Boulder, Colorado, USA.

- Google Earth Engine and Disaster Risk Modeling workshop, December 17-18, 2013, Google Headquarters, Mountain View, California, USA.
- Studies of Precipitation, flooding, and Rainfall Extremes Across Disciplines (SPREAD) workshop, June 16-21, 2013, Colorado State University, Fort Collins, Colorado, USA.
- NSF-EarthCube Workshop on Earth System Modeling Coupling, February 11-12, 2013, UC Irvine, California, USA.
- 3rd SMAP Cal/Val Workshop, November 14-16, 2012, Oxnard, California, USA.
- ESRI User Conference 2012, July 23-27, 2012, San Diego, California, USA.
- International Conference on Effective Land-Water Interface Management for Solving Agriculture - Fishery - Aquaculture Conflicts in Coastal Zones, March 1-3, 2005, Bac Lieu, Vietnam.

TRAINING COURSES

- **NEMS/GFS 2013 Summer Modeling School** on the NOAA operational Global Forecast System at the NCEP Environmental Modeling Center, Maryland. 2013.
- **NASA Jet Propulsion Laboratory's Center for Climate Sciences Inaugural Summer School**. California Institute of Technology in Pasadena, California. 2011.
- **SPSS and Dreamweaver**. University of Melbourne. 2008.
- **EAP Consolidation.** Australian Development Scholarship Center in Hanoi. 2006.
- **Application of GIS in natural resources management.** Nong Lam University. 2006.
- **Methodology and Classroom Skills in University Teaching.** Nong Lam University. 2005.
- **Certificate of ISO 9001 – Version 2000 in Education.** Nong Lam University. 2004.

LEADERSHIP/SERVICE

- **Co-founder – Secretary General**, Association of Vietnamese Students and Professionals in the United States, and www.sinhvienusa.org 2013-2015.
- **Vice President**, Vietnamese Youth and Student Association in California 2012-2014.
- **Coordinator**, Green Summer Campaign in remote areas of Gia Lai Province August 2009.
- **Coordinator**, Green Summer Campaign in remote areas of Gia Lai Province August 2003.

PROFESSIONAL AFFILIATIONS

- American Geophysical Union (**AGU**).
- American Meteorological Society (**AMS**).
- American Society of Civil Engineers (**ASCE**).

- Community Surface Dynamics Modeling System (**CSDMS**).
- **IEEE**

ABSTRACT OF THE DISSERTATION

Developing a high resolution coupled hydrologic-hydraulic model (HiResFlood-UCI) for flood modeling

by

Phu Dinh Nguyen

Doctor of Philosophy in Civil Engineering

University of California, Irvine, 2014

Distinguished Professor Soroosh Sorooshian, Chair

Floods are among the most devastating natural disasters which affect millions of people worldwide. Forecasting floods to provide warnings to the public in a timely manner is crucially important, however, this is a very challenging task. HiResFlood-UCI was developed by coupling the National Weather Service's (NWS) distributed hydrologic model (HL-RDHM) with the hydraulic model BreZo (developed by Sanders and Begnudelli) in order to estimate localized flood depths and velocities. A semi-automated technique of efficient unstructured mesh generation for BreZo was developed. HiResFlood-UCI was implemented for the ELDO2 catchment in Oklahoma. Using synthetic precipitation input, the model was tested for various components including HL-RDHM parameters (a priori versus calibrated), channel and floodplain Manning n values, DEM resolution (10m versus 30m), and computation mesh resolution (10m+ versus 30m+). Simulations show that HiResFlood-UCI produces reasonable results with the *a priori* parameters from NWS. Sensitivities to hydraulic model resistance parameters, mesh resolution, and DEM resolution are also identified, pointing to the importance of model calibration and validation for accurate prediction of localized flood intensities. HiResFlood-UCI

performance was examined using six measured precipitation events as model input for validation of the streamflow at the outlet and an interior point. Validation builds confidence in model predictions of river discharge, flood extent and localized velocities, which are fundamental to reliable flood warning.

HiResFlood-UCI was implemented for flood forecasting in the Cedar River Basin using real-time remote sensing precipitation PERSIANN-CCS data. The model was evaluated for the historical 2008 Iowa flood. The results show HiResFlood-UCI with real-time PERSIANN-CCS was able to capture the observed hydrographs and reasonably match the USDA's AWiFS 56m resolution flood imagery over the most impacted area in the extended Cedar Rapids region. This is promising for a global high resolution flood warning system pairing HiResFlood-UCI with PERSIANN-CCS in the near future.

Chapter 1. Introduction

1.1 Floods and flash floods

Floods are one of the most hazardous disasters in society. Floods account for 15 percent of all fatalities related to natural hazards (World Meteorology Organization – WMO, 2011). Fig. 1-1 shows the world-wide flood statistics from 1950 to 2010 using data from the Center for Research on the Epidemiology of Disasters (CRED, http://www.emdat.be). There was a significantly increasing trend in the number of floods occurring, number of deaths, number of people affected and economic damage over the past half century. In the 1990s, approximately 100 thousand people died and 1.4 billion people were affected by floods as a result of the severe flooding happening in China. Between 1987 and 1997, 44 percent of all floods occurred in Asian countries causing 288,000 deaths and economic damage of $136 billion (UNESCO, 2014, available online at http://webworld.unesco.org/water/wwap/facts_figures/managing_risks.shtml). The global warming leads to an increase in precipitation intensity in many parts of the world which may cause more severe floods. Strauss and Kulp at Climate Central organization (2014) predicted that about 2.5 percent of the world population live in an area likely to be impacted by flooding by the end of the 21st century.

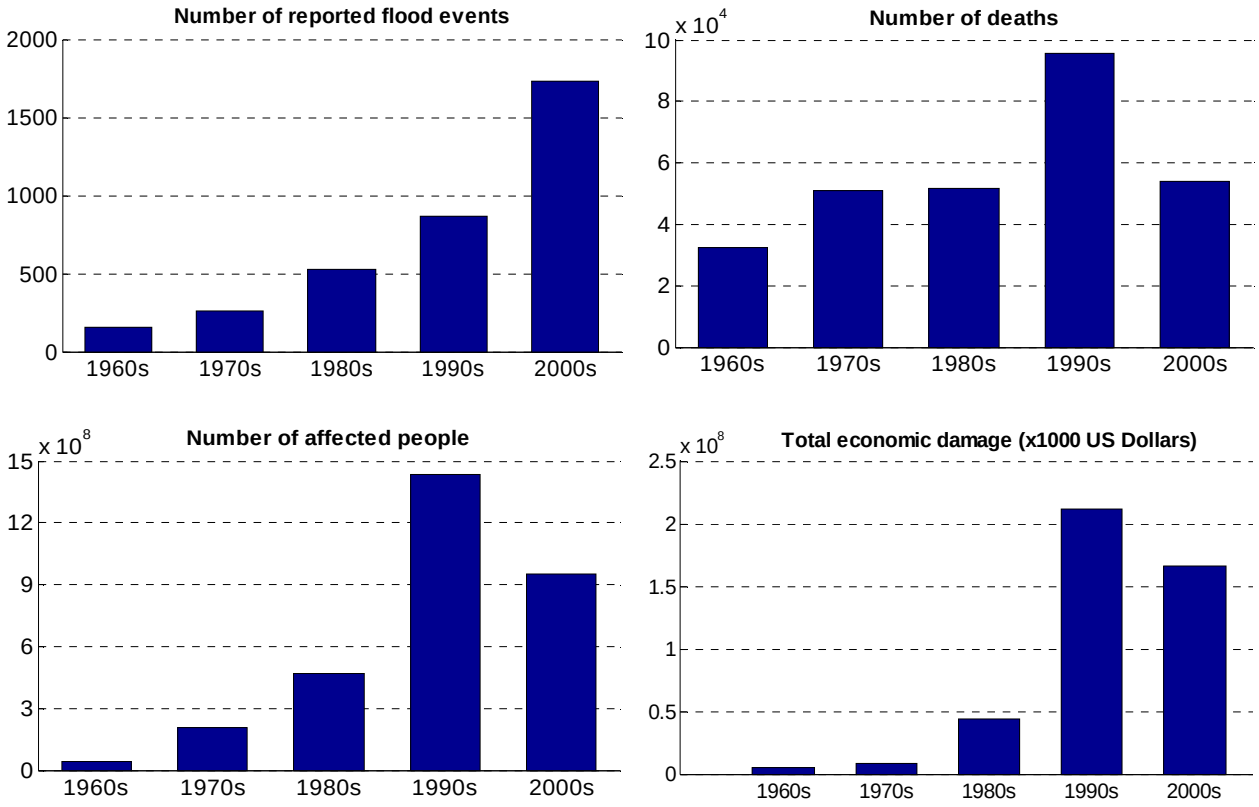

Fig. 1-1. Flood statistics from 1950 to 2010 using data from CRED

It is sometimes confusing for the public to distinguish the difference between the definitions of floods and flash floods. Flash floods are one kind of floods which have short duration but can result in many fatalities. A flood happens when prolonged rainfall over several days, intense rainfall over a short period of time, or an ice or debris jam causes a river or stream to overflow and flood the surrounding area.

A flash flood can occur within six hours of a rain event, or after a dam or levee failure, or following a sudden release of water held by an ice or debris jam. The use of the word "flash" here is synonymous with "urgent." (http://www.nws.noaa.gov/floodsafety/floodsafe.shtml). Flash floods usually occur in streams and small watersheds, about 260km^2 (Davis, 1998). Such

watersheds often have rapid responses to intensive rainfall because of their steep slopes, saturated soils and impermeable surfaces (Hapuarachchi *et al.,* 2011).

1.2 Modeling floods

Many efforts have been made to improve flood modeling and forecasts for the past decade through the improvements of data collecting capabilities and modeling techniques. Flood modeling can be categorized into two types of models: data-driven and hydrological models. The former use a statistical relationship between rainfall and river flow to generate flow simulation while the latter can be lumped, semi-lumped or distributed models.

In data driven models, statistical or machine learning techniques (Neural network) can be used to generate flows based on a training process with historical rainfall - discharge data (Sahoo *et al.*, 2006; Piotrowski *et al.*, 2006; Kim & Barros, 2001). This type of models is often simple to set up and gives acceptable results but requires long term data records (Hapuarachchi *et al.*, 2011). On the other hand, many hydrological models have been developed and applied for flood modeling and forecasting. Lumped models are commonly used for these purposes (Kobold & Brilly, 2006; Sirdas & Sen, 2007); however, distributed models have recently become more common because of data availability (i.e. the current NWS flash flood guidance system; Borrell *et al.*, 2006).

Hydrologic models as simplified representations of a part of the hydrologic cycle have served as important tools for modeling flash flooding. Based on the application and type of data available, hydrologic models have been designed with various levels of complexity from the so-called lumped (e.g. HBV, Bergstrom, 1995; Sacramento Soil Moisture Accounting - SAC-SMA, Burnash *et al.*, 1973) to semi-lumped (e.g. VIC – Liang *et al.*, 1994) and distributed (e.g. HL-

RDHM – Koren *et al.*, 2003, 2004, 2007). Lumped models treat the whole system as one element with single inputs and outputs at a time and do not account for the spatial variability over the domain (Khakbaz *et al.*, 2012). On the other hand, distributed models, which can capture the heterogeneities in the watershed characteristics and hydrometeorological forcings, are suggested to better represent the physical mechanisms of the reality. New technologies in the field of remote sensing enable distributed data of earth surface characteristics (topography, soil types, land uses) and forcing inputs (precipitation, temperature, evapotranspiration, etc.) available for distributed models. In addition to forcing data, remote sensing information, such as surface water data from the Surface Water and Ocean Topography mission (SWOT, to be launched in 2020), will be useful for distributed calibration/validation efforts of distributed models in the near future (Mersel *et al.*, 2013).

The Office of Hydrologic Development (OHD) at the National Weather Service (NWS) conducted the distributed model intercomparison project phases 1&2 (DMIP1&2, Smith *et al.*, 2004, 2012a, 2012b) in the regions of Oklahoma, Arkansas and Missouri. The DMIP experiments were designed to compare the performance of distributed models amongst themselves and to the currently operational lumped model (SAC-SMA) in various aspects of hydrologic modeling such as outlet hydrographs, interior-point hydrographs, model complexity, model calibration, *a priori* parameters and soil moisture. Reed *et al.* (2004) concluded, from the results of DMIP1 concluded, that in most of the cases of the experiments, lumped models showed better overall performance than distributed models. DMIP2 results suggested that distributed models can account for spatial features of basins and precipitation, and also preserve the water balance in catchments (Smith *et al.*, 2012b).

A hydrologic model even lumped or distributed normally involves two main components: rainfall-runoff estimator and routing scheme. In the latter, water is routed either using a routing equation in lumped models or through a cell "conceptual" channel system in distributed models. This can be considered as a weakness of hydrologic models for flood modeling because the "true" physical characteristics of the rivers/channels are not accounted for. Therefore, hydraulic models such as 1D HEC-RAS (US Army Corps of Engineers - USACE), MIKE FLOOD (Danish Hydraulic Institute - DHI), BreZo (Sanders & Begnudelli), and LISFLOOD-FP (University of Bristol) have been applied to simulate floods (Horritt & Bates, 2002; Patro *et al.*, 2009; Begnudelli & Sanders, 2006; Bates *et al.*, 2010). One of the main advantages of hydraulic models is that they can simulate water flowing in the 'true' river systems. This provides more information of flash floods in spatial distribution.

Many efforts have been made to take advantage of both hydrologic and hydraulic models by coupling them together in a system for flood modeling purposes. In regional scale, Kim *et al.* (2012) coupled the Triangulated Irregular Network-Real Time Integrated basin Simulator (tRIBS) with an Overland Flow Model (OFM) for a watershed of 64 km^2. Bonnifait *et al.* (2009) coupled TOPMODEL with a 1D hydraulic model named CARIMA for reconstructing the catastrophic flood event in the Gard region of France. In large scale, a coupled hydrologic/hydraulic framework of the Interactions between Soil-Biosphere-Atmosphere (ISBA) and LISFLOOD-FP (Bates *et al.*, 2010; Neal *et al.*, 2012) was developed for the Ob River in Siberia (Biancamaria *et al.*, 2009). More recently, Schumann *et al.* (2013) were successful in coupling the widely used VIC (Liang *et al.*, 1994) with LISFLOOD-FP for forecasting daily flood inundation in large scale for the Lower Zambezi River.

1.3 Research motivation

Due to the nature of their design, current coupled hydrologic/hydraulic model systems tend to suffer the inherent trade-off between capturing fine details through the utilization of high resolution and covering extensive areas. A flexible computational mesh makes the proposed coupled system feasible for large areas while maintaining the ability to capture flood details where needed (i.e. closer to the river). The design of the proposed coupling framework itself is unique in that it has the capability to easily switch from uncoupled to coupled mode. In an operational sense, this is extremely valuable as the hydrologic model may be permanently running for an entire large region, such as a river forecast center area, and when a more localized area requires detailed simulation of a flooding event the hydraulic component may be activated.

1.4 Research objectives

This research aims to develop a high resolution coupled hydrologic/hydraulic model (HiResFlood-UCI) for flash flood modeling. The Hydrology Laboratory Research Distributed Hydrologic model (HL-RDHM) is coupled with a hydraulic model, BreZo (Sanders & Begnudelli) for flash flood modeling in high resolution at river scale. Further applications of the coupled model are to simulate past severe flash floods, flash flood forecasts and flash flood analysis with various scenarios.

The objectives of this dissertation are:

1) ***Developing HiResFlood-UCI for flood modeling purposes.***
2) ***Developing a semi-automated technique of efficient unstructured mesh generation for HiResFlood-UCI.***

3) ***Testing the sensitivities of HiResFlood-UCI with synthetic precipitation data for various components including hydrologic parameters (a priori versus calibrated), hydraulic Manning n values, DEM resolution (10m versus 30m), and computation mesh (10m+ versus 30m+).***
4) ***Validating HiResFlood-UCI for both streamflow and flooded maps for real extreme precipitation events.***
5) ***Applying HiResFlood-UCI for flood forecasting using real-time remote sensing precipitation data.***

1.5 Outline of the research

The remainder of this dissertation is organized into seven chapters. Chapter 2 describes in details the development of the coupled hydrologic/hydraulic model named HiResFlood-UCI for flood modelling. Chapter 3 addresses the method for calibration of HiResFlood-UCI. Chapter 4 describes the statistical metrics used in model validation. Chapter 5 presents the test of HiResFlood-UCI with hydraulic roughness parameters, default HL-RDHM parameters, DEM resolution and mesh resolution. Chapter 6 is devoted to the validation of HiResFlood-UCI using streamflow observation with NEXRAD Stage 4 radar precipitation data. Chapter 7 presents the application of HiResFlood-UCI for flood forecasting using real-time remote sensing precipitation data. The summary and future works are described in Chapter 8.

Chapter 2. Model development

HiResFlood-UCI is a coupled model based on the heritage of HL-RDHM and BreZo. The coupled model uses HL-RDHM as a rainfall-runoff generator and replaces the routing scheme of HL-RDHM with the 2D hydraulic model (BreZo) for better simulating floods at river scale. HL-RDHM was chosen for the hydrologic component in the HiResFlood-UCI because this model is one of the most reliable hydrologic models, which was well developed and calibrated, especially for the U.S. BreZo has originally been developed for simulating flood extent and flow velocity at river scale and it has been successfully applied for dam breaks (Begnudelli & Sanders, 2006; Begnudelli & Sanders, 2007; Sanders, 2007; Begnudelli *et al*., 2008).

2.1 Model heritage

2.1.1 Hydrologic component (HL-RDHM)

The Hydrology Laboratory - Research Distributed Hydrologic Model (HL-RDHM) was developed by the National Weather Service (NWS) Office of Hydrologic Development (OHD), with the basic concepts and structures originated by the Nile Forecast System by Koren and Barrett (1995). HL-RDHM has been developed and implemented for the Contiguous United States (CONUS) for hydrologic research and development. Detailed information can be found in the user manual V.3.2.0 (NWS, 2011). HL-RDHM has been widely used for hydrologic studies including Smith *et al.* (2004), Moreda *et al.* (2006), Reed *et al.* (2007), Tang *et al.* (2007), Yilmaz *et al.* (2008), Wagener *et al.* (2009), Khakbaz *et al.* (2012), Smith *et al.* (2012a), and Smith *et al.* (2012b).

In SAC-SMA, unlike other distributed models with fixed values for sub-domains or the entire domain, an advanced algorithm was designed to derive *a priori* parameters from soil and land use data. Forcing data of HL-RDHM include next generation radar (NEXRAD) precipitation data and surface temperature for Snow-17.

HL-RDHM is a distributed hydrologic model which was designed and implemented for the entire CONUS at a spatial resolution of 1 Hydrologic Rainfall Analysis Project (HRAP) grid (~4km). HL-RDHM structure can also be applied for any cell resolution and time step length. The model involves 3 main modules: Snow-17, SAC-SMA, hillslope and channel routing (Fig. 2-1).

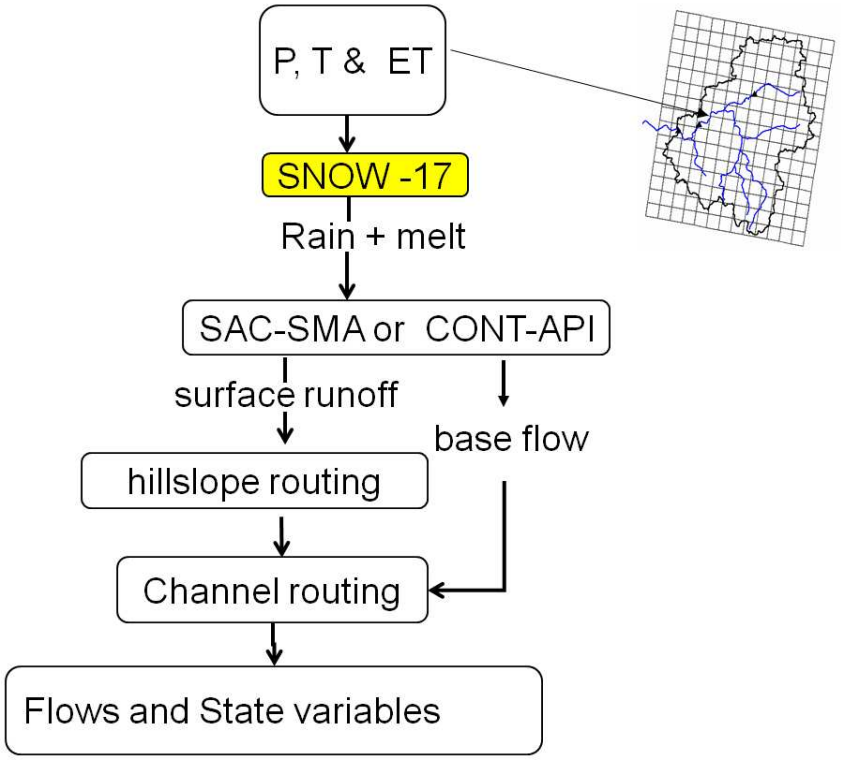

Fig. 2-1. Schematic structure of HL-RHDM system (NWS, 2011)

Snow-17

The NWS snow accumulation and ablation model (Snow-17) available within HL-RDHM was developed by Anderson (1973). Snow-17 is a conceptual index model for simulating the processes of snowmelt and snow accumulation based on air temperature. The model structure is illustrated in Fig. 2-2. Snow-17 has air temperature and precipitation as model inputs. Snow-17 uses air temperature as the index to determine the energy exchange across the snow-air interface. In distributed application of Snow-17 in HL-RDHM, the depletion curve can be set to a straight line or a snow or no snow relationship for each pixel. More description of the Snow-17 can be found in Anderson (1973), Anderson (2006), and NWS (2011).

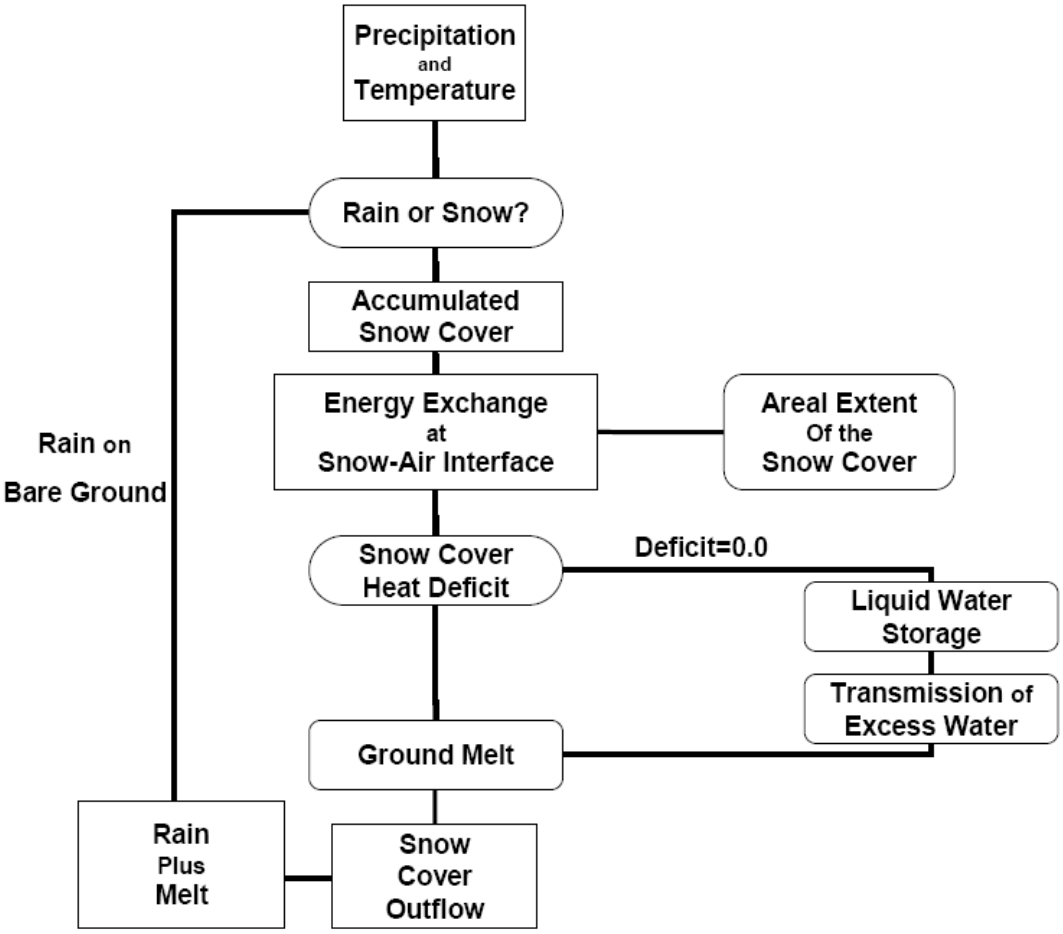

Fig. 2-2. Flowchart of Snow-17 model (Anderson, 2006)

SAC-SMA

SAC-SMA is the heart of the HL-RDHM model. Fig. 2-3 represents the schematic of the SAC-SMA model. SAC-SMA has two conceptual layers, upper and lower zone storages. Each layer has two basic components, tension water and free water. Tension water is defined as the water that can only be removed from the soil by evaporation or evapotranspiration. The water which can be filled in the voids of the soil and eventually drains out of the soil is considered free water. The upper zone tension water is restricted to the volume of water which can be applied to the dry soil before any component of leakage takes place from the soil. Direct runoff is the fraction of

runoff which is due to rainfall over permanent imperious areas of the basin which drains directly to the stream channel. Surface runoff is the fraction of streamflow generated when rainfall exceeds infiltration. Another component of moisture in the unsaturated zone is called the "upper zone free water" which moves laterally through the soil to provide interflow and moves vertically into deeper levels of the soil as percolation. The "lower zone tension water" is the water necessary to fully satisfy moisture requirements based on the molecular attraction between dry soils and moisture excluding free water in the interstices between the soil molecules. Baseflow is a combination of lateral drainage from lower zone supplementary and primary free water storages. Subsurface outflow is the drainage from lower zone free water storages to aquifers that do not discharge to the stream channel within the basin. More details about SAC-SMA model can be found in Burnash *et al.* (1973) and Burnash (1995).

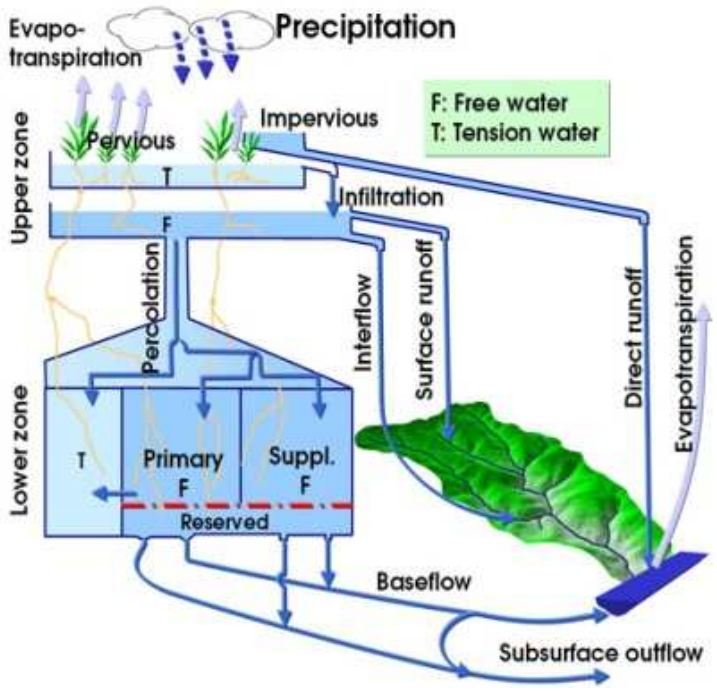

Fig. 2-3. Schematic structure of SAC-SMA model

Hillslope and channel routing

The routing scheme within HL-RDHM has two components, hillslope and channel routing (Fig. 2-4). The hillslope runoff consists of fast (surface) and slow (subsurface) flows. In SAC-SMA, direct runoff and surface runoff are considered as fast flow, and interflow and baseflow as slow flow. Within a cell, fast runoff is routed over a conceptual uniform hillslope system then combined with the slow flow component and flow from upstream pixels routed through a cell conceptual channel. In the channel routing process, water is moved from upstream to downstream through a topographically based cell-to-cell connectivity sequence (NWS, 2011).

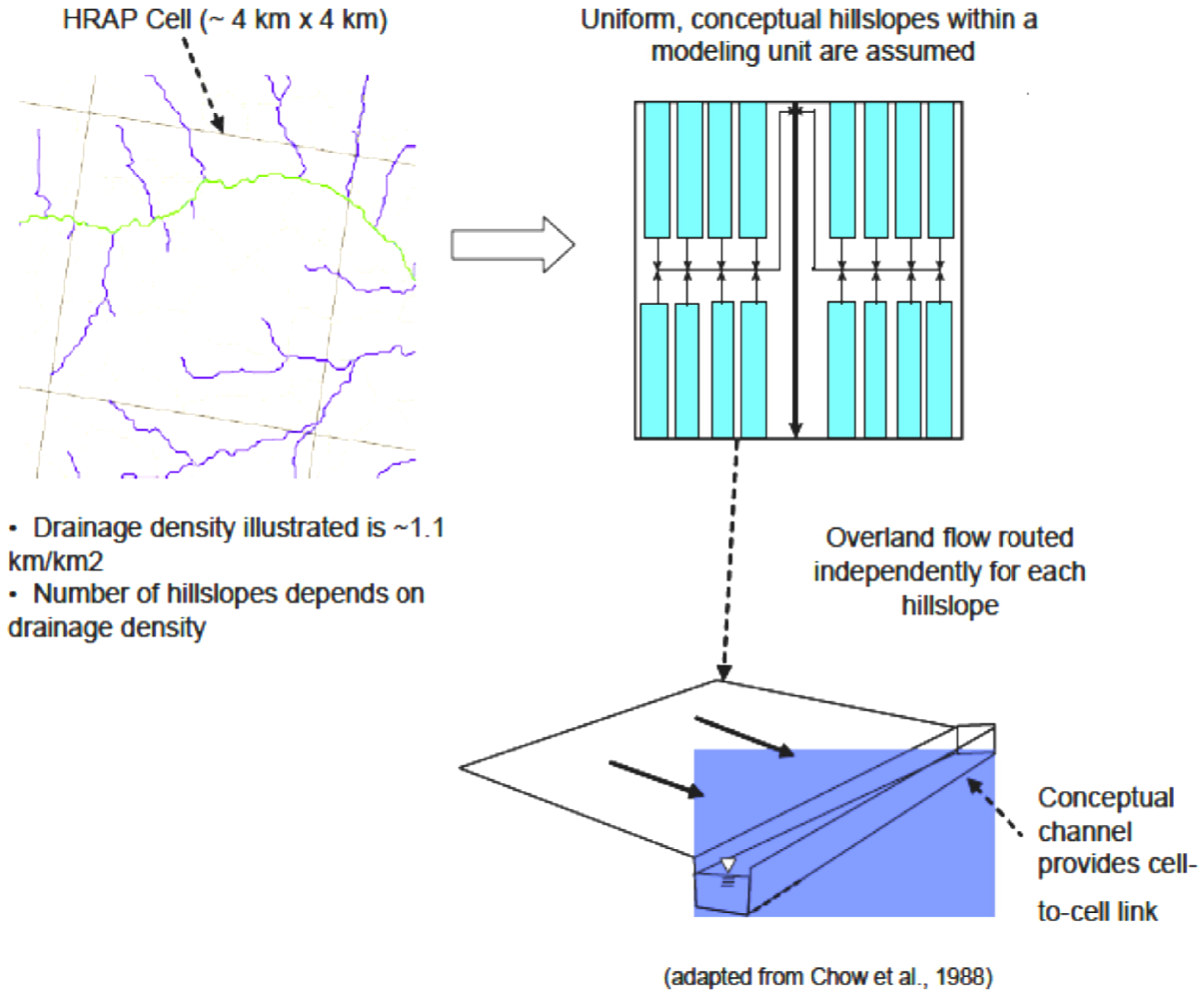

Fig. 2-4. Schematic structure of routing scheme in HL-RHDM system (NWS, 2011)

2.1.2 Hydraulic component (BreZo)

BreZo is a hydraulic model which solves the 2D shallow-water equations using Godunov-type finite volume method with unstructured grid of triangular cells. The shallow-water equations can be rewritten in integral form as follows (Bradford & Sanders, 2002).

$$\frac{\partial}{\partial t}\int_{\Omega}\mathbf{U}\,d\Omega+\oint_{\partial\Omega}(\mathbf{F}\,dy-\mathbf{G}\,dx)=\int_{\Omega}\mathbf{S}\,d\Omega \tag{1}$$

where U = (h uh vh)^T is vector of flow variables. F and G are flux terms. S is source term. F, G and S are computed as follows.

$$\mathbf{F}=\begin{pmatrix} hv \\ hu^2+\frac{1}{2}gh^2 \\ huv \end{pmatrix} \qquad \mathbf{G}=\begin{pmatrix} hv \\ huv \\ hv^2+\frac{1}{2}gh^2 \end{pmatrix} \qquad \mathbf{S}=\begin{pmatrix} 0 \\ -gh\frac{\partial z}{\partial x}-c_D u\sqrt{u^2+v^2} \\ -gh\frac{\partial z}{\partial y}-c_D v\sqrt{u^2+v^2} \end{pmatrix} \tag{2}$$

h is flow depth; u and v are velocities in x and y directions respectively. z is bed elevation, C_D is drag coefficient computed from Manning formula $C_D = gn^2/h^{1/3}$, where *n* is the bed's Manning roughness value.

A detailed description of the Godunov-type finite volume method solving the 2D shallow water equations in BreZo can be seen in Bradford & Sanders (2002), Begnudelli & Sanders (2006), Begnudelli *et al.* (2008). One of the primary advances of the model is that it was designed for working with an unstructured grid of triangular cells which enables the model to simulate the water flow in varying shapes of the channel/river systems.

Parameters of BreZo are surface friction (Manning, Chezy or Darcy-Weisbach), wind (optional), Coriolis Effect (optional) and viscosity (optional). BreZo is flexible for setting initial conditions, boundary conditions (open, free slip wall, inflow, and outflow), inputs (multiple point sources), outputs (discharge, water level, flow velocity). The advanced technique of cross-section zoning enables the user to estimate accumulative flows through a cross section. Another advanced technique is for implementing tide as a type of boundary which is useful for modeling flash floods and inundation in coastal areas. A more detailed description, demo and implementation of BreZo can be found at http://sanders.eng.uci.edu/brezo.html.

2.2 HiResFlood-UCI

A new coupling framework named HiResFlood-UCI (**Hi**gh Resolution **Flood** model - **U**niversity of **C**alifornia, **I**rvine) has been developed to couple the two models working together to simulate flash floods. HiResFlood-UCI has two basic components: distributed hydrologic HL-RDHM model for rainfall-runoff generation and BreZo for water flow routing. The whole coupling process is followed the steps below, illustrated in Fig. 2-5. The model employs HL-RDHM as a rainfall-runoff generator in coarse resolution to produce surface runoff which will be zoned into point source hydrographs at the sub-catchment outlets. With point source input, BreZo simulates the spatial distributions of water depth and velocity of the flow in the river/channel and flood plain. The coupled model is being implemented and tested for some catchments before being applied for the whole CONUS and other parts of the world. HL-RDHM and BreZo components are run in parallel. The framework is designed for processing the results from HL-RDHM to the form which BreZo can read as inputs.

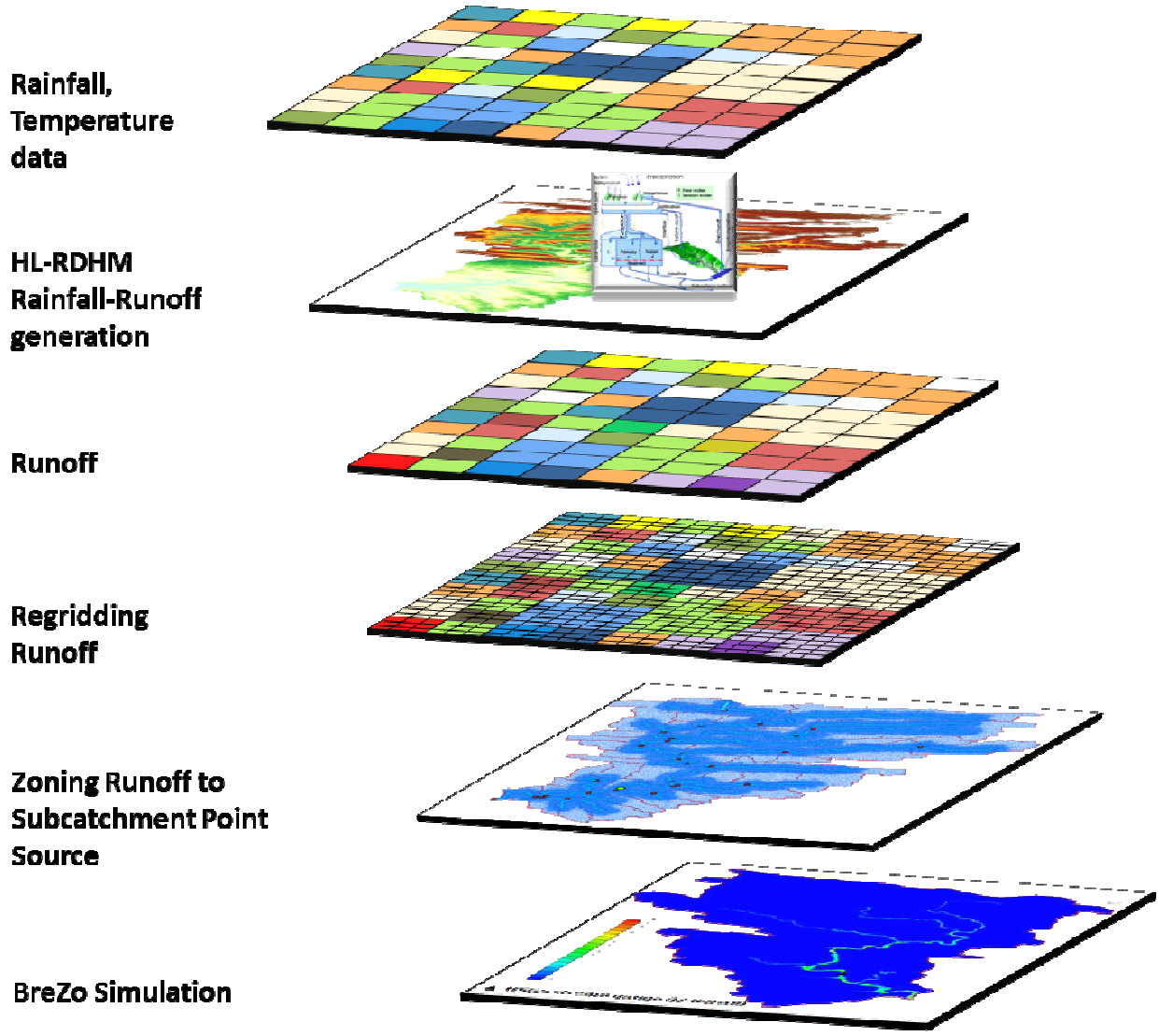

Fig. 2-5. HiResFlood-UCI coupling framework

2.2.1 Set up HL-RDHM

HL-RDHM can be executed over the whole CONUS with the *a priori* parameter set provided by NWS to provide surface and subsurface runoffs. The model can also be set up for a specific domain in the CONUS using calibrated parameter adjustment coefficients provided by NWS.

Hourly rainfall (i.e. Stage IV; PERSIANN – Hsu *et al.*, 1997) and temperature (i.e. North America Land Data Assimilation Systems – NLDAS) data in coarse resolution (i.e. 4km) are input to HL-RDHM serving as a rainfall-runoff generator to produce surface and subsurface runoff volumes in the same resolution

2.2.2 Reprocessing runoffs

The runoff from HL-RDHM in coarse resolution (i.e. 1HRAP~4km, 1/2HRAP~2km) needs to be regridded into finer resolution (i.e. 10m) to capture the subcatchment shapes when mapping to the subcatchments. Each subcatchment has a specific hydrograph associated with a given location along the stream at the point nearest to the centroid of the subcatchment and serving as a point source for BreZo. Multiple point sources are then simulated within BreZo to produce flash flood information in appropriate spatial and temporal distributions in the river/channel systems and floodplains.

2.2.3 BreZo simulation and output processing

BreZo is set up with initial conditions (water level or depth, flow velocity) and boundary conditions (free, wall, inflow and outflow). BreZo initial conditons in the channels and overland flood plains can be assigned a uniform condition (i.e. dry condition), using the observed data (water level or depth, flow velocity) or the condition from a warm-up run. BreZo reads the subwatershed runoff hydrographs as pointsource input. The time step for the model run is assigned to a value which allows the global maximum Courant number $Cr \leq 1$ for model stability.

The cross-sections are set at the points of interest to produce discharges. Flooded-area maps and flow velocity maps can be output into Tecplot (vizualization software, http://www.tecplot.com/)

or ArcGIS format. ArcGIS interpolation tools can be used to process the flooded maps and flow velocity maps from triangular mesh into regular grids for spatial evaluation or comparison.

2.3 Method of designing efficient mesh in HiResFlood-UCI

One of the most important parts of implementation of HiResFlood-UCI is the design of efficient high resolution triangular mesh. For a catchment, DEM is downloaded from USGS's National Hydrology Dataset (NHD) at 10 or 30m resolution. ArcGIS was employed to process the watershed delineation for subcatchments, subcatchment centroids, stream networks. Using buffering techniques in ESRI ArcGIS and the software named Triangle (Shewchuk, 1996) the mesh can be created with various resolutions ranging from high resolution (i.e. 10m side in triangle elements) along the river where floods often happen, coarser and coarser (i.e. 30m, 100m, 200m side in triangle elements) far away from the river network. Depending on the users' particular application, the size of the buffer zones may be adjusted to ensure the capture of more or less detail as needed. This is especially relevant for mainstream width considerations. For example, this mesh development has been applied for the Cedar River watershed in Iowa (mainstream width approximately 200m) where buffer size (each side of the stream) of the finest mesh was 100m, and a 25m size was used for the finest mesh buffer for the Upper Little Missouri River watershed (mainstream width approximately 50m). The Triangle refines the triangular mesh based on an area constraint. The term of mesh resolution in the model is the length of a leg in a right isosceles triangle which has the equivalent area in the mesh refinement. The computational cost for modeling depends on the number of elements N_E in the domain and the number of time steps N_T as follows,

$$C \sim kN_E N_T \tag{3}$$

where C is the computational cost, k is a factor depending on the numerical scheme (Kim *et al.*, 2014). The proposed mesh design method allows for modeling the whole basin with a minimized number of elements while areas that are important during a flash flood still have the mesh in high resolution. In comparison with a mesh of uniform resolution the same as the highest resolution in the proposed method, the computational cost can be reduced as follows,

$$\frac{C_P}{C_U} = \frac{N_{E-U}}{N_{E-P}} \tag{4}$$

where C_P, C_U, $N_{E\text{-}P}$, and $N_{E\text{-}U}$ are the computational costs and numbers of elements of the mesh designed by the proposed method and the uniform resolution mesh respectively.

The elevation of each node of the triangular element is interpolated from the DEM using ArcGIS Interpolation Tools. The boundary conditions are assigned to the domain during the mesh creation using Triangle.

Chapter 3. Model calibration

3.1 Calibration for HL-RDHM

HL-RDHM is available with an *a priori* parameter set for the CONUS. The procedure of calibration for HL-RDHM is described in detail in the HL-RDHM User's Manual (NWS, 2011). The objective function used in HL-RHDM is the multi-scale objective function as follows:

$$F = \sqrt{\sum_{k=1}^{n} \left(\frac{\sigma_1}{\sigma_k}\right)^2 \sum_{i=1}^{m_k} \left(q_{0,k,i} - q_{s,k,i}(X)\right)^2} \quad (5)$$

where $q_{o,k,i}$ and $q_{s,k,i}$ are observed and simulated flows averaged over time interval k. σ_k is the standard deviation of the observed discharge, n is the total number of scales used, and m_k is a number of ordinates at the scale k.

Calibration of lumped hydrologic models is challenging (Sorooshian and Gupta, 1983; Duan *et al.*, 1992; Sorooshian, *et al.* 1993), distributed hydrologic models have an even more complicated calibration process. Global optimization techniques such as Shuffled Complex Evolution – University of Arizona (SCE-UA by Duan *et al.*, 1992) have been employed successfully in calibration for lumped hydrologic models. However, these techniques generally require a large number of iterations and this may lead to difficulty in application for calibration for distributed hydrologic models. Moreover, global optimization may not transfer well the complexity of the spatial patterns of the pedologic and physiographical characteristics of a large domain into the distributed parameter grids (NWS, 2011). HL-RDHM has a built-in local search technique named Stepwise Line Search (SLS, Kuzmin *et al.*, 2008) which provides a limited optimization based on *a priori* parameters.

HL-RHDM is flexible for users to choose manual or auto automatic calibration mode for a certain number of the parameters in SAC-SMA and routing components. Fig. 3-1 shows the calibration process for SAC-SMA component in HL-RHDM. On one hand, distributed *a priori* parameters of SAC-SMA for a basin are derived from soil texture, hydrologic soil group and land cover/use (Koren *et al.*, 2003). On the other hand, the model is calibrated in lumped or semi-lumped mode to obtain the area average parameters. The *a priori* parameters are rescaled using the area lumped parameters. SLS is used to search for a set of uniform scale factors that result in the best match of the simulated discharge with the observed hydrograph at the basin outlet.

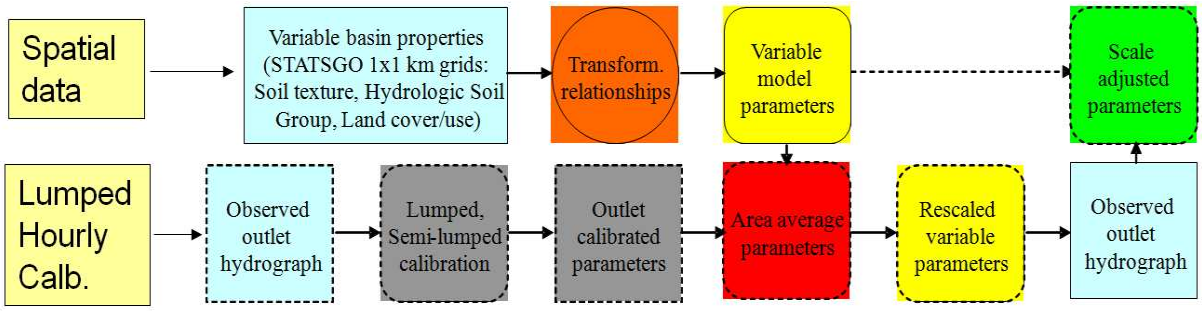

Fig. 3-1. Schematic diagram of SAC-SMA parameter calibration process (Smith *et al.*, 2006)

Fig. 3-2 shows the calibration process for the channel routing parameters in HL-RDHM. A similar process to the calibration method used in SAC-SMA is applied to the channel routing calibration. Channel routing parameters at the basin outlet can be derived from the measured data including discharge, top width and cross-section. The spatially variable basin properties including slope, area, and drainage density are used to calculate the variable channel routing parameters. SLS technique is applied to find the uniform rescale factor set for the simulated discharge best fitting the observed hydrograph at the basin outlet.

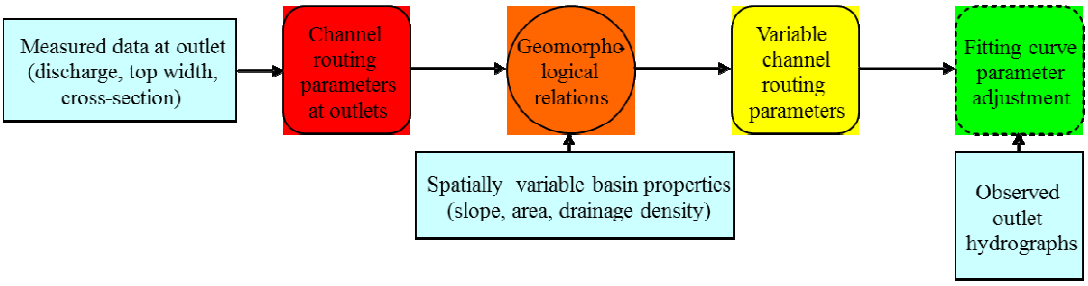

Fig. 3-2. Schematic diagram of channel routing parameter calibration process (Smith *et al.*, 2006)

3.2 Calibration for BreZo

HL-RDHM and BreZo in the coupled HiResFlood-UCI can be calibrated separately. At the current development, BreZo component is manually calibrated by tuning the Manning *n* roughness values to best fit the hydrograph at the catchment outlet. A new procedure is under development for automatic calibration for BreZo using SCE-UA algorithm (Duan *et al.*, 1992). For flood simulation purposes, optimal Nash-Sutcliffe efficiency (NSE) is used as the objective function in calibration process for BreZo component.

---

where n is the total number of observations, q_o is the observed discharge (m^3/s), and q_s is the simulated discharge (m^3/s) for each time step t.

For areas where there are no stream gauge observation data, an *a priori* parameter set is used for HL-RDHM and Manning *n* roughness values are chosen from Chow's look-up table (Chow, 1959) based on the catchment characteristics.

Chapter 4. Statistical metrics

4.1 Point comparison

The model was validated across the time periods of extreme flood events (excluding the time of calibration process) using three metrics: Root Mean Square Error (RMSE), BIAS and Nash-Sutcliffe efficiency (NSE).

$$\mathrm{RMSE} = \sqrt{\frac{1}{n}\sum_{t=1}^{n}\left(q_o(t) - q_s(t)\right)^2} \quad (7)$$

where n is the total number of observations, q_o is the observed discharge (m^3/s), and q_s is the simulated discharge (m^3/s) for each time step t.

BIAS indicates the tendency of the simulated flows in comparison with gauge observations. A BIAS of 0 is optimal. Positive values indicate an overestimation while negative values indicate a tendency to underestimate.

$$\mathrm{BIAS} = \frac{\sum_{t=1}^{n}(q_s(t) - q_o(t))}{\sum_{t=1}^{n} q_o(t)} \quad (8)$$

CORR is the most commonly used measure for evaluating the goodness of fit of two hydrographs (McCuen & Snyder, 1975). CORR ranges from -1 (negatively correlated) to 1 (correlated). The ideal value of CORR is 1 and CORR of 0 indicates no correlation between the hydrographs.

$$\mathrm{CORR} = \frac{\sum_{t=1}^{n}(q_0(t) - \bar{q}_0)\sum_{t=1}^{n}(q_s(t) - \bar{q}_s)}{\sqrt{\sum_{t=1}^{n}(q_0(t) - \bar{q}_0)^2}\sqrt{\sum_{t=1}^{n}(q_s(t) - \bar{q}_s)^2}} \quad (9)$$

NSE is used to assess the predictive power of the model. The ideal value of NSE is 1. Negative NSE values indicate that the mean of observations is a better predictor than the model.

4.2 Spatial comparison

The unique advancement of the model is its capability to produce the spatio-temporal distribution of water flow in the channel/river network as well as in the flood plains in high resolution. The spatial outputs (flooded-area maps, flow velocity) from the model in an unstructured triangular cell mesh were regridded into regular grid of 10m x 10m for comparison. Three main metrics (probability of detection - POD, false-alarm ratio - FAR, and critical success index - CSI) were used with three statistics: hits (having flood in both simulation and observation), misses (flood in observation but not in simulation) and false alarms (flood in simulation but not in observation). For these spatio-temporal experiments, no areal observations are available. With that, they are used only for the sensitivity tests, taking the baseline run (see description of baseline run in Table 4-1) as the "observation".

Table 4-1. Contingency table used in flooded map validation

		AWiFS image	
		Flooded	Not flooded
Predicted by HiResFlood-UCI	Flooded	Hit	False alarm
	Not flooded	Miss	-

POD indicates the fraction of observed floods (from aerial images) that were correctly simulated. POD ranges from 0 to 1. POD of 1 means that floods were correctly simulated; 0 means no flooding detected by the model.

$$\mathrm{POD} = \frac{\mathrm{hits}}{\mathrm{hits} + \mathrm{misses}} \tag{10}$$

FAR measures the fraction of simulated flooding that was not associated with observation. Similar to POD, FAR of 1 indicates that all floods were not associated with observation, FAR of 0 indicates that no simulated floods found in observation.

$$\mathrm{FAR} = \frac{\mathrm{false\ alarms}}{\mathrm{hits} + \mathrm{false\ alarms}} \tag{11}$$

CSI measures the skill of the system ranging from 0 meaning no skill to 1 meaning perfect skill:

$$\mathrm{CSI} = \frac{\mathrm{hits}}{\mathrm{hits} + \mathrm{misses} + \mathrm{false\ alarms}} \tag{12}$$

Chapter 5. Testing HiResFlood-UCI with synthetic precipitation

5.1 Research domain

Baron Fork at Eldon, Oklahoma (NWS forecast point ELDO2, Fig. 5-1) was chosen as the study area because it can be seen as a flashy catchment and data is available from the Distributed Model Intercomparison Project – Phase 2 (DMIP2, Smith *et al*., 2012a&b). ELDO2 is an 808km^2 catchment of the Baron Fork River on the border of Oklahoma and Arkansas. The USGS stream gauge 07197000 (latitude 35°55'16", longitude 94°50'18") is located at Eldon, Oklahoma. The USGS stream gauge 07196900 (latitude 35°52'48", longitude 94°29'11") is located at Dutch Mills, Arkansas, covering a drainage area of 105km^2. ELDO2 is a natural watershed which has limited manmade raised linear features such as levees, roadways, and railways.

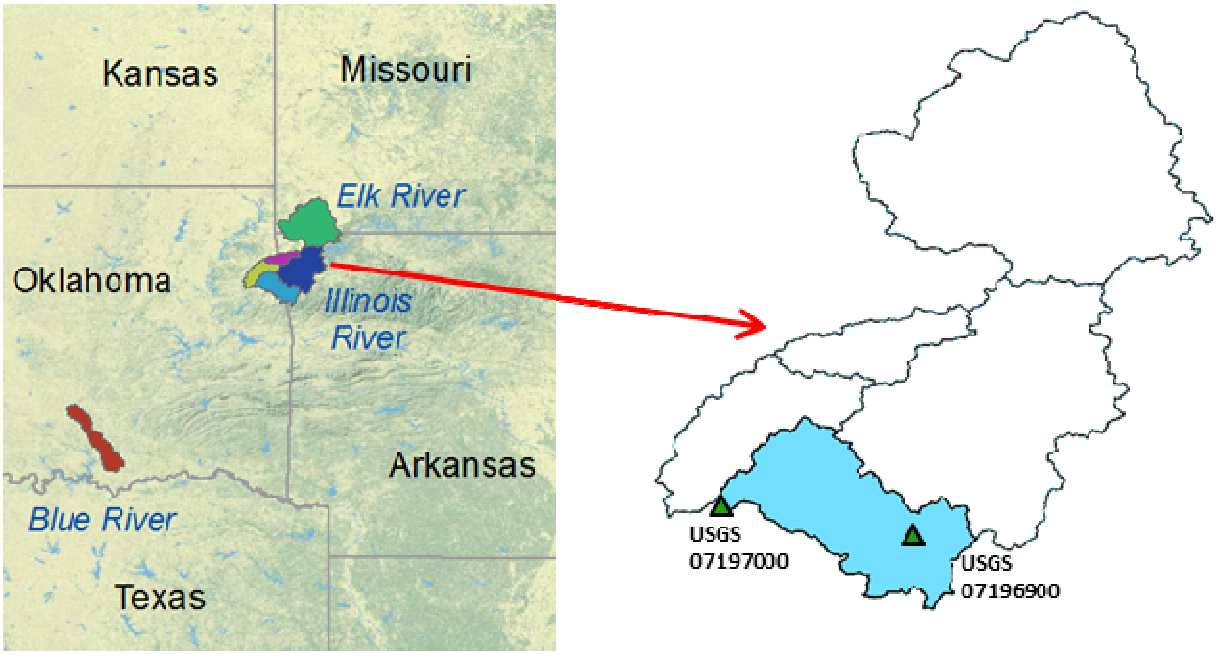

Fig. 5-1. Research area: ELDO2 catchment in DMIP2 experiment

5.2 Data collection

Topographic data is crucially important in flood modeling (Sanders, 2007). The digital elevation model (DEM) data at 10m (1/3 second) and 30m (1 second) resolution based on the national elevation data (NED) was downloaded from USGS's National Hydrography Dataset (NHD, http://viewer.nationalmap.gov/viewer/nhd.html?p=nhd). The 10m and 30m DEMs have vertical accuracies of ±1.55 m and ±2.44 m root mean square error (RMSE) respectively (Gesch *et al.*, 2014).

The DMIP2 project (http://www.nws.noaa.gov/oh/hrl/dmip/2/data_link.html) offers projection and boundary shape files to extract ELDO2 catchment.

5.3 Model implementation

5.3.1 Set up HL-RDHM component

HL-RDHM version 3.2.0 was set up for the ELDO2 catchment. Distributed *a priori* parameter values of SAC-SMA model and Routpix9 routing technique were adjusted by a set of calibrated coefficients provided by NWS. The model was set at 1 HRAP resolution and an hourly time step to produce time-series at basin outlet and interior point discharges, and gridded surface flow.

5.3.2 Set up BreZo component

A new framework was proposed to design an efficient mesh for BreZo which allows for modelling large domains. First, ELDO2 was extracted from the DEM map of Illinois River basins (Fig. 5-2). ESRI ArcGIS terrain processing tools were used for watershed delineation to derive the stream network and 119 sub-catchments. Subcatchment centroids were created and then snapped into the nearest stream serving as the subcatchment hydrograph point sources (Fig. 5-3).

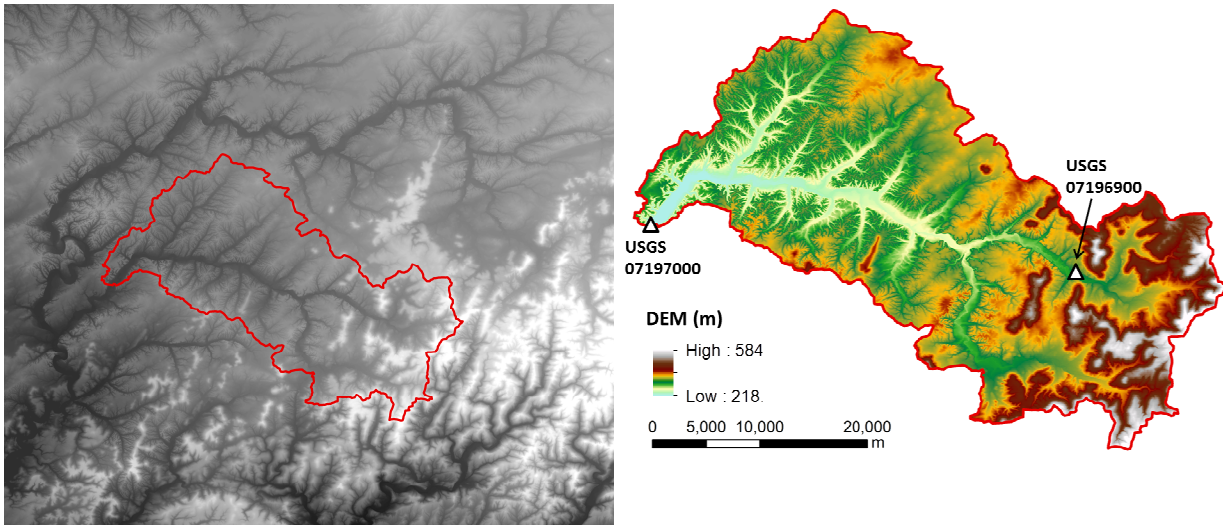

Fig. 5-2. DEM of ELDO2 extracted from USGS NHD database

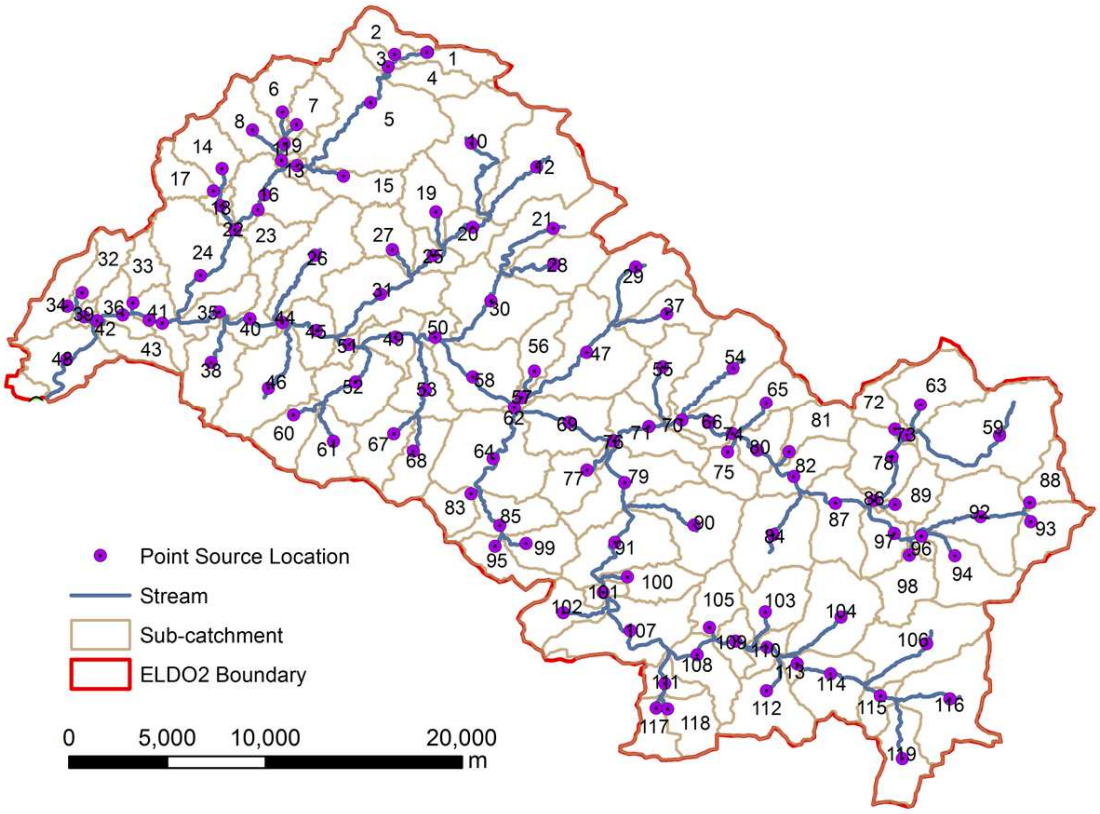

Fig. 5-3. Subcatchments, Stream network and Point sources of ELDO2

Rather than having a uniform high resolution mesh for the entire basin, the proposed procedure enables the design of an unstructured triangular mesh with various resolutions. Areas along the river network are more important in flash flood simulation than those far away from the river. Four zones based on the distance from the stream were created using buffering tools in ArcGIS (Table 5-1 and Fig. 5-4). Two meshes were created in this experiment. The first mesh (Case 1) has the highest resolution of 10 m while the other (Case 2) was designed with the highest resolution of 30m.

Table 5-1. Mesh resolution related to the distance from the river

Buffer zone	Distance from river (m)	Mesh resolution			
		Case 1		Case 2	
		Size (m)	**Area** (m^2)	**Size** (m)	**Area** (m^2)
1	25	10	50	30	450
2	100	30	450	50	1,250
3	500	100	5,000	100	5,000
4	5,000	200	20,000	200	20,000

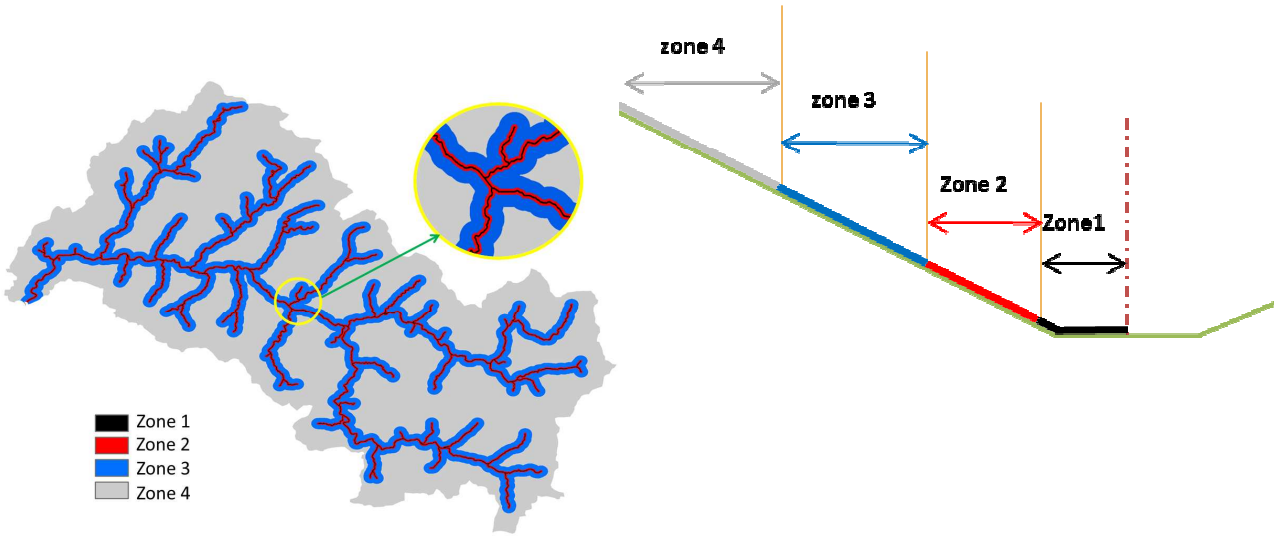

Fig. 5-4. Mesh design of ELDO2 catchment for BreZo: 4 zones with various resolutions (Table 5-1)

ArcGIS interpolation tools and the Triangle software (Shewchuk, 1996) were used with the refinement option based on cell areas to create the final mesh (Fig. 5-5).

In terms of an efficient mesh, the final 10m+ resolution mesh (Case 1) has 802,405 elements and is significantly more efficient compared to the mesh of 25,589,112 elements designed with a uniform 10m resolution. This leads to an approximately 32-fold reduction in computational time.

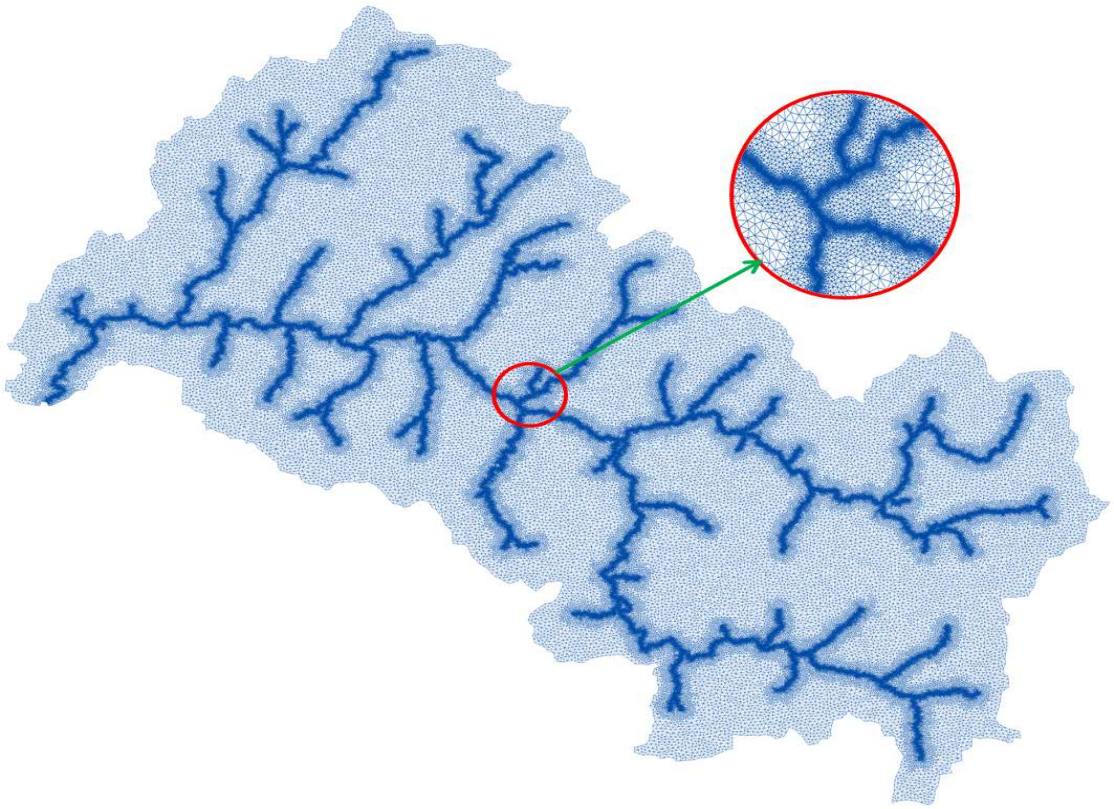

Fig. 5-5. Final unstructured triangular cell mesh of ELDO2 for BreZo in Case 1 (Table 5-1)

5.4 Scenario description

This experiment used a uniform synthetic rainfall input of 2 continuous hours of 87.38 mm/hr created from the partial duration series (PDS)-based precipitation frequency estimates with 90% confidence intervals for 2 hours, 1% probability at USGS 7197000.

The precipitation was uniformly distributed over the entire catchment in an attempt to negate effects that natural, distributed precipitation will have on discharge, particularly on the timing of events. The main purpose of using synthetic data in this experiment is to capture the impact of changing certain model elements such as channel and floodplain roughness (Manning *n*), DEM resolution, mesh resolution, and calibration of the hydrologic model. Table 5-2 highlights the various model runs that were used to explore model response to changes in the aforementioned

model components. The baseline run employs the average Manning *n* value for the channel and floodplain as provided by Chow (1959), uses the calibrated hydrologic model parameters as provided by the NWS, a 10m DEM, and a mesh resolution with the finest grids near the river at a 10m resolution.

Table 5-2. Scenario description: Testing HiResFlood-UCI with Manning *n* values (Runs 1-6), HL-RDHM *a priori* parameters (Run 7), DEM 30m resolution (Run 8) and mesh 30m+ resolution (Run 9)

Scenario	Manning value – Channel	Manning value – Floodplain	HL-RDHM parameter	DEM resolution	Mesh resolution
Baseline	0.0925	0.0975	Calibrated	10m	Case 1 (10m+)
Run1	0.0350	0.0350	Calibrated	10m	Case 1 (10m+)
Run2	0.0638	0.0663	Calibrated	10m	Case 1 (10m+)
Run3	0.1213	0.1288	Calibrated	10m	Case 1 (10m+)
Run4	0.0350	0.1600	Calibrated	10m	Case 1 (10m+)
Run5	0.1500	0.0350	Calibrated	10m	Case 1 (10m+)
Run6	0.1500	0.1600	Calibrated	10m	Case 1 (10m+)
Run7	0.0925	0.0975	*a priori*	10m	Case 1 (10m+)
Run8	0.0925	0.0975	Calibrated	30m	Case 1 (10m+)
Run9	0.0925	0.0975	Calibrated	10m	Case 2 (30m+)

Significant attention was given to the evaluation of roughness parameter choice because of the potential tradeoffs of having different floodplain and channel roughness. Runs 1-6 explore combinations of high and low parameter values in both the channel and the floodplain in an effort to examine the entire spectrum of possible outcomes that may result from a possibly uninform roughness choice.

Run 7 addresses the outcome of using the *a priori* parameter grids for HL-RDHM (based on soil surveys) rather than calibrated grids. This is a realistic scenario in that some basins may not have a stream gauge at the outlet to allow for calibration of the hydrologic model. Run 8 explores the outcome of using a 30m DEM grid as the base for generating the mesh, which is currently the finest resolution available in many parts of world. Run 9 investigates the use of a slightly coarser mesh with the finest grids at 30m. It should be noted that although the option to consider even coarser mesh resolution exists, the main intent of this work to provide high resolution flood information begins to deteriorate with a mesh coarser than 30m.

5.5 Results

One major innovation of HiResFlood-UCI is the capability to generate and display distributed high resolution flow information for an entire basin. Fig. 5-6 shows the resulting map of maximum flow depth for the baseline simulation using synthetic precipitation as input. Similarly, Fig. 5-7 shows the maximum flow velocity for the baseline run.

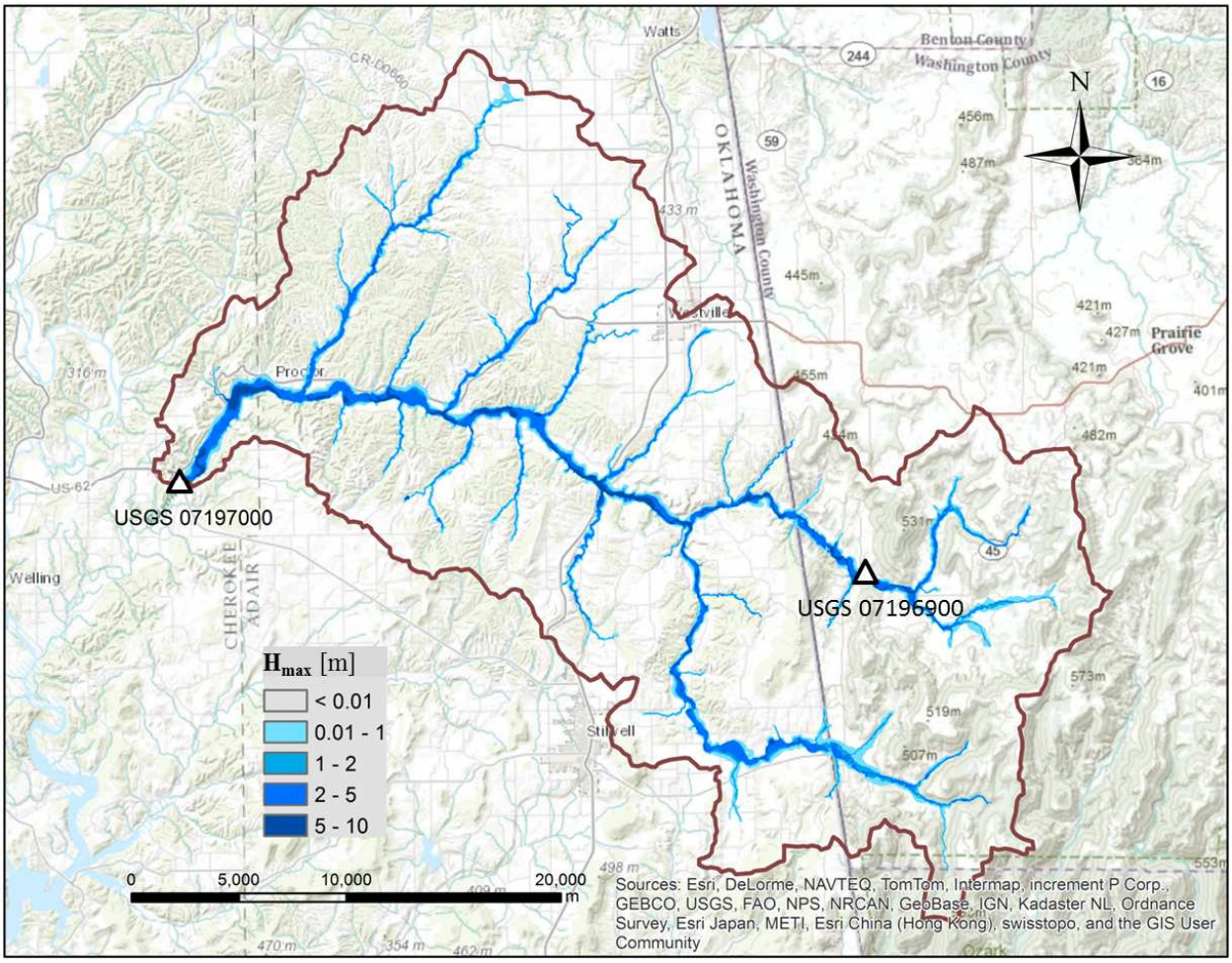

Fig. 5-6. Flooded map in Baseline scenario. H_{max} is the maximum water depth in the simulation

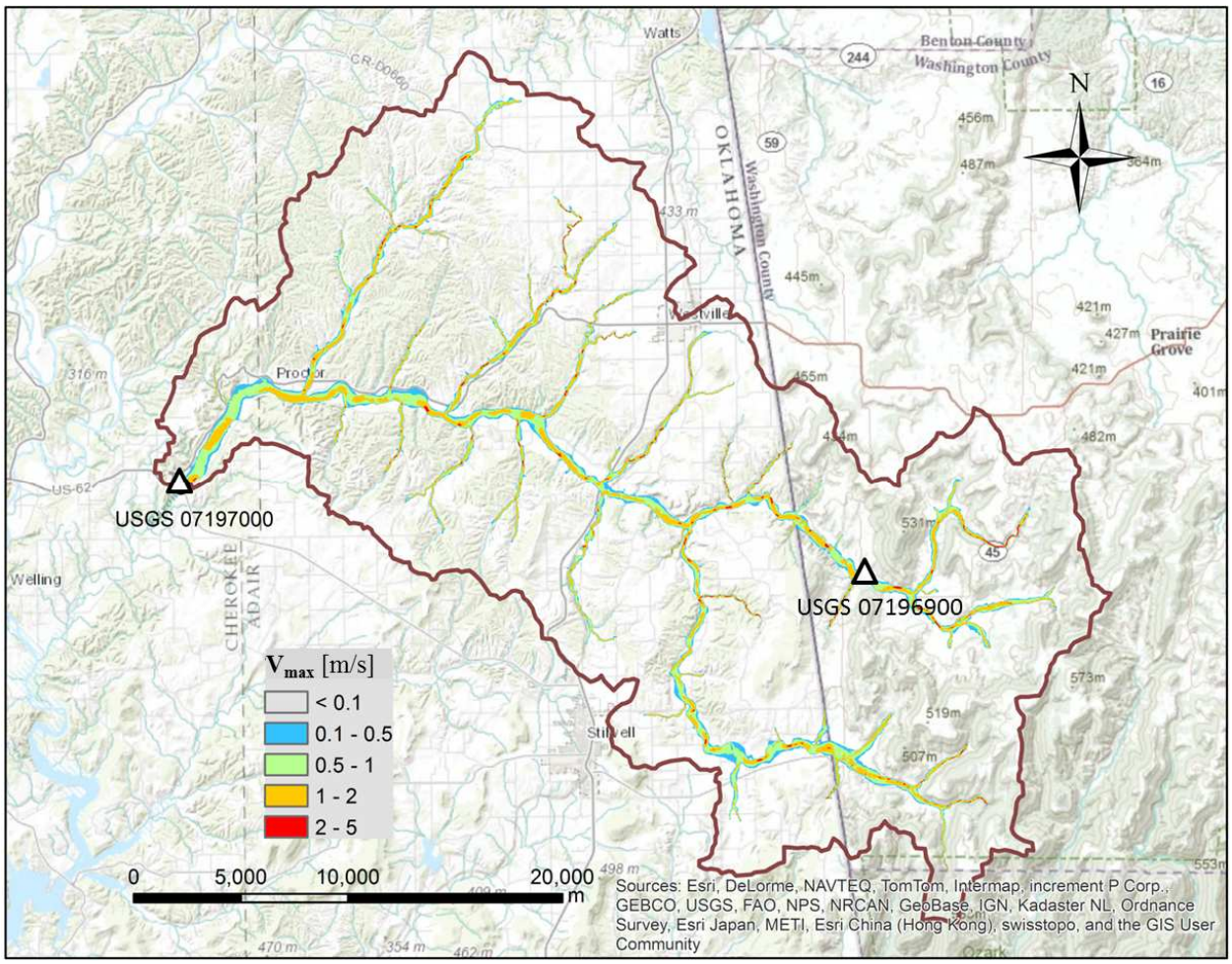

Fig. 5-7. Flow velocity in Baseline scenario (see description of Baseline scenario in Table 5-2)

5.5.1. Testing HiResFlood-UCI with HL-RDHM a priori parameters

When the hydrologic model is run using *a priori* parameter grids as opposed to those calibrated for the DMIP2 experiment, the overall impact on basin discharge is minimal in the synthetic precipitation experiment (Fig. 5-8 and Table 5-3). Peak timing is unchanged and only a slight reduction of the first major peak and a slight increase of the secondary peak are noticeable. Additionally, the tail of the recession limb becomes slightly fatter compared to that of the baseline run. Although anecdotal, the low sensitivity of the coupled model system to using *a priori* parameter grids for the hydrologic model rather than calibrated grids is encouraging. There are some cases where basins are ungauged, and calibration of the hydrologic model

component using discharge observations is impossible. The results show that, for at least this basin, the inability to further calibrate the *a priori* parameter grids does not significantly depreciate the overall quality of the coupled system

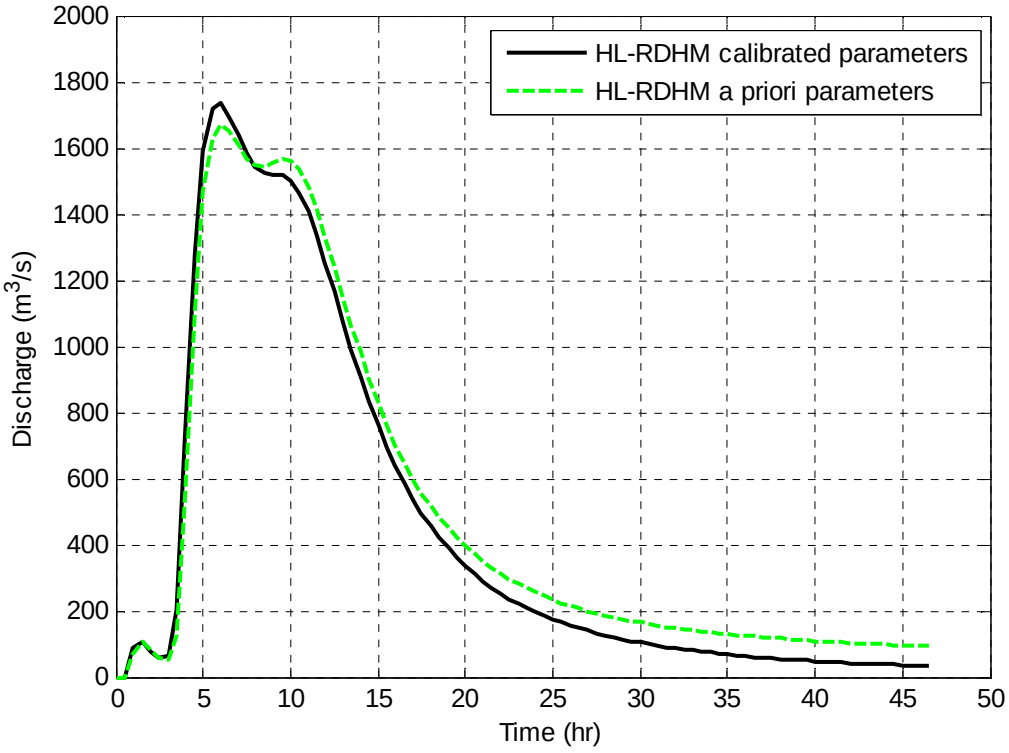

Fig. 5-8. HiResFlood-UCI with HL-RDHM *a priori* parameters

Table 5-3. Testing HiResFlood-UCI with HL-RDHM *a priori* parameters (Run7, see scenario description in Table 5-2)

Scenario	H_{max} (m)	V_{max} (m/s)	Peak Flow (m^3/s)	RMSE (m^3/s)	BIAS -	NSE -	CSI -	POD -	FAR -
Baseline	10.25	5.69	1733.47	-	-	-	-	-	-
Run7	10.34	5.46	1670.70	65.13	0.09	0.99	0.99	1.00	0.01

5.5.2 Hydraulic roughness parameter sensitivity

The outcomes of the hydraulic roughness parameter sensitivity tests for the synthetic precipitation experiment point to the importance of careful identification of the roughness parameter in both the channel and floodplain (Fig. 5-9 and Table 5-4). This is particularly evident through the evaluation of runs 4 and 5 (minimum channel roughness, maximum floodplain roughness and vice versa respectively) – see Table 5-2. While the effect of changing the roughness parameters is more substantial in run 5, both runs had the same outcome of an increasing peak, an earlier timing of the peak, and a steepening of the recession limb. This suggests that neither parameter significantly dominates the other, thus accurate characterization of both is important. Not surprising are the hydrographs resulting from runs 1 and 6. Run 1 utilizes the smallest Manning *n* for both the channel and floodplain and intuitively features a hydrograph with a sharp peak and a quickly descending recession limb. Accordingly, run 6 shows the opposite with the smallest, most drawn-out peak of all runs as it uses the highest roughness parameters.

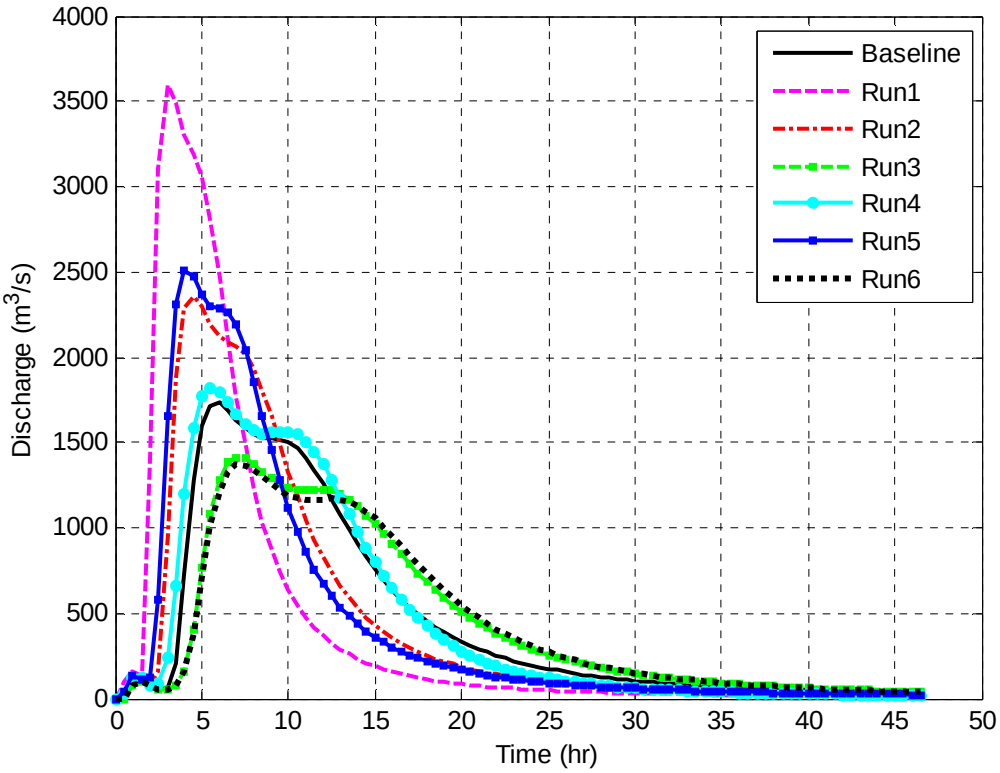

Fig. 5-9. Testing Roughness parameter for Runs 1-6 listed in Table 5-2

Table 5-4. Testing hydraulic roughness sensitivity (see Scenario description in Table 5-2)

Scenario	H_{max} (m)	V_{max} (m/s)	Peak Flow (m^3/s)	RMSE (m^3/s)	BIAS -	NSE -	CSI -	POD -	FAR -
Baseline	10.25	5.69	1733.47	-	-	-	-	-	-
Run1	10.26	9.04	3593.42	793.04	0.026	-1.09	0.90	0.90	0.00
Run2	10.19	6.93	2362.20	341.73	0.013	0.61	0.96	0.96	0.00
Run3	10.44	4.22	1414.13	203.55	-0.004	0.86	0.98	1.00	0.02

Run4	10.64	9.04	1822.03	92.07	0.021	0.97	0.94	0.95	0.01
Run5	10.39	6.02	2504.80	435.10	0.011	0.37	0.96	0.96	0.00
Run6	10.59	5.69	1368.55	225.04	-0.004	0.83	0.98	1.00	0.02

5.5.3 Testing HiResFlood-UCI with DEM 30m resolution and Mesh 30m+ resolution

Of the three sensitivity tests investigated other than the Manning's *n* roughness sensitivity, the one that had the most negative impact on the resulting area-based statistics was increasing the DEM resolution from 10m to 30m. This decrease in quality of flood extent-based metrics is intuitive for an increase in DEM resolution as the hydraulic model relies heavily on topography to govern flood dynamics. While this scenario suffered the worst area-based statistics compared to the other sensitivity tests, the quality reduction was not so severe that it would warrant not using the coupled system if only a 30m were available. The point-based outlet statistics suggest the same, as the NSE remains near 1 and the bias is the lowest compared to the other two non-roughness sensitivity runs.

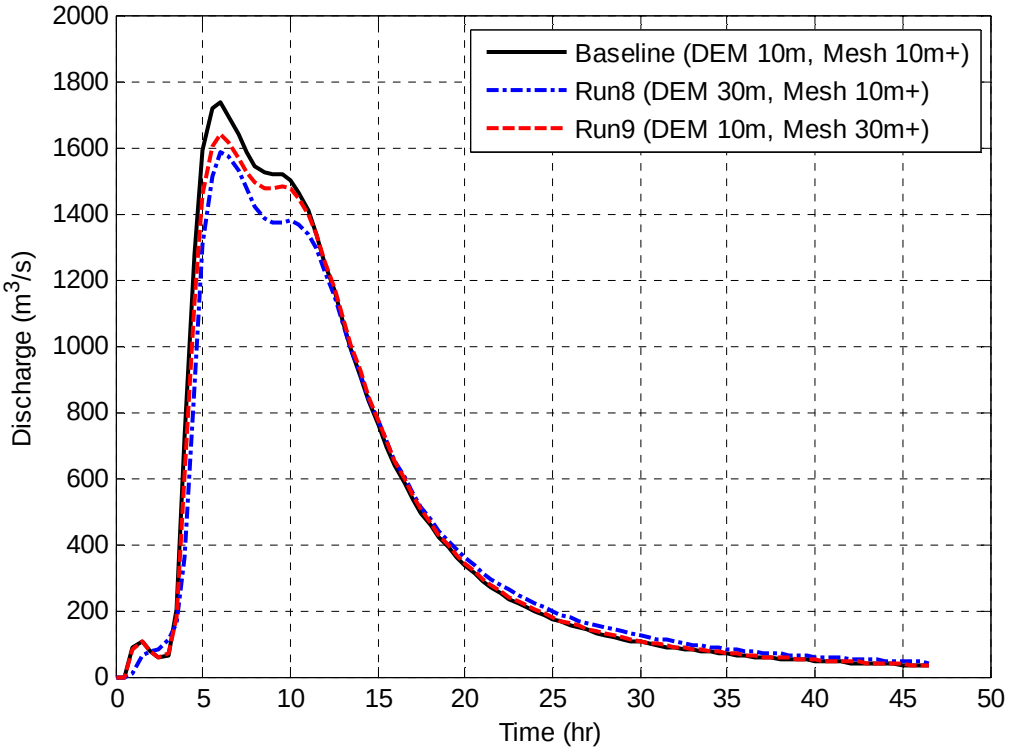

Fig. 5-10. Testing HiResFlood-UCI with DEM 30m resolution and Mesh 30m+ resolution

Table 5-5. Testing HiResFlood-UCI with DEM 30m resolution (Run8) and mesh 30m+ resolution (Run9, see scenario description in Table 5-2)

Scenario	**H_{max}**	**V_{max}**	**Peak Flow**	**RMSE**	**BIAS**	**NSE**	**CSI**	**POD**	**FAR**
	(m)	(m/s)	(m^3/s)	(m^3/s)	-	-	-	-	-
Baseline	10.25	5.69	1733.47	-	-	-	-	-	-
Run8	12.43	6.09	1583.30	81.23	-0.04	0.98	0.71	0.85	0.18
Run9	10.07	6.65	1636.67	33.08	-0.02	1.00	0.84	0.99	0.16

The mesh resolution sensitivity test suggests there is little change compared to the baseline scenario, especially in terms of outlet statistics, when the mesh resolution was increased from

10m+ to 30m+ (Fig. 5-10 and Table 5-5). Not surprisingly, POD is slightly lower than 1 and FAR is slightly higher than 0. It is unreasonable to expect a coarser mesh to perfectly capture the details of a finer mesh. However, the differences are quite small for this synthetic study, and when modeling very large basins, it may be necessary to use a 30m+ mesh rather than a 10m+ mesh to save computational expenses. This aspect of the sensitivity analysis suggests that a 30m+ mesh would not be unreasonable for use, particularly in very large basins.

5.6 Conclusions

Using synthetic precipitation input, the model was tested for various components including HL-RDHM parameters (*a priori* versus calibrated), channel and floodplain Manning *n* values, DEM resolution (10m versus 30m) and computation mesh resolution (10m+ versus 30m+). Simulations with calibrated versus *a priori* parameters of HL-RDHM show that HiResFlood-UCI produces reasonable results with the *a priori* parameters from NWS. Sensitivities to hydraulic model resistance parameters, mesh resolution and DEM resolution are also identified, pointing to the importance of model calibration and validation for accurate prediction of localized flood intensities. From Figs. 5-8 -5-10, it can be concluded that the model is more sensitive to Manning *n* values than to the other parameters.

Chapter 6. Validating HiResFlood-UCI using streamflow observation with NEXRAD Stage 4 precipitation data

6.1 Research domain and data collection

The research domain in this experiment is ELDO2, described in details in Chapter 5. Hourly 4km NEXRAD radar rainfall data from 1995 to 2001 over the basin was from DMIP2. The National Centers for Environmental Prediction/Environmental Modeling Center (NCEP/EMC) hourly 4km Stage IV rainfall data from 2002 to 2011 for the entire CONUS was downloaded from the National Center for Atmospheric Research (NCAR) website (http://data.eol.ucar.edu/codiac/dss). The temperature data in this experiment is from the North America Land Data Assimilation System (NLDAS, http://ldas.gsfc.nasa.gov/nldas).

Hourly streamflow data from 2000 to 2011 at the U.S. Geological Survey (USGS) stream gauge 07197000 was retrieved from USGS's National Water Information System (NWIS, http://nwis.waterdata.usgs.gov/nwis/) for calibrating and validation based on the streamflow at the watershed outlet. The 15-minute streamflow and gauge height data at USGS 07196900 (available from 2007) was downloaded from NWIS for validating the predicted streamflow and flood stage at the interior point of the watershed.

6.2 Model implementation

The HiResFlood-UCI model was implemented for 6 real flooding events in the ELDO2 basin. These events were selected based on the highest observed streamflow for which precipitation data were concurrently available. The flooding event in June of 2000 was selected as a calibration run, and 5 additional events (April 2004, March 2008, April 2008, October 2009, and April 2011) were run as validation events. Fig. 6-1 highlights the total precipitation distribution

of each of these events as they appear on the HRAP grid. The selected precipitation events represent a range of possible storm types, allowing for insight into how the model responds to given different scenarios. March 2008 and April 2008 represent lighter but longer storms, whereas June 2000 and April 2011 have much more intense and generally shorter storms. Additionally, some storms are multimodal (April 2004 and April 2011), while the others represent more continuous events. The hyetographs in Fig. 6-1 depict the various storm events.

BreZo component was initialized for each event with a warm-up run that provides a low flow discharge similar to the observed discharge at the watershed's outlet and at the beginning of the simulation. These events were also simulated using the NWS standard HL-RDHM with its native routing scheme rather than BreZo. This is an important investigation to make certain that the additional information gained from using HiResFlood-UCI such as flow velocity, depth, and areal flood extent, are not at the expense of the quality point discharge information that HL-RDHM already provides.

Manual calibration of the Manning *n* values was conducted for the floodplain and river channel. Calibration efforts were based on optimizing NSE for the outlet hydrograph. The flood event from June 21-23, 2000 was used as the calibration period. This resulted in a channel roughness value of $n1$=0.07 and a floodplain roughness of $n2$=0.10, and yielded a NSE of 0.90. These roughness parameter values were subsequently used in the remaining five validation flood events.

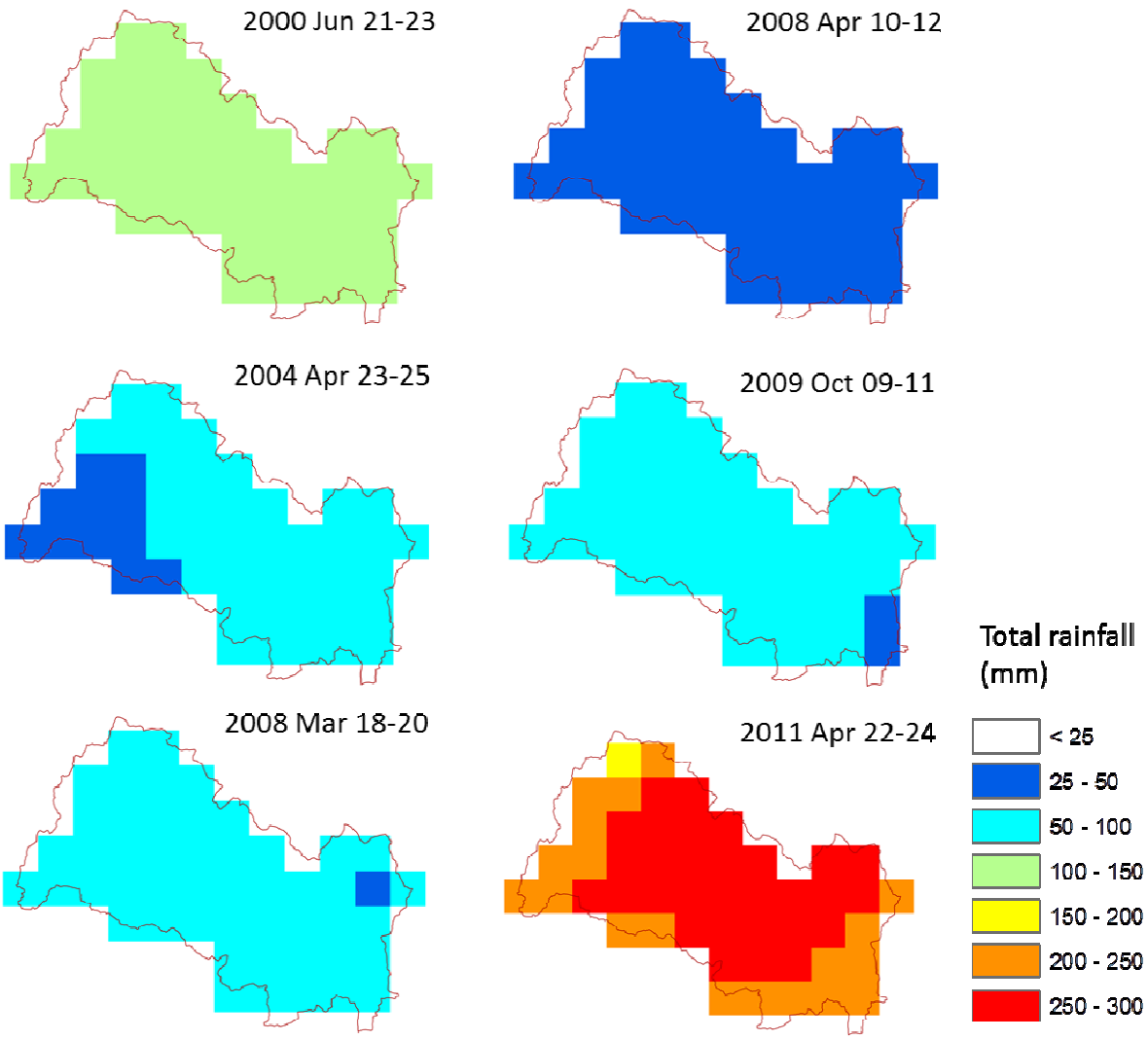

Fig. 6-1. Total Rainfall (mm) of extreme events in ELDO2 from 2000 to 2011

6.3 Results and discussion

6.3.1 Discharge at the watershed outlet

The simulated hydrographs from the two models at the outlet for the 6 case studies are compared with each other and with the gauge observations (Figs. 6-2 - 6-7). The results show that in terms of simulating the flood magnitudes, HiResFlood-UCI performs comparable to HL-RDHM but neither shows dominance in comparison to gauge observations. In terms of simulating peak

timing the maximum difference is about 2 hours, but no systematic tendency is detected. In terms of the timing difference of the two models with observation, the maximum was around 3 hours and again, no special trend was evident. Table 6-1 summarizes the statistics of the case studies for both models with the USGS gauge at the ELDO2 outlet serving as the "true" observation. In all of the selected cases, the statistics for HL-RDHM are quite similar to those of HiResFlood-UCI, and no one model decisively dominates the other. This is an encouraging result as HiResFlood-UCI is able to provide additional information, particularly spatially distributed high resolution flow depth and velocity, while at the same time not sacrificing the quality outlet flow information that HL-RDHM was designed to generate.

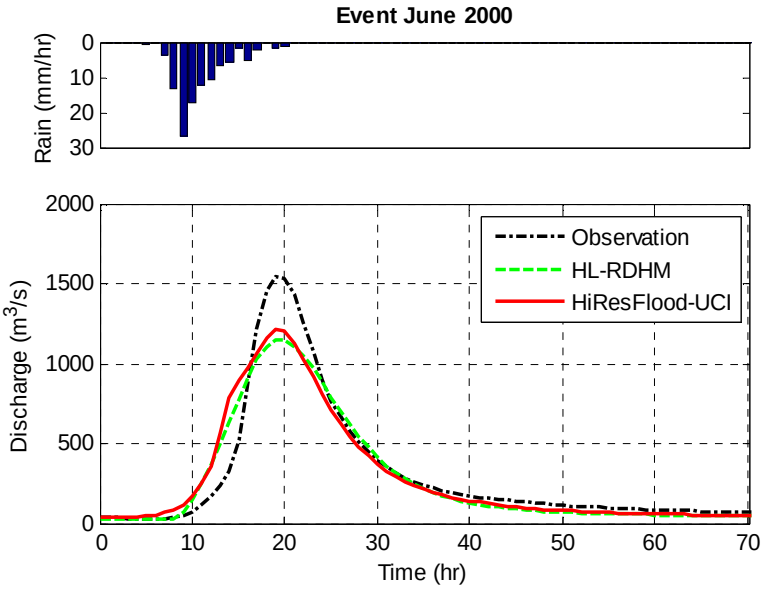

Fig. 6-2. Simulation results at watershed outlet

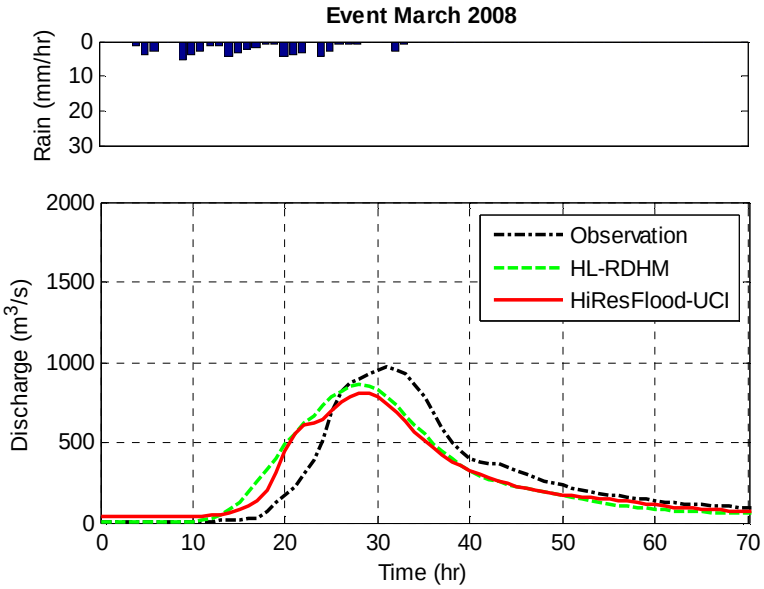

Fig. 6-3. Simulation results at watershed outlet

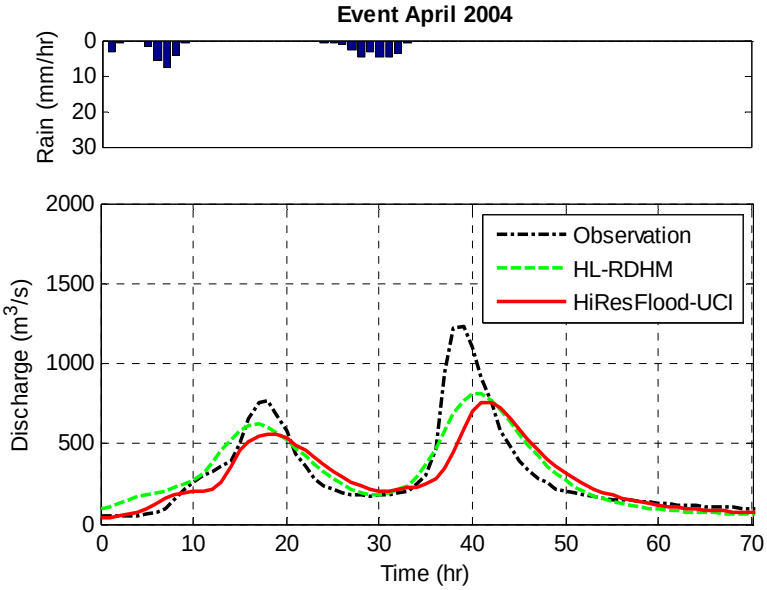

Fig. 6-4. Simulation results at watershed outlet

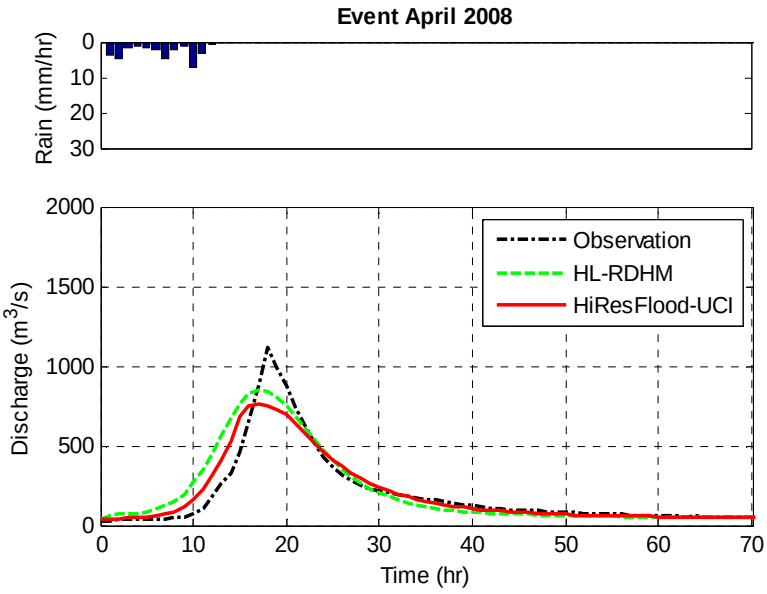

Fig. 6-5. Simulation results at watershed outlet

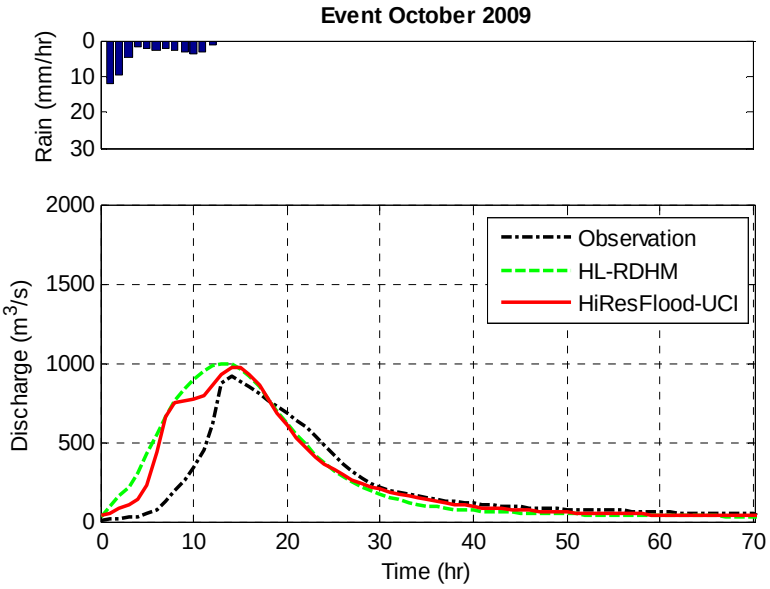

Fig. 6-6. Simulation results at watershed outlet

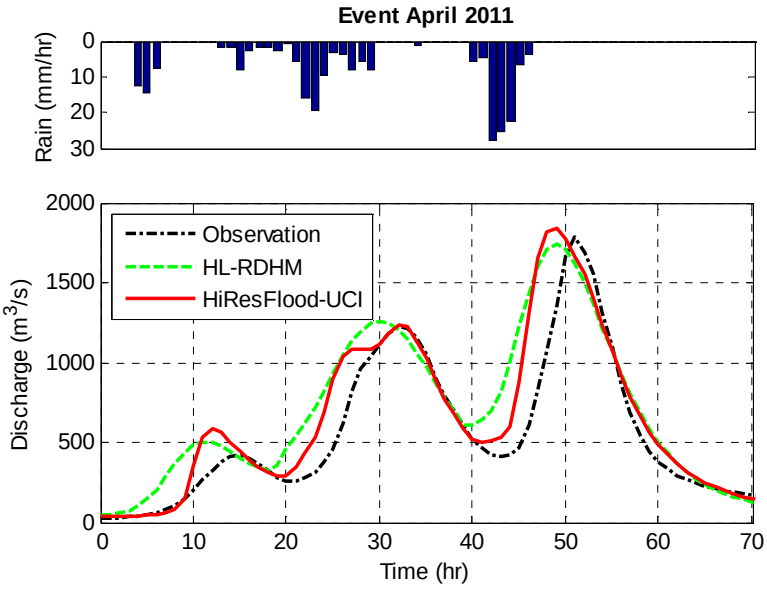

Fig. 6-7. Simulation results at watershed outlet

Table 6-1. Statistics of event simulations at watershed outlet. The event in June 2000 was used for model validation

Event	Observation/ Simulation	Peak flow (m^3/s)	Peak flow error (%)	Phase error (hr)	RMSE (m^3/s)	BIAS -	NSE -
June 2000	USGS Observation	1548.90	-	-	-	-	-
	HL-RDHM	1144.30	-26.12	1	116.76	-0.09	0.91
	HiResFlood-UCI	1200.00	-22.53	0	123.03	-0.06	0.90
April 2004	USGS Observation	1234.60	-	-	-	-	-
	HL-RDHM	808.40	-34.52	-1	124.99	0.04	0.80
	HiResFlood-UCI	756.27	-38.74	-3	170.27	-0.07	0.63
March 2008	USGS Observation	971.27	-	-	-	-	-
	HL-RDHM	862.79	-11.17	-3	129.58	-0.06	0.80
	HiResFlood-UCI	813.00	-16.30	-3	121.49	-0.08	0.83
April 2008	USGS Observation	1121.30	-	-	-	-	-
	HL-RDHM	851.63	-24.05	-1	100.87	0.07	0.83
	HiResFlood-UCI	762.00	-32.04	-1	80.47	-0.04	0.89

October 2009	USGS Observation	911.80	-	-	-	-	-
	HL-RDHM	996.37	9.28	-1	179.10	0.17	0.51
	HiResFlood-UCI	976.00	7.04	1	146.04	0.14	0.67
April 2011	USGS Observation	1781.10	-	-	-	-	-
	HL-RDHM	1740.10	-2.30	-2	260.11	0.25	0.67
	HiResFlood-UCI	1840.00	3.31	-2	208.97	0.17	0.78

6.3.2 Discharge at interior point

Since the USGS stream gauge 07196900 at Dutch Mills was installed in 2007 as part of DMIP2 project, the observed streamflow is available for validation at the interior point for only 4 events in March and April 2008, October 2009 and April 2011. Figs. 6-8 – 6-11 and Table 6-2 show the simulation discharges of the four events at the interior point. Similarly to the HL-RDHM Rupix9 routing technique, HiResFlood-UCI well captured the hydrographs at the interior point during the events (NSE ranges from 0.89 to 0.97). The predicted flood peak times by HiResFlood-UCI are very accurate, within 1 hour. The results suggest that HiResFlood-UCI is capable of preserving the advantage of the distributed hydrologic model HL-RDHM in simulating streamflow at interior points of the watershed.

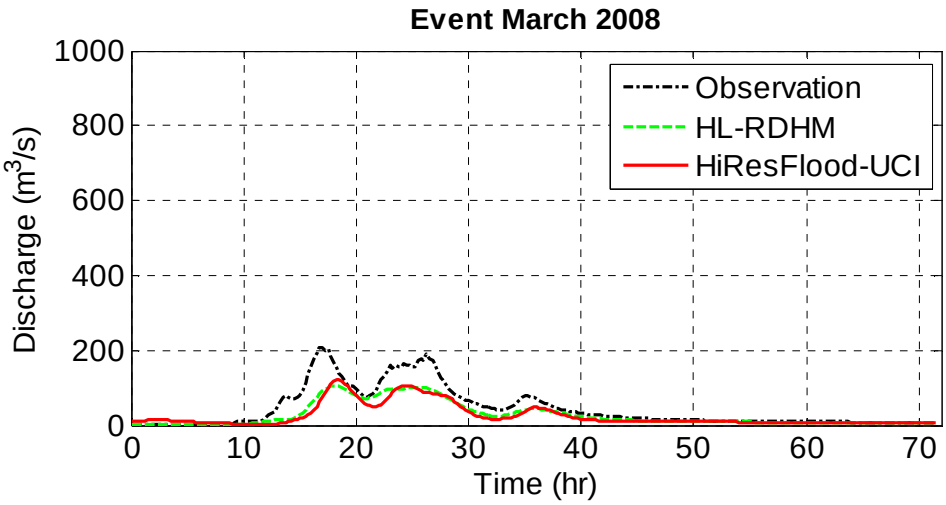

Fig. 6-8. Simulation results at interior point USGS 07196900

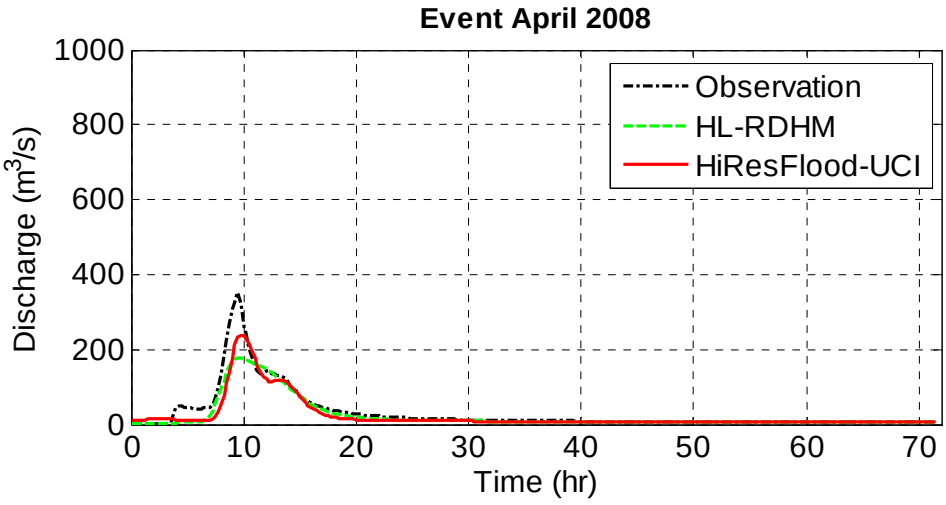

Fig. 6-9. Simulation results at interior point USGS 07196900

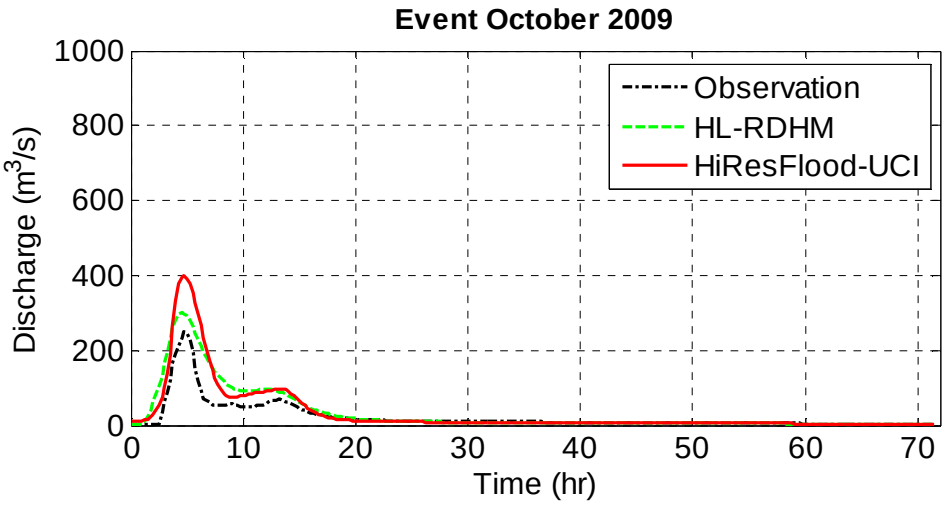

Fig. 6-10. Simulation results at interior point USGS 07196900

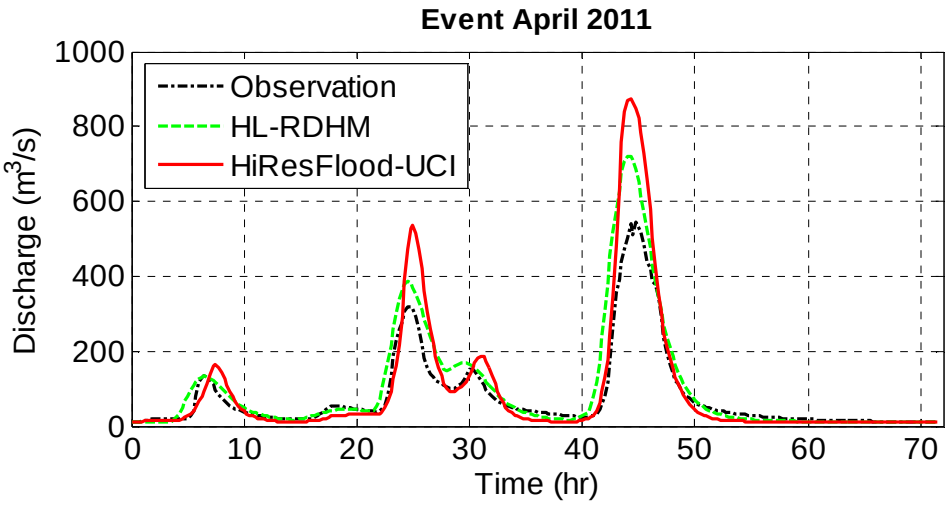

Fig. 6-11. Simulation results at interior point USGS 07196900

Table 6-2. Statistics of event simulations at interior point USGS 07196900

Event	Observation/ Simulation	Peak flow	Peak flow error	Phase error	RMSE	BIAS	NSE
		(m^3/s)	(%)	(hr)	(m^3/s)	-	-
March 2008	USGS Observation	208.41	-	-	-	-	-
	HL-RDHM	104.92	-49.66	1	30.12	-0.38	0.68
	HiResFlood-UCI	128.18	-38.50	1	34.88	-0.42	0.56
April 2008	USGS Observation	353.96	-	-	-	-	-
	HL-RDHM	177.22	-49.93	0	23.70	-0.251	0.83
	HiResFlood-UCI	237.89	-32.79	0	22.12	-0.25	0.85
October 2009	USGS Observation	251.74	-	-	-	-	-
	HL-RDHM	300.50	19.37	0	29.60	0.45	0.44

	HiResFlood-UCI	398.74	58.39	0	36.55	0.52	0.15
April 2011	USGS Observation	546.51	-	-	-	-	-
	HL-RDHM	721.90	32.09	0	57.10	0.27	0.73
	HiResFlood-UCI	874.77	60.06	0	73.64	0.20	0.56

6.3.3 Flooded maps and flow velocity

Figs. 13-15 highlight the spatial distribution of the maximum water depth (H_{max}) and velocity for each pixel in the ELDO2 catchament for the April 2011 event. The value of HiResFlood-UCI is exemplified by this series of figures in that they provide a clear picture of the most extreme depth and velocity for the entire basin (Figs. 6-12 and 6-13), but maintain a high enough resolution such that highly localized impacts (i.e. flooding of individual fields) can be seen (Fig. 6-14). While some existing models (i.e. MIKE FLOOD, BreZo) are capable of capturing inundation at high resolutions, often it is only of a select river reach or a very small catchment due to computational expense. The coupled structure HiResFlood-UCI allows for effiicient production of high resolution, spatial flow information for the whole catchment. While for some events, the estimated hydrograph from HiResFlood-UCI may be similar to that of HL-RDHM, the HiResFlood-UCI provides important information such as flow depth and velocity that is not available from commonly used hydrologic models. Flow depth and velocity are very important

for flood warning, and the proposed HiResFlood-UCI can potentially be used to enhance NWS's flood warning capabilities.

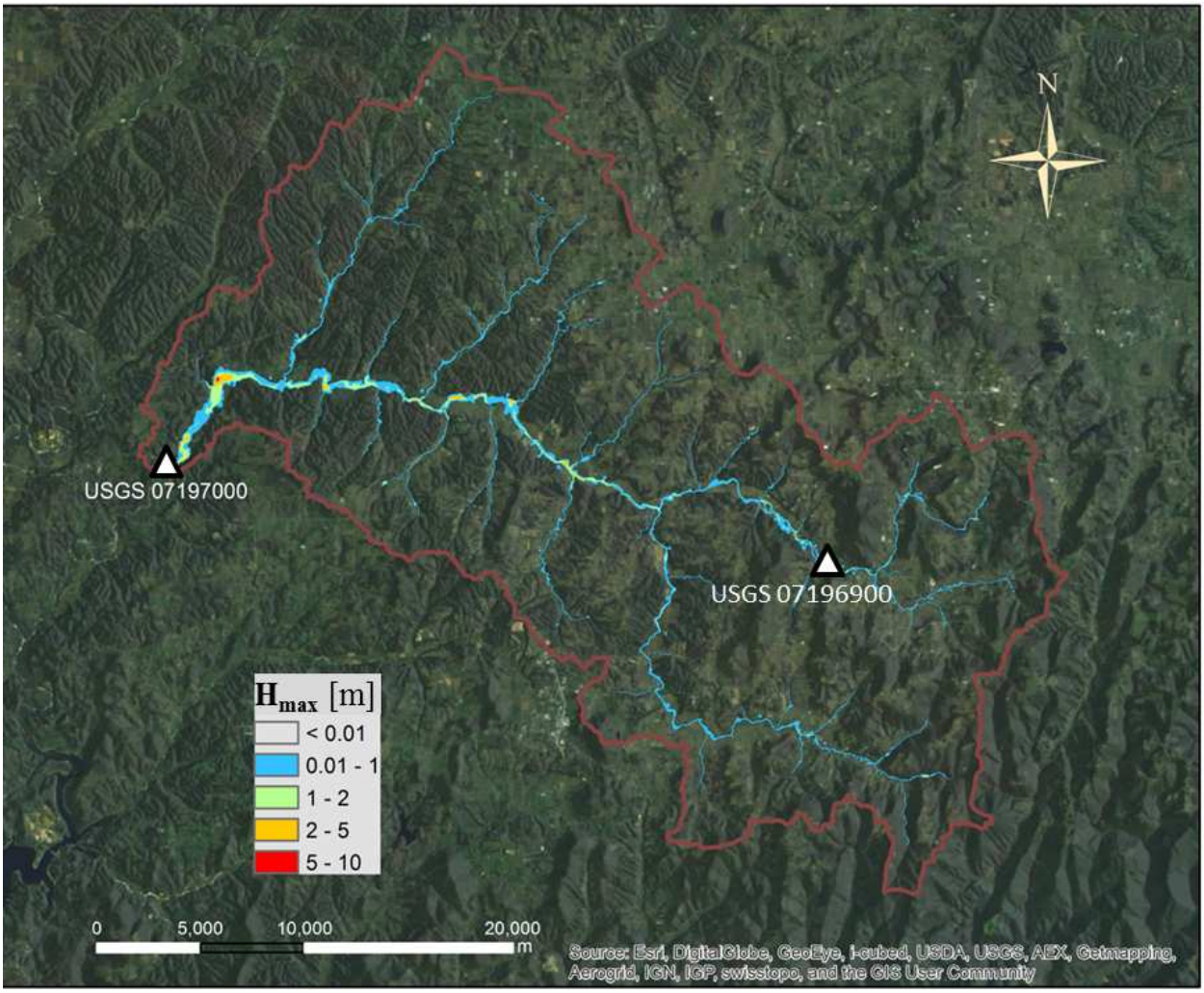

Fig. 6-12. Flooded-area map of ELDO2 in extreme event in April 2011

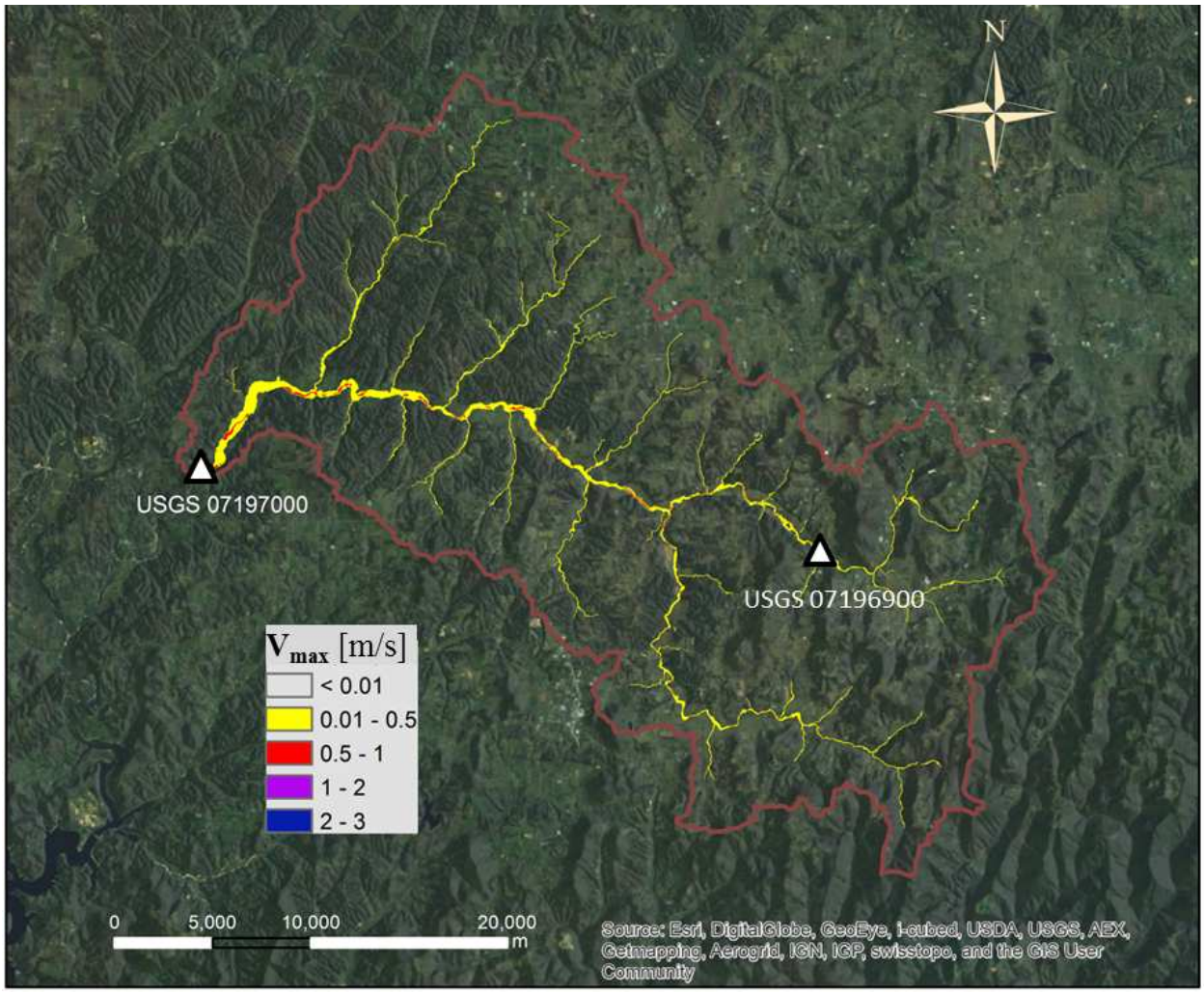

Fig. 6-13. Flow velocity of ELDO2 in extreme event in April 2011

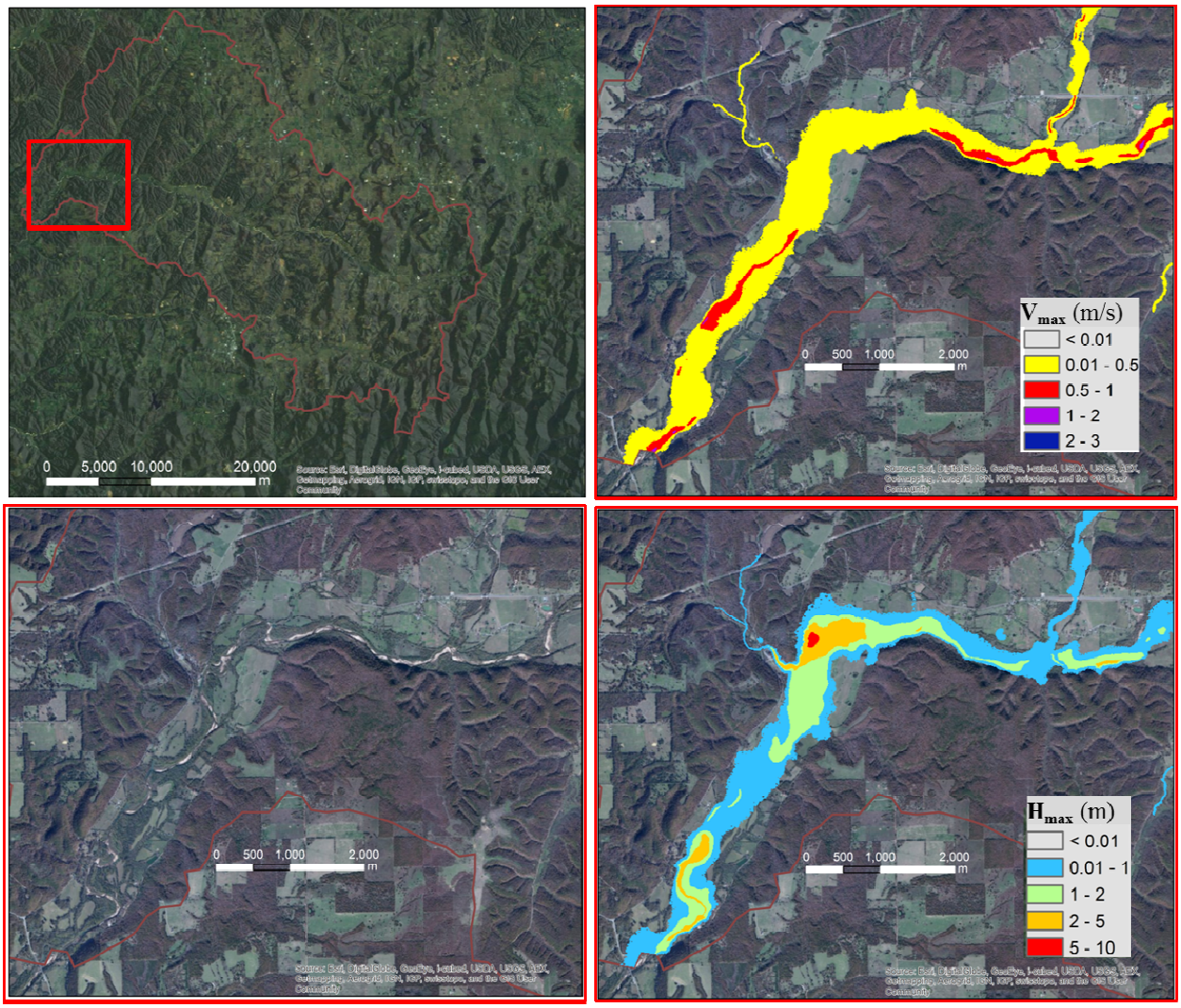

Fig. 6-14. Details of Flooded map and Flow velocity of ELDO2 in event April 2011

6.3.4. Validation of the floodplain inundation using observed gauge height

Validation of the flooded maps was performed at a USGS gauge located at an interior point of the ELDO2 catchment (Fig. 6-15). A cross section of the channel at the gauge location was constructed from a 10m DEM, with elevation being relative to the datum of the gauge. Simulated flood stage was retrieved using the flood extent maps and flow depth information produced by HiResFlood-UCI in conjunction with the channel cross section.

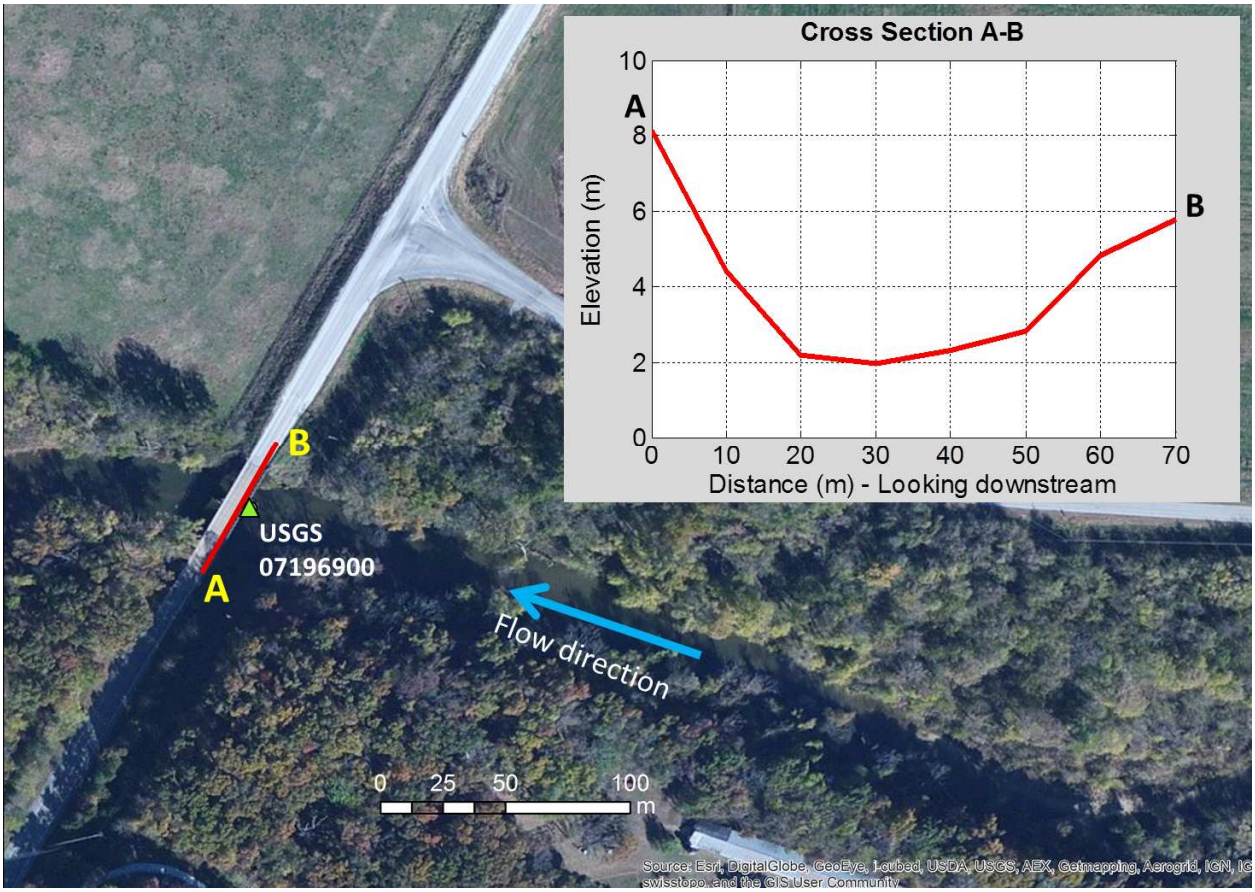

Fig. 6-15. USGS 07196900 gauge station site. Cross section derived from 10m DEM at gauge USGS 07196900, elevation with respect to the gauge datum (300.676m National Geodetic Vertical Datum of 1929, NGVD29)

The simulated and observed flood stage of the four validation events at the interior point are shown in Figs. 6-16 - 6-19. While the difference between simulated and observed flood stage is substantial for all events (40-70% error or 1.81-2.08m), the simulation error is significantly reduced during flood peaks (5-29% error or 0.19-0.82m). Table 6-3 summarizes the flood peak stage and event stage errors for each of the validation events. Large errors in stage height for low flow periods at this site are not unexpected, as the 10m DEM remains too coarse to capture the fine details of this small stream. However, the simulated stage greatly improved during

flooding, which is the most important period for HiResFlood-UCI because the model's purpose is to capture details of high flow events.

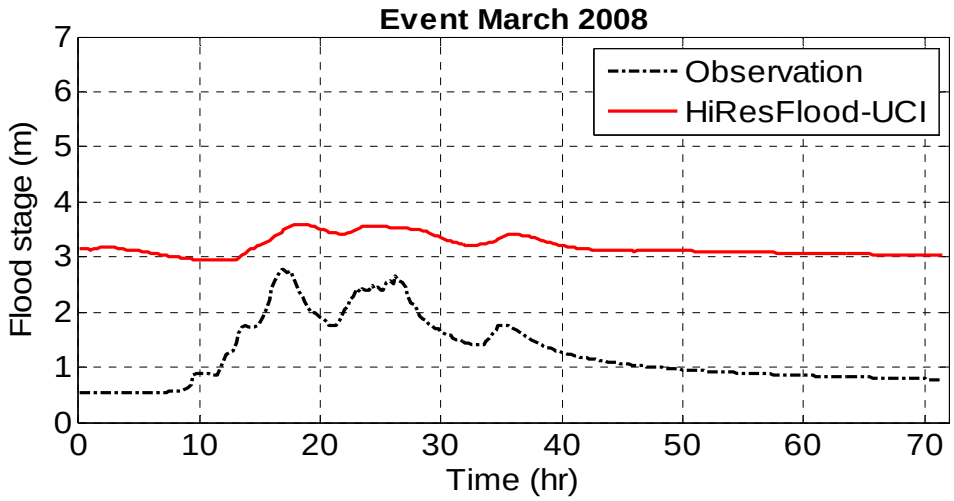

Fig. 6-16. Flood stage (m) with respect to the datum of gauge USGS 07196900 (300.676m NGVD29)

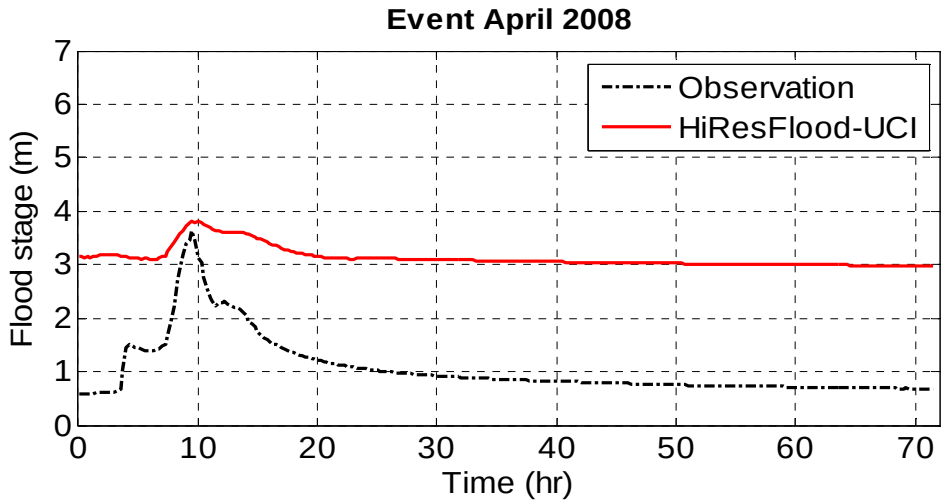

Fig. 6-17. Flood stage (m) with respect to the datum of gauge USGS 07196900 (300.676m NGVD29)

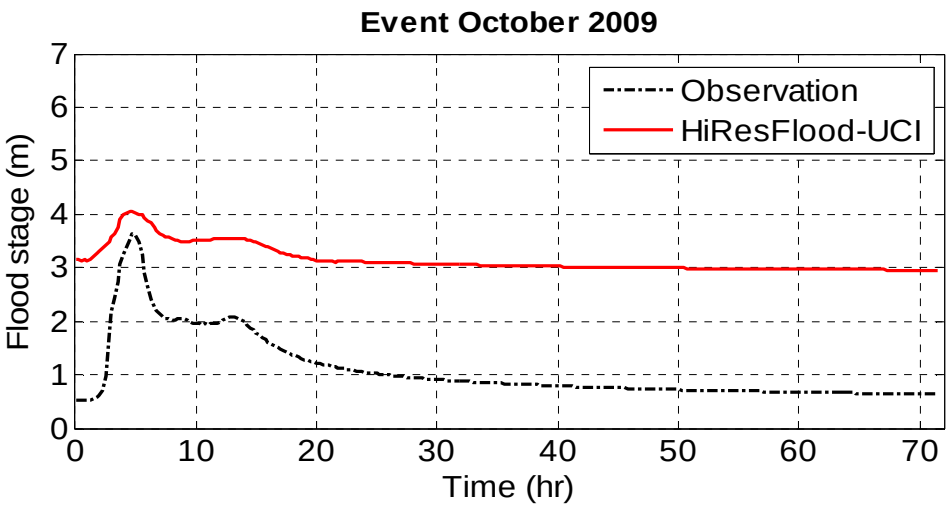

Fig. 6-18. Flood stage (m) with respect to the datum of gauge USGS 07196900 (300.676m NGVD29)

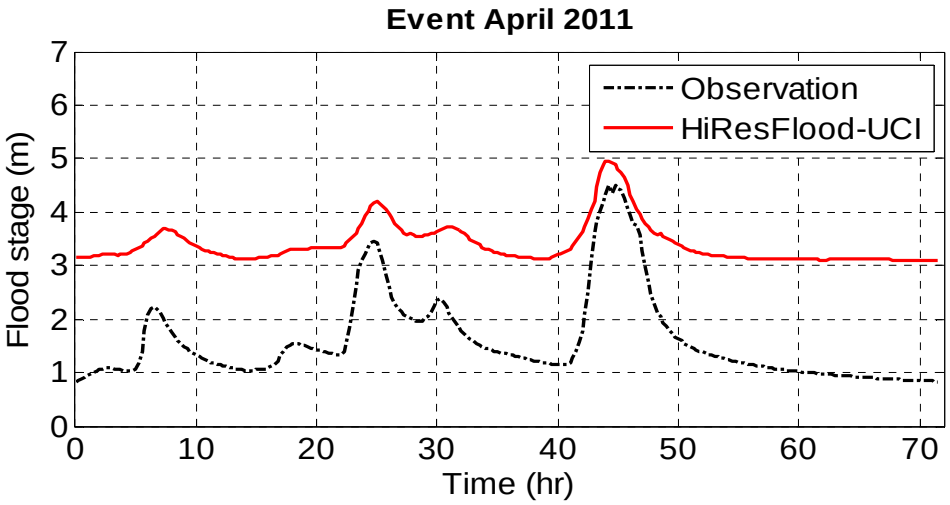

Fig. 6-19. Flood stage (m) with respect to the datum of gauge USGS 07196900 (300.676m NGVD29)

Table 6-3. Statistics of flood stage with respect to the datum of gauge USGS 07196900

Event	Observation/ Simulation	Flood Stage (m)	Flood Stage error (m)	Event stage error (m)
March 2008	USGS Observation	2.78	-	-
	HiResFlood-UCI	3.60	0.82	1.94
April 2008	USGS Observation	3.63	-	-
	HiResFlood-UCI	3.82	0.19	2.08
October 2009	USGS Observation	3.64	-	-
	HiResFlood-UCI	4.04	0.40	2.06
April 2011	USGS Observation	4.51	-	-
	HiResFlood-UCI	4.96	0.45	1.81

6.4 Conclusions

HiResFlood-UCI performance was examined using 6 measured precipitation events as model input for validation of the streamflow at the outlet. The Nash-Sutcliffe Efficiency (NSE) obtained ranges from 0.629 to 0.904. The model was also validated for the flooded map using USGS observed water level at an interior point. The predicted flood stage error is 0.82m or less, based on a comparison to measured stage. Validation of stage and discharge predictions builds confidence in model predictions of flood extent and localized velocities, which are fundamental to reliable flash flood warning.

Chapter 7. Application of HiResFlood-UCI for flood forecasting using real-time remote sensing precipitation data

7.1 Introduction

The primary hydrologic forcing into a catchment responsible for floods is extreme rainfall. Other types of floods can be caused by dam breaks, high tides and snow melting. Many efforts have been made by various organizations across the world to prevent/mitigate the impact of floods on society; however, modeling and forecasting floods caused by extreme precipitation, especially flash floods, are still very challenging (Borga *et al*., 2011). The difficulty exists with two main aspects: modeling techniques and data acquisition. Currently, flood forecasting techniques can be classified into three main groups: (1) those based on precipitation forecast/nowcast data; (2) those based on hydrologic/hydraulic models which use rainfall and river stage observations; and (3) the two former techniques combined (WMO, 1981).

Hydrologic and hydraulic models have been used to model floods driven by rainfall data from various sources: gauges, radars, satellites and numerical forecast models. Precipitation data is a key variable in flood modeling. Gauge data can be the most reliable as "true observation" but it is "point" data and difficult to extrapolate over a relatively large area. Furthermore, the gauge observation network is neither dense enough nor uniform in global scale, especially in rural, mountainous areas where floods occur more often. Radars have been used to estimate precipitation for flood warnings but they are expensive to operate and their coverage is also limited.

Remote sensing technologies have emerged since the 1970s and have consistently advanced, showing great potential for near real-time precipitation estimation for high resolution (i.e. 4 km)

global scale flood forecasting and warning. . The satellites launched by NASA and NOAA in the past several decades (i.e. NASA'S Tropical Rainfall Measuring Mission - TRMM, NOAA's Geostationary Operational Environmental Satellite series - GOES), and others launched by other international organizations offer great opportunities for developing global flood warning systems. Those systems include the Global Flood and Landslide Monitoring System by NASA (Hong *et al*., 2007), Global Flash Flood Guidance System (GFFGS) developed by the U.S. Hydrologic Research Center, Global Flood Alert System (GFAS) developed in Japan by ICHARM (http://www.icharm.pwri.go.jp/research/ifas/), and the Global Flood Monitoring System (http://flood.umd.edu/) by the University of Maryland (Wu *et al*., 2014). All the models provide very basic warnings on where there is possible potential for floods to occur. None of them can show the details of the floods, e.g. spatio-temporal distribution of water depth and flow velocity at river scale, which are crucially important in flood analysis and warnings.

Together with the rapid evolution in remote sensing technologies, more data with larger coverage and finer spatio-temporal resolution have been available for use. Furthermore, with numerous contemporary and future missions such as NASA's Global Precipitation Measurement (GPM, launched in 2014), and NASA's Soil Moisture Active Passive (SMAP, to be launched in 2015), NASA offers the unique opportunity to better understand the physics of floods in order to develop a new generation of models, which will improve global flood forecasting. Moreover, powerful computing systems motivate modelers to use high resolution hydrologic/hydraulic models to simulate the water flow in rivers and flood plains as realistically as possible to protect people and mitigate the damages of their properties caused by extreme flood hazards.

Satellite-based surface water measurements are becoming routine for flood observations and forecasting. Information from satellite sensors such as Landsat Thematic Mapper (TM),

Advanced Wide Field Sensor (AWiFS), Moderate Resolution Imaging Spectroradiometer (MODIS), Advanced Synthetic Aperture Radar (ASAR), Advanced Microwave Scanning Radiometer – Earth observing system (AMSR-E), and Ocean Topography Experiment (TOPEX)/Poseidon radar altimeter can be used to estimate flood inundation, water level, and river discharge (Hossain *et al*., 2014a&b; Khan *et al*., 2014; Alsdorf, *et al*., 2007; Bjerklie *et al*., 2005; Brakenridge *et al*., 2005; Bates *et al*., 1997; Behrangi *et al*., 2011). The NRT Global MODIS Flood Mapping system recently developed by NASA for near real-time global flood monitoring and its archived data will be a great resource for validating the proposed system (http://oas.gsfc.nasa.gov/floodmap). The NASA's Surface Water Ocean Topography (SWOT, launched 2020) will provide global river discharge observation (Mersel *et al*., 2013), which is promised to be a revolutionary resource for flood observation and forecasting in addition to validation of flood modelling at a global scale.

The Iowa Flood Center (IFC) hosted a National Aeronautics and Space Administration (NASA) Global Precipitation Measurement (GPM) validation field campaign in the spring of 2013 known as Iowa Flood Studies. The focus of the IFloodS campaign was to explore advantages and weaknesses of satellite precipitation products in terms of their application towards understanding and forecasting hydrologic processes (IFloodS – Krajewski *et al*., 2013).

This section of the dissertation presents an application of the recently developed coupled hydrologic-hydraulic model HiResFlood-UCI (Nguyen *et al*., 2014) with near real-time satellite precipitation data (PERSIANN-CCS) for flood forecasting and inundation mapping in the Cedar River in Iowa. The system was validated for the historical 2008 Iowa flood event using high resolution imagery from the Advanced Wide Field Sensor (AWiFS) of flood extent provided by the U.S. Department of Agriculture (USDA), and observations from U.S. Geological Survey

(USGS) streamflow gauges along the main channel of the Cedar River. The modeling framework uniquely integrates areal imagery into a coupled hydrologic-hydraulic modeling framework, and offers a unique avenue for validation and verification of inundation models. This work aims to supplement the efforts of the IFloodS campaign through application of the HiResFlood-UCI model to a major flood event within the IFloodS domain. The application is done in the context of using near real-time satellite precipitation data in a forecasting environment.

7.2 Near real-time satellite precipitation PERSIANN-CCS

PERSIANN-CCS (Hong *et al.*, 2004) is a near real-time satellite precipitation product. Precipitation is estimated by algorithms developed by the scientists at the Center for Hydrometeorology & Remote Sensing (CHRS) at the University of California, Irvine (UCI). The product has high spatio-temporal resolution at hourly, 0.04^{o}x0.04^{o}, quasi-global coverage from 60N to 60S. PERSIANN-CCS algorithms estimate precipitation from GEO-IR (Infrared) imagery using artificial neural networks (ANNs) and cloud classification system techniques. More detailed description on the development of PERSIANN-CCS algorithms, product validation, and application can be found in Hsu *et al.* (1997), Sorooshian *et al.* (2000), Hong *et al.* (2004), Hong *et al.* (2007), and Hsu *et al.* (2013). Since PERSIANN-CCS is available in near real-time with about 1 hour delay, it is suitable for use in providing flood warnings to the public and flood disaster managers (Sorooshian *et al.*, 2013; Nguyen *et al.*, 2014).

7.2 Research domain and data used

The Cedar River is a 544km river in Minnesota and Iowa with a drainage area of approximately 20,000km^2 (Fig. 7-1). The Cedar River flows through two major cities (Waterloo and Cedar Rapids) in Iowa. Agriculture is the main land use in the Cedar River Basin (Linhart & Eash, 2010).

The Digital Elevation Model (DEM) at 30m resolution with vertical accuracy of ±2.44m in Root Mean Square Error (RMSE) was downloaded from USGS's National Hydrology Dataset (NHD). Near real-time global PERSIANN-CCS precipitation data at 0.04 degree resolution is retrieved from UCI CHRS's server. The original PERSIANN-CCS is in geographical projection (lat/lon), so it is necessary to convert the data to the Hydrologic Rainfall Analysis Projection (HRAP, 1 HRAP ~ 4km) using the code provided by NWS (available at http://www.nws.noaa.gov/oh/hrl/dmip/lat_lon.txt) for HiResFlood-UCI.

For model validation, hourly USGS streamflow data at gauges along the Cedar River was retrieved from USGS's National Water Information System (NWIS, http://nwis.waterdata.usgs.gov/nwis/).

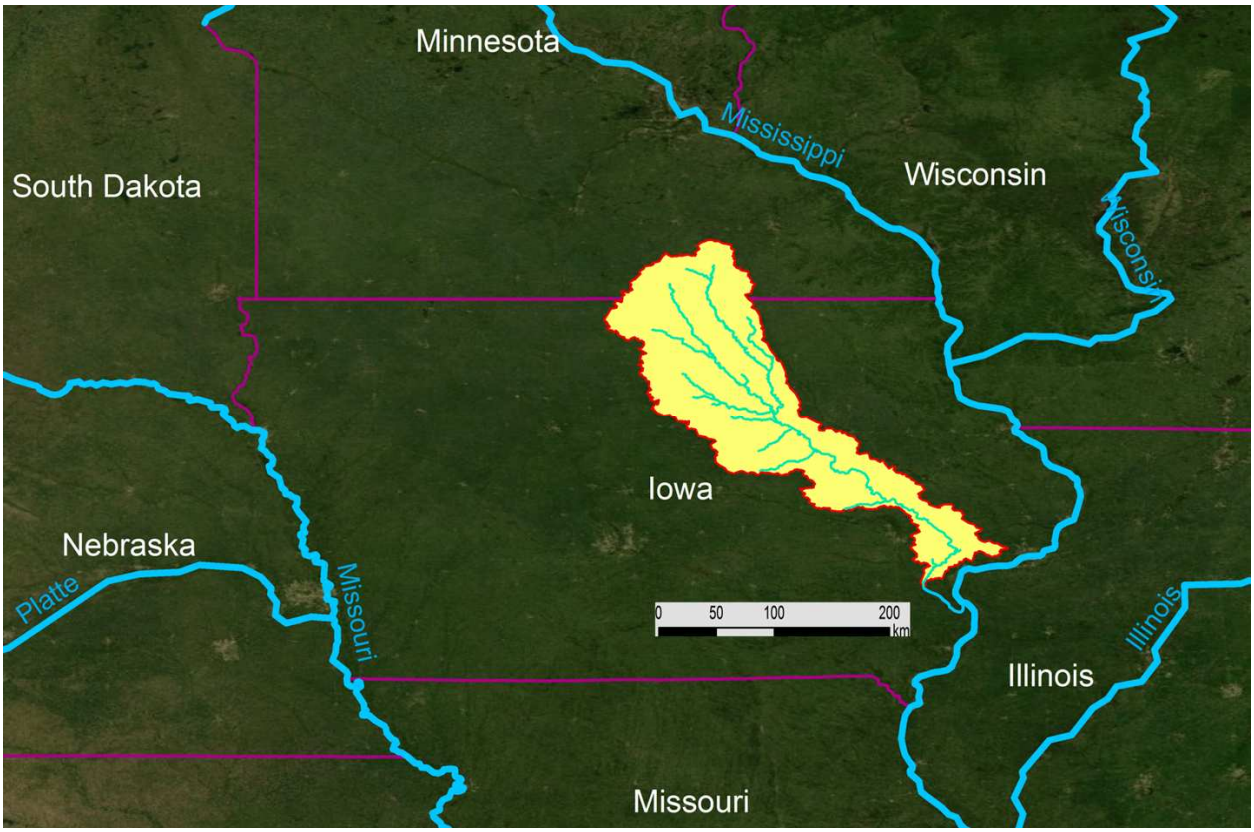

Fig. 7-1. Cedar River Watershed

7.2 Model implementation

HiResFlood-UCI was set up for Cedar River Watershed following the procedure in Nguyen *et al.* (2014). HL-RDHM was set at an hourly time step, 1 HRAP resolution. HL-RHDM was implemented with the *a priori* parameters (Koren *et al.*, 2003) from NWS.

From USGS 30m DEM (Fig. 7-2), Cedar River Watershed was delineated into 29 subcatchments using ESRI ArcGIS terrain processing tools (Fig. 7-3). The unstructured triangular mesh was designed using Triangle software (Shewchuk, 1996) with buffering sizes and area constraints described in detail in Table 7-1. The highest resolution along the river network and within 100m from the river center line is 30m.

Manning *n* values for the channel and floodplain of Cedar River were selected from Chow's look-up table (Chow, 1959) at 0.045 and 0.060 respectively.

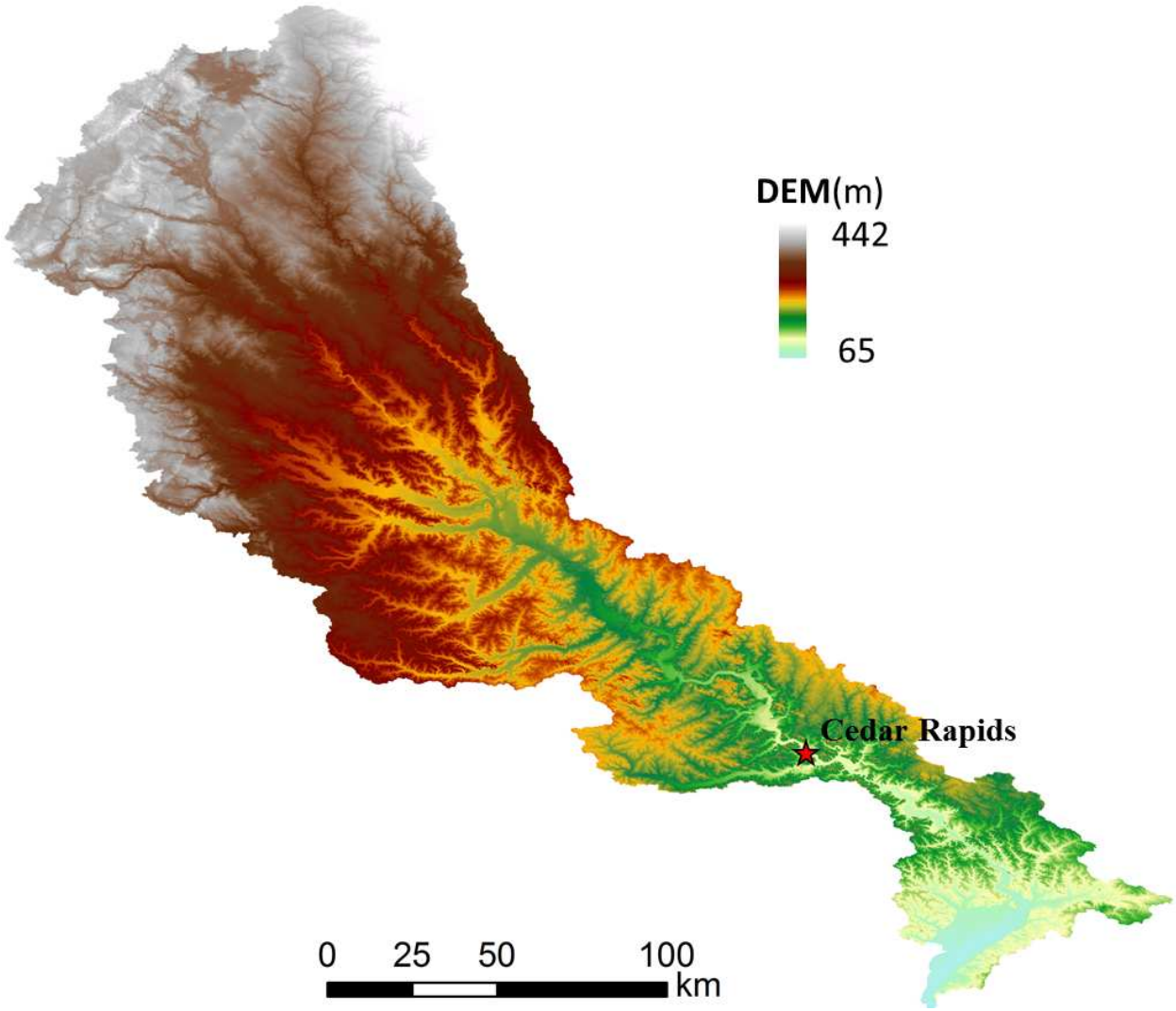

Fig. 7-2. DEM of Cedar River Watershed

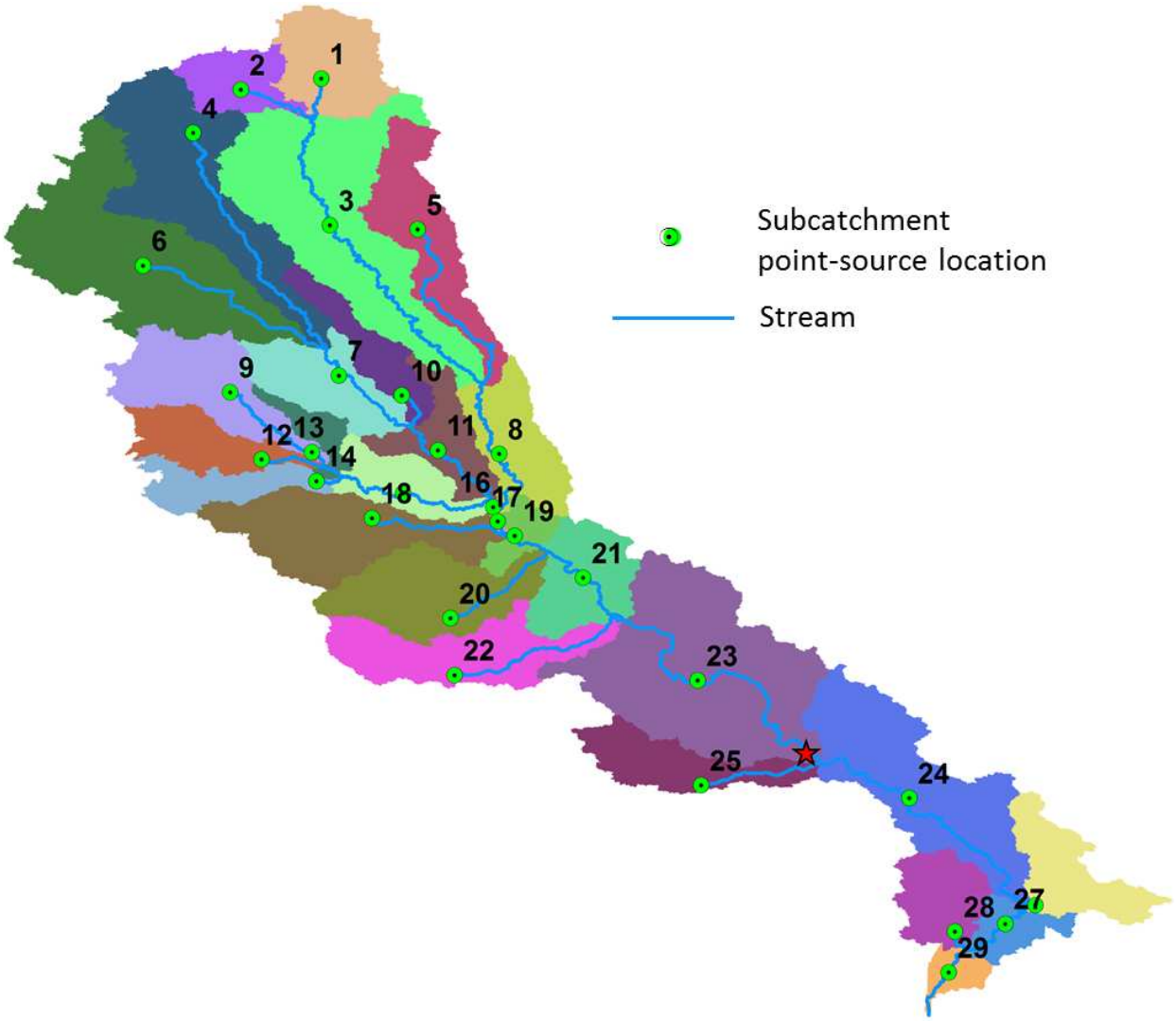

Fig. 7-3. Watershed delineation results including streams, subcatchments and point-source locations

Table 7-1. Mesh design for BreZo

Buffer zone	Distance from river (m)	Mesh resolution	
		Size (m)	**Area** (m^2)
1	100	30	450
2	500	50	1,250
3	1,000	100	5,000
4	5,000	500	125,000
5	20,000	1,000	500,000

7.3 Application of the model for simulating the historical 2008 Iowa flood

7.3.1 Description of the Iowa flood 2008

A sweep of several storms associated with sequential frontal system passages over the Midwestern U.S. was the primary contributor to the historic 2008 flood. The state of Iowa averaged 167mm of rain above normal for the period of May 29th – June 12th. This occurred following an unusually heavy snowpack during the winter of 2007-2008, which provided enough snowmelt to saturate soils and elevate river levels prior to the arrival of the late spring storms.

The 2008 flood is the largest flood on record for the Cedar River Basin, and had a peak discharge representing a 0.2-1% annual recurrence at the Cedar River stream gauge near the outlet (Linhart

& Eash, 2010). The streamflow measured by USGS's stream gauge on the Cedar River at Cedar Rapids reached to 3,964m^3/s, twice the maximum record of 110 years (Smith *et al.*, 2013).

7.3.2 Data collection

Precipitation from PERSIANN-CCS for May 29th – June 25th of 2008 was collected to use as forcing data in the simulation. Additionally, Stage 2 radar precipitation data for the same time period was obtained for a comparison to the satellite product. Stage 2 data was selected for comparison because it too is a near real-time product that could be used in a forecasting setting (albeit, limited to the U.S.). Figs. 7-4 and 7-5 show a comparison of precipitation totals for the 2008 flood event for both products. Overall, both products exhibit similar precipitation total patterns. The PERSIANN-CCS estimates less precipitation than Stage 2. PERSIANN-CCS estimates less precipitation than Stage 2. This tendency to underestimate extremes is a common disadvantage of satellite precipitation products (Mehran & AghaKouchak, 2014). It can be seen that both products have an area of maximum total precipitation located upstream of the Cedar Rapids area, where the most damaging flooding in the basin occurred.

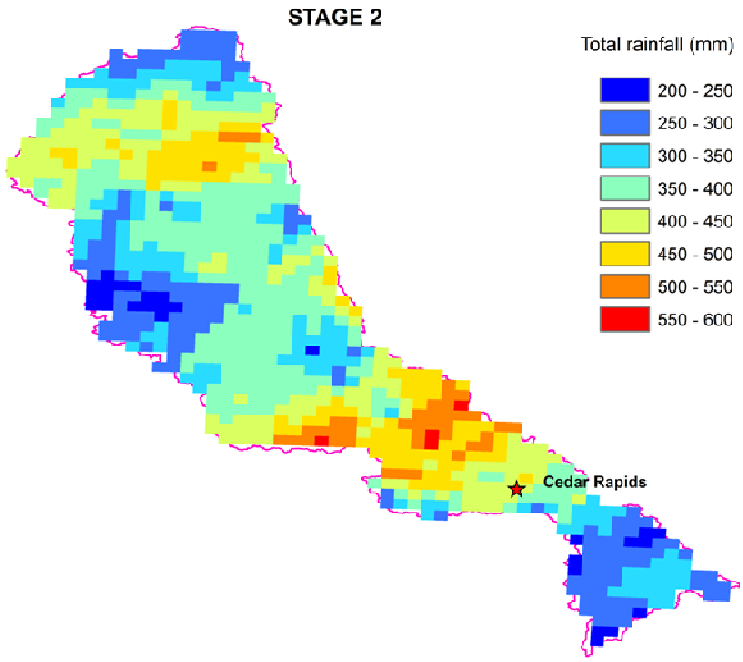

Fig. 7-4. Total precipitation during the event from 29 May 00:00 to 25 June 23:00 2008: Stage 2

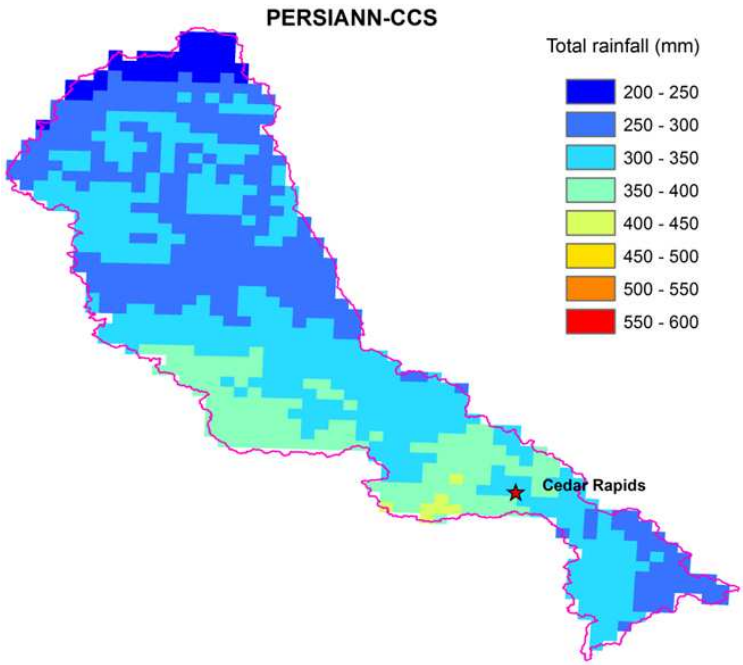

Fig. 7-5. Total precipitation during the event from 29 May 00:00 to 25 June 23:00 2008: PERSIANN-CCS

Using the Stage 2 precipitation as a baseline, spatial statistics were calculated between PERSIANN-CCS and Stage 2. Figs. 7-6 – 7-8 highlight these spatial relationships. The highest RMSE is found in the central basin, which coincides with the location of the maximum total precipitation band. Areas with the highest positive biases are detected in the southern and western regions of the basin and areas with strongest negative biases exhibited throughout the northern and central basin. The correlation coefficient pattern closely mimics that of RMSE, with the lowest correlation being in the central basin.

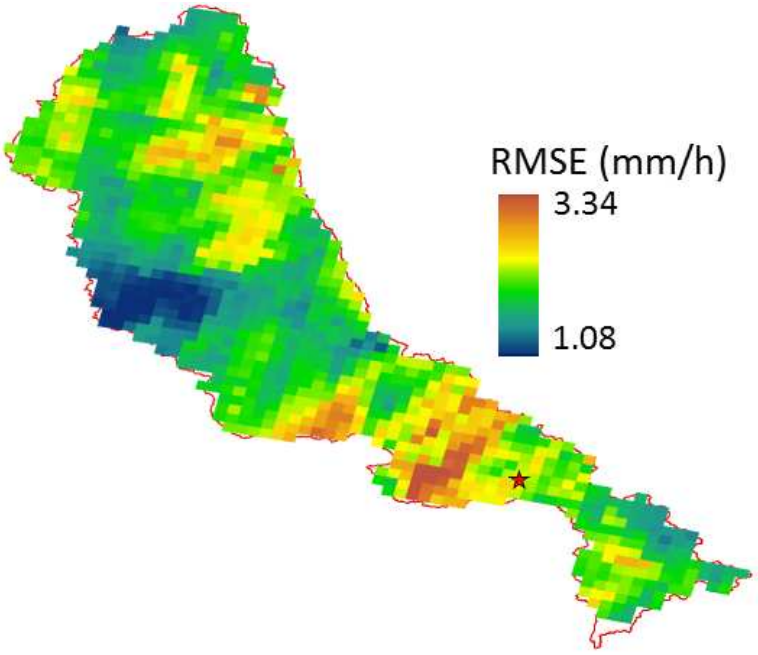

Fig. 7-6. Comparison statistics between Stage 2 and PERSIANN-CCS hourly precipitation from 29 May 00:00 to 25 June 23:00 2008

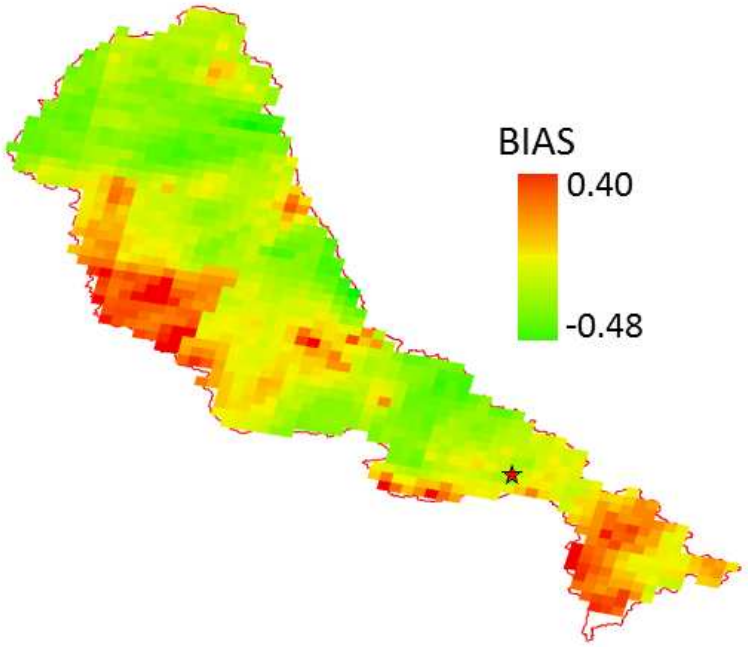

Fig. 7-7. Comparison statistics between Stage 2 and PERSIANN-CCS hourly precipitation from 29 May 00:00 to 25 June 23:00 2008

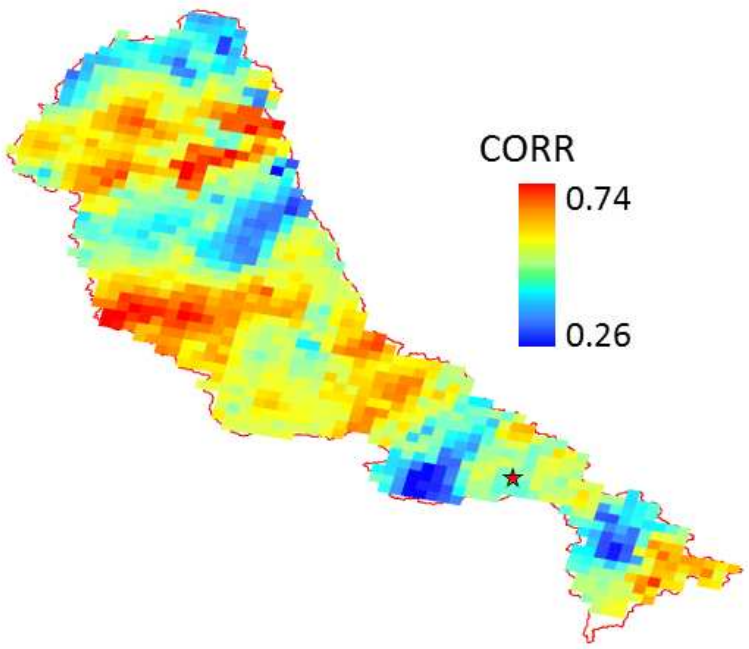

Fig. 7-8. Comparison statistics between Stage 2 and PERSIANN-CCS hourly precipitation from 29 May 00:00 to 25 June 23:00 2008

Observations from 7 USGS streamflow gauges scattered across the basin were used to analyze the simulated hydrographs produced by HiResFlood-UCI. Locations and IDs of these gauges are shown in Fig. 7-9.

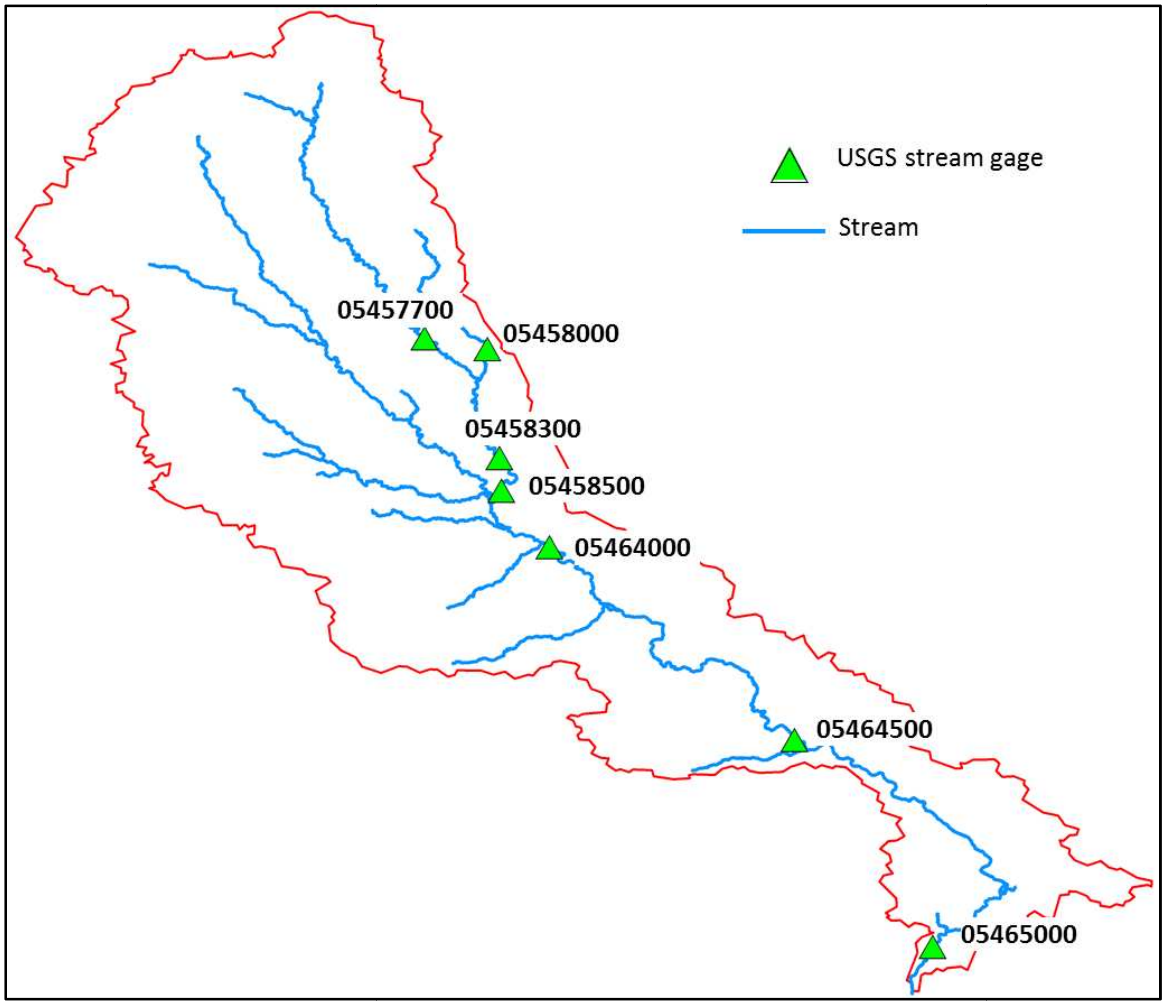

Fig. 7-9. USGS streamflow gage IDs and locations in the Cedar River Watershed used for validation

This research used the AWiFS flood extent data from USDA. Johnson and Lindsey (2008) suggest AWiFS (56m resolution) as an excellent compromise between Landsat (30m resolution but not frequent enough), and MODIS (250m resolution but more frequent). AWiFS imagery is taken from the AWiFS sensor aboard the Indian Remote Sensing – Polar satellite launch vehicle 6 (IRS-P6). AWiFS imagery has 56m resolution at nadir with a swath of 740km and a 5-day revisit (Indian Remote Sensing Agency, 2003). The AWiFS images over the Iowa area on 29 May and 16 June 2008 were classified into flood/non-flood then converted into vector format

(shapefile) by USDA. The data in shapefile format was downloaded from the USGS Hazard Data Distribution System (HDDS, http://hddsexplorer.usgs.gov/data). Fig. 7-10 illustrates the magnitude of the 2008 Iowa flood in the Cedar River Basin as seen by AWiFS.

As the figure shows, most of the basin's streamflow conditions are characterized with these images except the northern, most upstream segment is not fully covered. This was of little concern, as the most impacted area is the river towards the southern half of the basin, particularly near the Cedar Rapids area. This pre-classified product depicts flooded areas that are noisy and disconnected from the main channel. While these classifications may be correct (i.e. small ponds), both the pre-flood and post-flood images were manually cleaned such that only pixels of the main river channel and its tributaries were left. This allows for a more straightforward analysis of the model's performance of flooding the actual river by negating any influence the isolated ponds (not connected to the main river) would have on performance metrics.

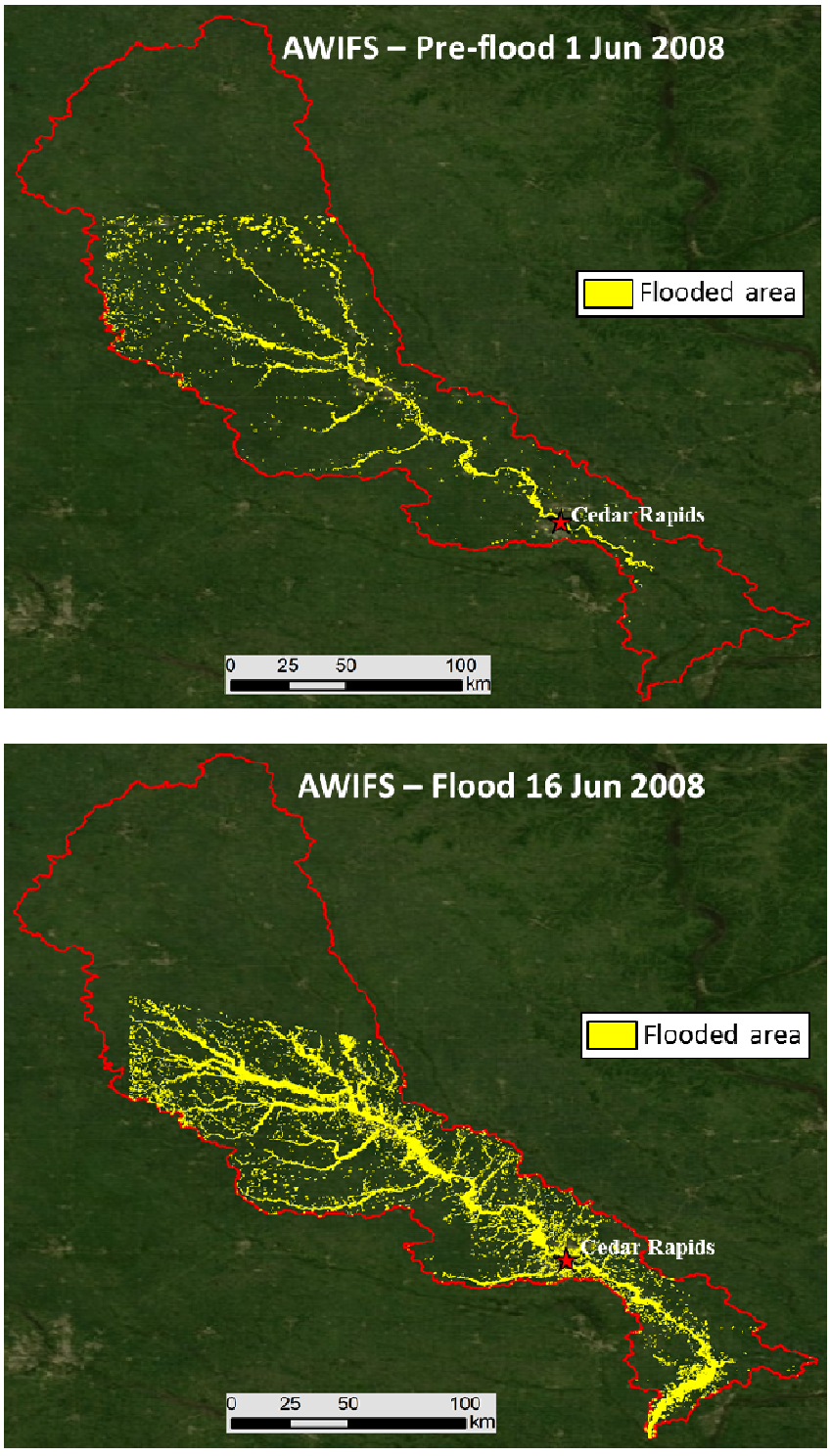

Fig. 7-10. AWiFS areal images of pre-flood (1 June 2008) and flood (16 June 2008)

7.3.3 Results and discussion

Streamflow validation

Fig. 7-11 shows the simulated and observed hydrographs at each of the 7 USGS gauge locations in the Cedar River Basin during the 2008 Iowa flood event. Hourly basin average precipitation as captured by Stage 2 radar and PERSIANN-CCS is also highlighted in Fig. 7-11. The major flood level at each gauge location as defined by the NWS is plotted as well. In general, both simulations replicate the observed streamflow well in terms of event timing, but struggle in terms of peak magnitude. The PERSIANN-CCS simulation catches the general shape of the observed streamflow, as evidenced by high correlation values in Table 7-2, but underestimates flow magnitude overall. On the other hand, the Stage 2 simulation overestimates peak magnitude at some locations while underestimating at others, and features sharper, more frequent peaks than the observation and the PERSIANN-CCS simulation.

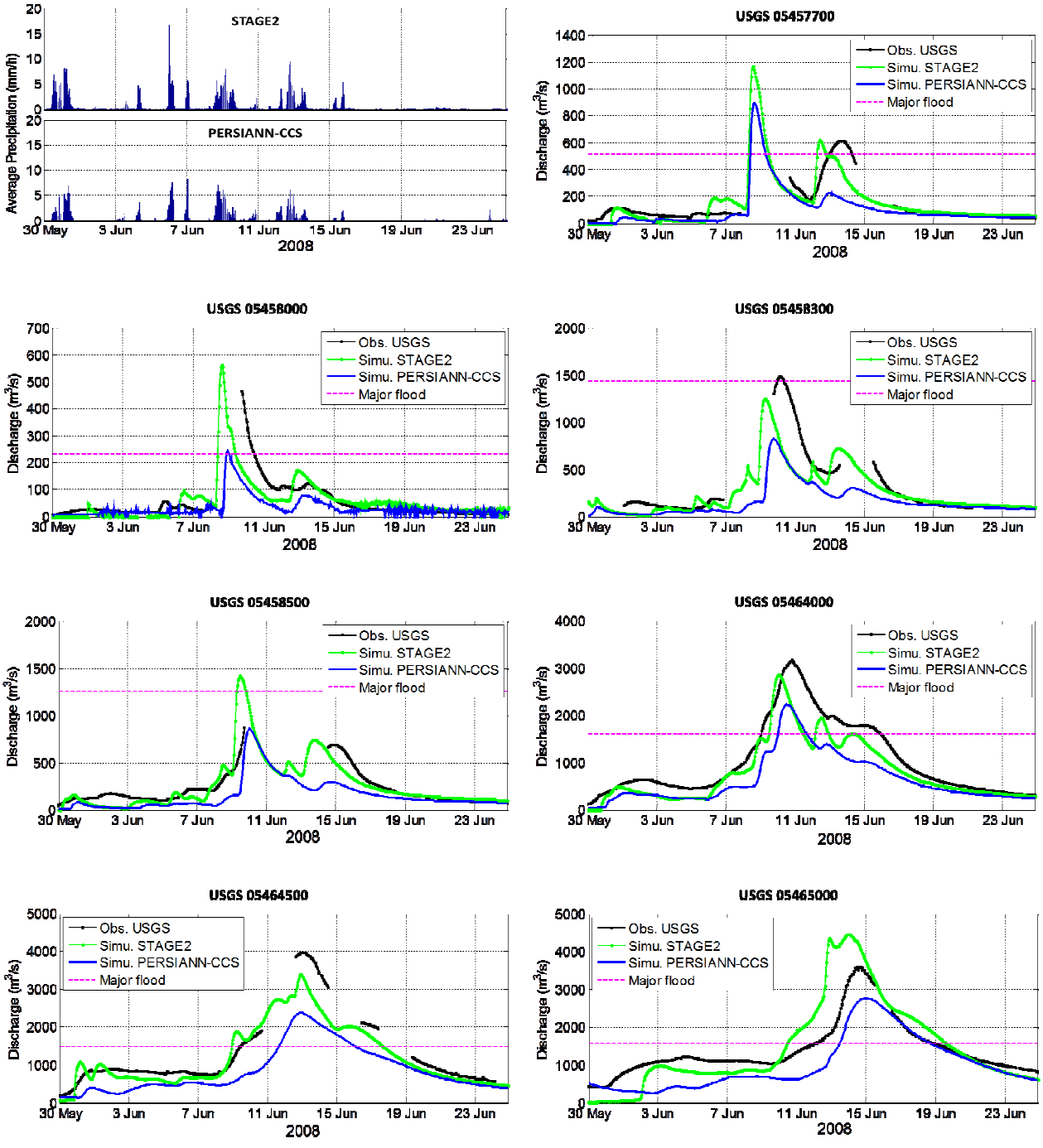

Fig. 7-11. Average precipitation, USGS observed hydrographs and model results from model with Stage 2 and PERSIANN-CCS precipitation data

Statistics in Table 7-2 highlight the differences in hydrographs produced throughout the basin when using Stage 2 radar data versus PERSIANN-CCS data as they compare to observed USGS

streamflow gauge measurements. RMSE values between the two simulations are comparable, but the Stage 2 simulation has a lower RMSE than the PERSIANN-CCS simulation at all gauges, except at the outlet. In nearly all of the cases, simulations using Stage 2 and PERSIANN-CCS have a negative bias, with the PERSIANN-CCS forced simulation having a larger bias. Since the model was run using *a priori* parameter grids, it is possible that with calibration, such bias could be reduced. For correlation, both simulations show a strong performance throughout the basin with the lowest value for either case at 0.72. The PERSIANN-CCS simulation slightly outperformed Stage 2 at all stream gauge locations except at the outlet in terms of correlation.

Table 7-2. Statistics of event simulations with STAGE2 and PERSIANN-CCS precipitation data comparing with USGS observed streamflow

USGS Streamflow Gauge	Precipitation Input	RMSE (m^3/s)	BIAS	CORR
05457700	Stage 2	77.79	-0.08	0.85
	PERSIANN-CCS	119.84	-0.51	0.87
05458000	Stage 2	46.50	-0.14	0.72
	PERSIANN-CCS	54.06	-0.50	0.87
05458300	Stage 2	233.32	-0.28	0.87
	PERSIANN-CCS	256.97	-0.48	0.97
05458500	Stage 2	139.07	-0.05	0.79
	PERSIANN-CCS	151.43	-0.54	0.86
05464000	Stage 2	353.32	-0.22	0.95
	PERSIANN-CCS	493.58	-0.39	0.99
05464500	Stage 2	328.10	-0.13	0.96
	PERSIANN-CCS	631.54	-0.42	0.97

	Stage 2	609.22	0.05	0.91
05465000				
	PERSIANN-CCS	518.85	-0.31	0.89

Inundation map validation

The model not only can provide a step-by-step picture of the flooded conditions, but it can also highlight the maximum impact (e.g. maximum depth and maximum flow velocity) at each location for an event. Fig. 7-12 is one example of such image, as it shows the maximum depth experienced during the flood event for the entire basin. Such information is not available from the commonly used hydrologic model, and it is a unique feature of the HiResFlood-UCI. The validation of the model simulation against the AWiFS product is carried out for a flood map at a certain time step. Also highlighted in Fig. 7-12 is the area that was selected for validation (the "extended" Cedar Rapids area). This area was chosen for its high flood impact and complete AWiFS coverage.

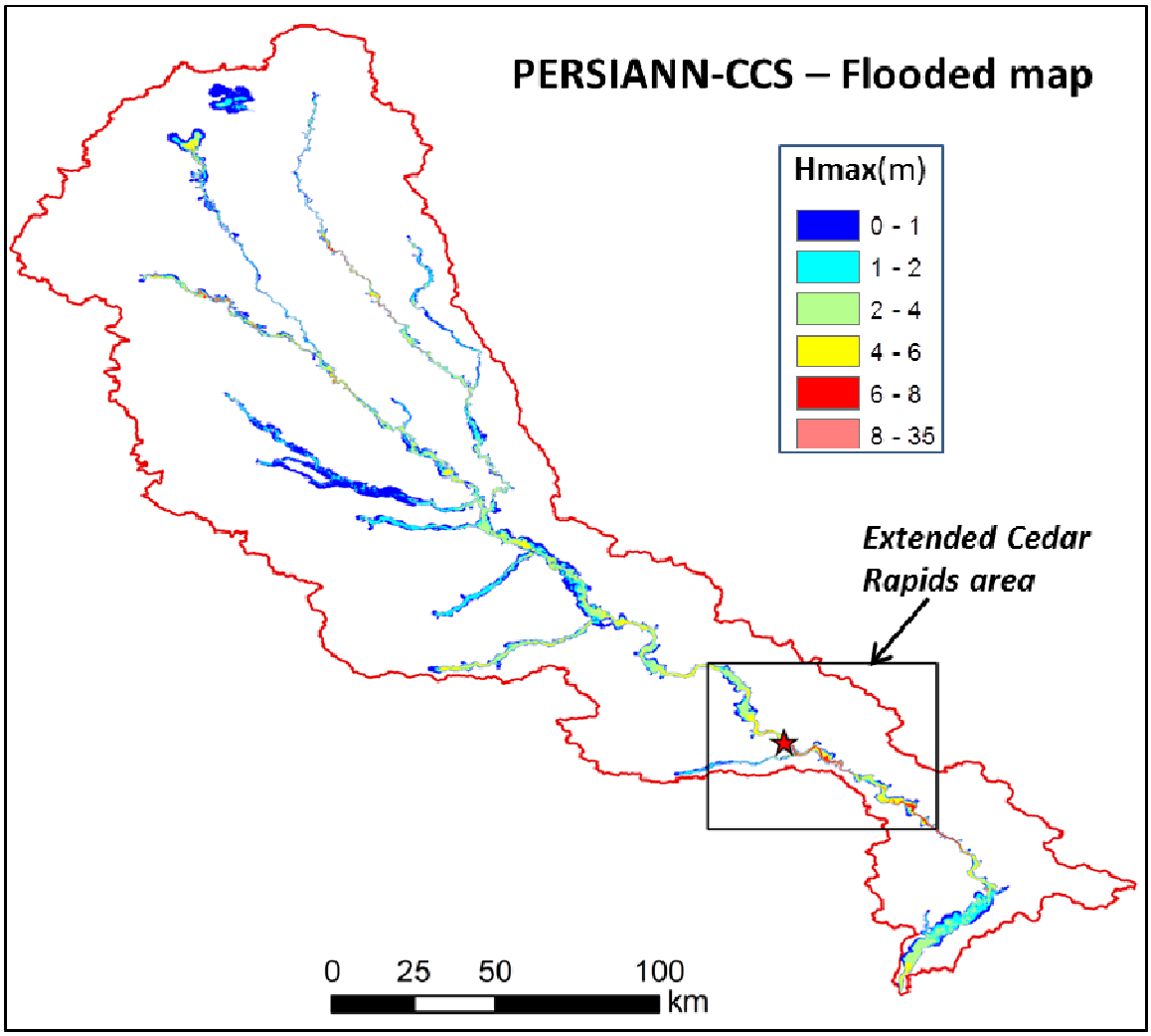

Fig. 7-12. Maximum flood depth (m) during the event simulated with PERSIANN-CCS, and extended Cedar Rapids area (Lat: 41.7393 - 42.1962^{o}N; Lon: 91.8782 – 91.2465^{o}W)

The cleaned, AWiFS imagery-based pre-flood and flood inundation maps for the Cedar Rapids and surrounding area are shown in Fig. 7-13. Fig. 7-14 shows the simulated inundation maps of the corresponding area for the Stage 2 and PERSIANN-CCS forced simulations for the flood on June 16th, 2008. The predicted flooded maps were interpolated into 56m resolution regular grid in order to be spatially compared with the AWiFS images.

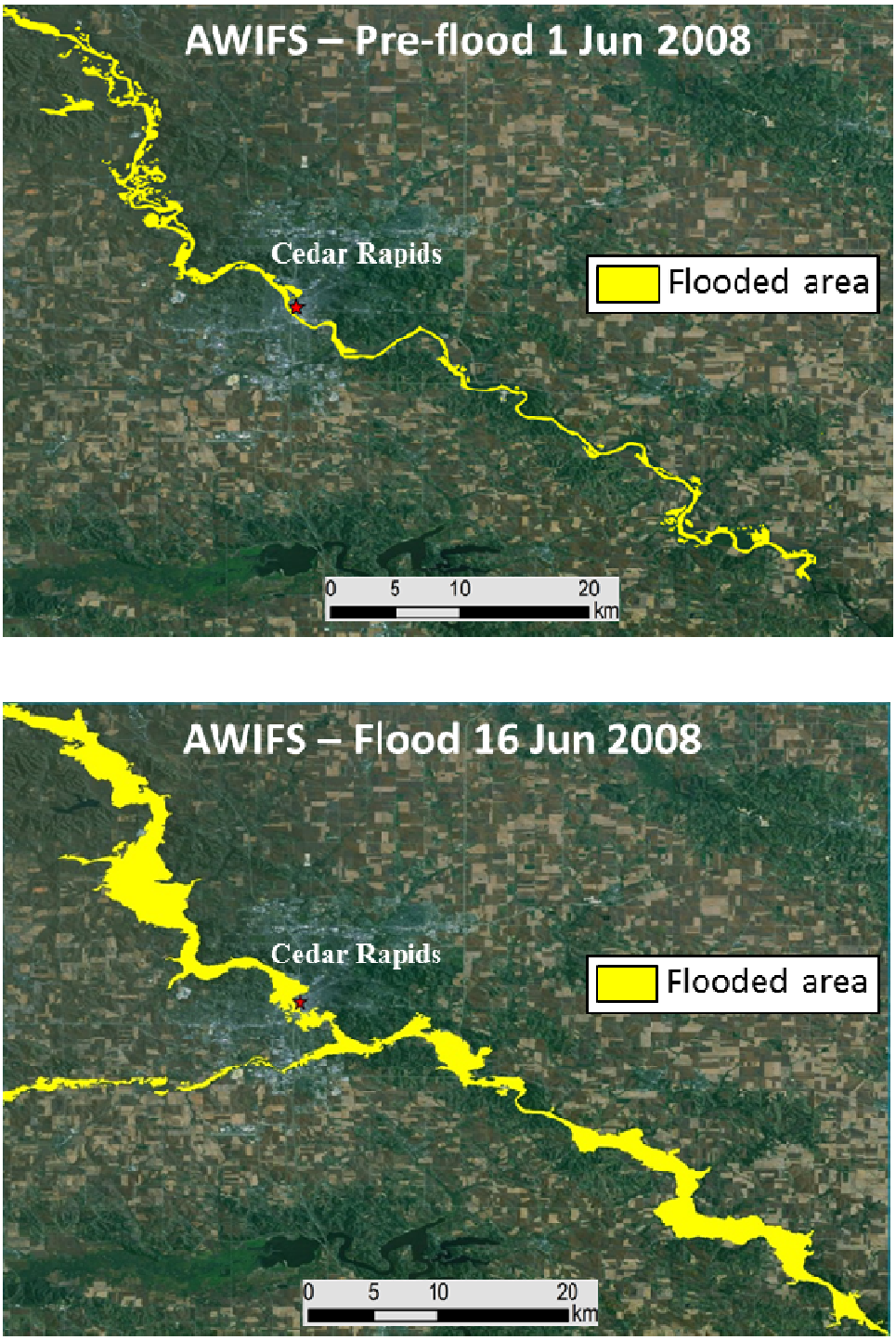

Fig. 7-13. Cleaned flooded maps of pre-flood and flood over the extended Cedar Rapids area

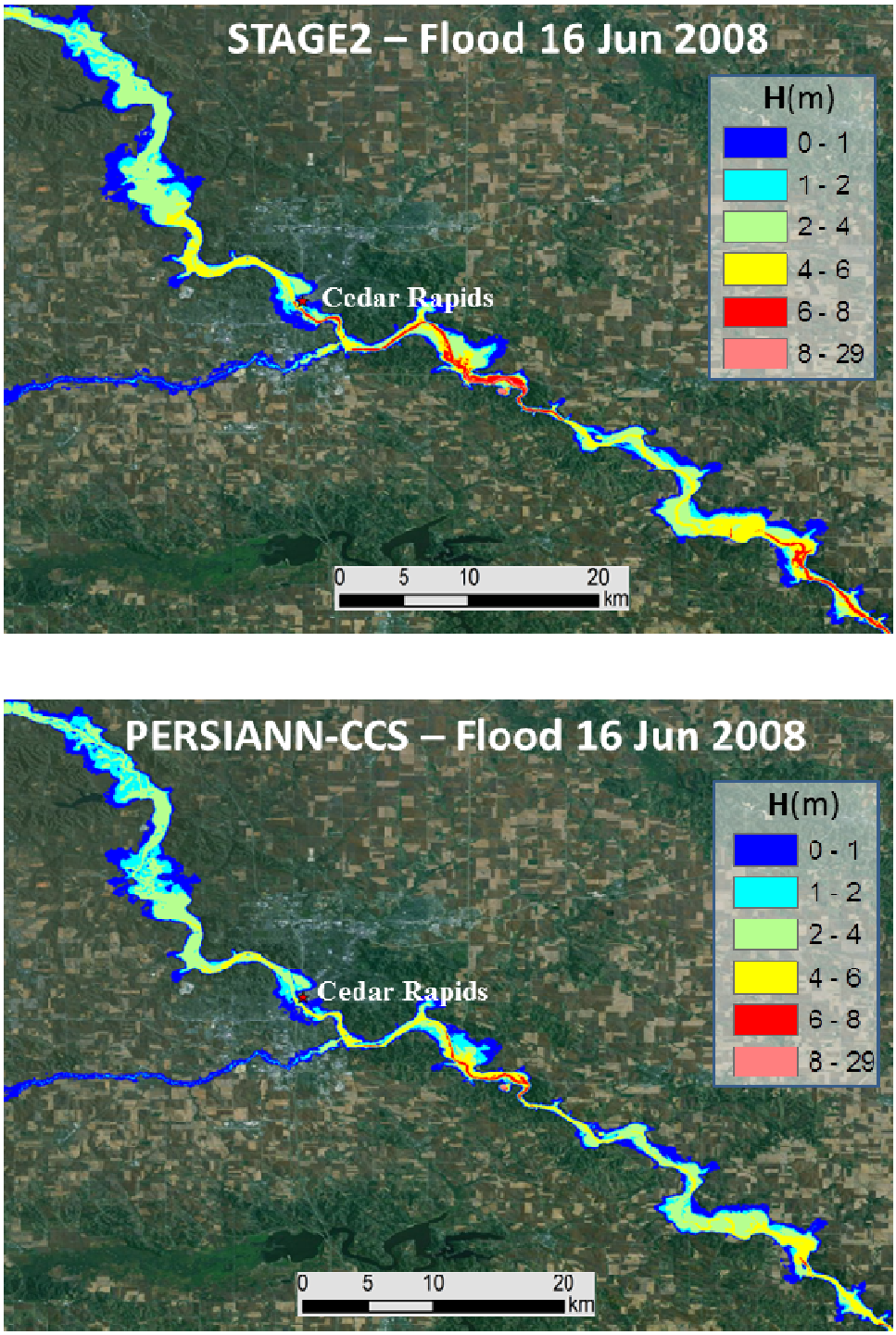

Fig. 7-14. Modeled flood depth maps with Stage 2 and PERSIANN-CCS precipitation data over the extended Cedar Rapids area

Fig. 7-15 shows the hit/miss/false alarm map for the simulations using each precipitation product. Using the AWiFS inundation maps as 'truth' the Stage 2 simulation overestimated the flood extent as exemplified by more false alarm pixels than missed pixels. On the other hand, the PERSIANN-CCS simulation tends to have more misses than the Stage 2 simulation. This is a somewhat expected by-product of PERSIANN-CCS showing less precipitation in the flood event total precipitation map (Figs. 7-4 and 7-5). In fact, previous satellite validation studies indicate that satellite precipitation data sets tend to underestimate precipitation especially at higher rain rates (AghaKouchak *et al.*, 2011, 2012). This can explain the underestimation of peak discharge relative to the Stage 2. However, the results show that satellite observations still provide comparable flood estimates, and inundation maps.

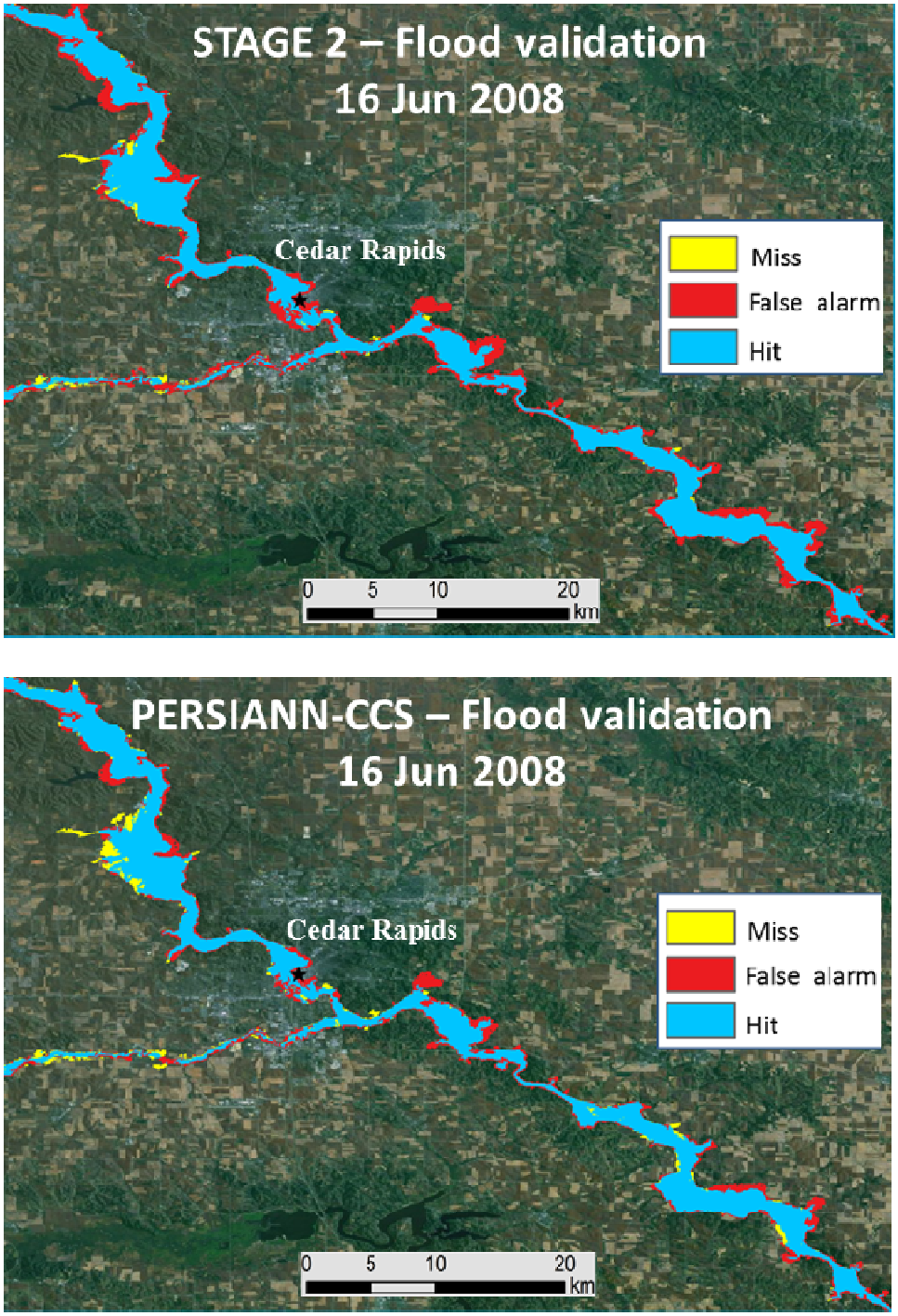

Fig. 7-15. Validations of flooded maps from the model (with Stage 2 and PERSIANN-CCS precipitation) using AWiFS areal imagery

Table 7-3. Statistics of flooded map validations for the extended Cedar Rapids area

Precip. input	CSI	POD	FAR
STAGE2	0.672	0.965	0.311
PERSIANN-CCS	0.727	0.925	0.227

Table 7-3 summarizes the spatial statistics for both simulations as they relate to the AWiFS maps of the extended Cedar Rapids area. The CSI for the PERSIANN-CCS simulation is slightly higher than the Stage 2 simulation, which suggests it correctly identified flooded pixels with few mistakes (miss or false alarm) compared to the Stage 2 run. Overall, both simulations performed reasonably well as the model was able to capture much of the detail present in the AWiFS-based maps when forced with both precipitation products. This highlights the value of satellite observations for flood forecasting and inundation mapping in remote regions where radar observations are not available (Sorooshian *et al.*, 2011).

7.4 Conclusions

The coupled hydrologic-hydraulic model HiResFlood-UCI was driven by near real-time remote sensing data in an effort to demonstrate flood inundation mapping capabilities of the model in a forecasting framework. Two near real-time precipitation products, PERSIANN-CCS satellite-based product and Stage 2 radar, were used as input for simulating the historic 2008 Iowa flood. This study exploited the rare AWiFS areal imagery of the Cedar River in the extended Cedar Rapids area before and during the flood as a means of validating the model generated flood

extent maps. Basin-internal and outlet hydrographs from the model were compared to corresponding observed gauges as a secondary investigation of model performance.

The AWiFS dataset of inundation extent for the 2008 Iowa flood event allowed for a unique experimental set up that encompasses three varieties of remote sensing for either simulation or validation. With AWiFS imagery as a baseline, simulations forced by both Stage 2 and PERSIANN-CCS produced flood maps of the extended Cedar Rapids area with high POD's (0.97 and 0.93 respectively).

Streamflow gauges located at basin interior points reveal high streamflow correlations with both simulations, with a minimum correlation of 0.72 for the Stage 2 simulation and 0.86 for the PERSIANN-CCS simulation. The Stage 2 simulation tends to replicate event magnitude better than the PERSIANN-CCS run, as evidenced by a 42% – 90% bias reduction from PERSIANN-CCS to Stage 2. However, the PERSIANN-CCS simulation captures the observed hydrograph shape more accurately as the Stage 2 run shows sharper, more frequent peaks. This is also supported by the PERSIANN-CCS run's higher correlation coefficients.

Chapter 8. Summary and Future direction

8.1 Summary

Floods are among the most devastating natural disasters which affect millions of people worldwide. Modeling and forecasting floods to provide warnings to the public in a timely manner is crucially important, but not without its challenges. This research aims to develop, test, and validate a new high resolution coupled hydrologic-hydraulic model HiResFlood-UCI for flood modeling. HiResFlood-UCI offers hydrographs, flow depth, inundated area, and flow velocity. An application of the model for a real flood event was carried out to build confidence on the model performance. The objectives mentioned in Chapter 1 were addressed and tested in this dissertation as follows:

1) Development of HiResFlood-UCI for flood modeling purposes.

A coupled hydrologic-hydraulic model for flood modeling called HiResFlood-UCI was developed. HiResFlood-UCI is the coupling of the NWS's hydrologic model (HL-RDHM) with the hydraulic model (BreZo) for flood modeling at decameter resolutions. The coupled model uses HL-RDHM as a rainfall-runoff generator and replaces the routing scheme of HL-RDHM with the 2D hydraulic model (BreZo) in order to predict localized flood depths and velocities. The system was designed to combine the strengths of the NWS's HL-RDHM distributed hydrologic model with those of the BreZo 2D hydraulic model.

2) Development of a semi-automated unstructured mesh generation technique for HiResFlood-UCI.

A semi-automated technique of unstructured mesh generation using ArcGIS and Triangle was developed to cluster an adequate density of computational cells along rivers. This approach is designed in such a way that numerical errors are negligible compared with other sources of error, but no more, so that computational costs of the hydraulic model are kept to the bare minimum. Depending on the users' particular application, the size of the buffer zones may be adjusted to ensure the capture of more or less details as needed. The proposed mesh design method allows for modeling the whole basin with a minimized number of elements while areas that are important during a flood still have the mesh in high resolution

3) Testing the sensitivities of HiResFlood-UCI with synthetic precipitation data for various components including hydrologic parameters (a priori versus calibrated), hydraulic Manning n values, DEM resolution (10m versus 30m), and computation mesh (10m+ versus 30m+).

The HiResFlood-UCI coupled hydrologic-hydraulic system was evaluated on several levels. Synthetic precipitation studies permitted investigation of various model aspects. Tests with calibrated versus *a priori* parameter grids for the hydrologic (HL-RDHM) component suggest that even with *a priori* parameter set, HiResFlood-UCI could still produce reasonable results. The roughness parameter for floodplain and channel in the hydraulic model (BreZo) component was evaluated using a range of roughness parameters and their combinations. The findings from this sensitivity test suggest that selection of channel and floodplain roughness should be done with care, as the model appears sensitive to these parameters. Additionally, no one roughness parameter dominated the other, and different combinations led to similar outlet flow results. Results when using coarser mesh resolution (30m+) and DEM resolution (30m) suggest that it is more imperative to have a high quality, high resolution DEM to derive the mesh, even if the mesh resolution is slightly coarser.

4) Validating HiResFlood-UCI for both streamflow and floodplain inundation mapping for real extreme precipitation events.

HiResFlood-UCI was evaluated using six real precipitation events in ELDO2 catchment as model input. The primary outcome of these experiments shows that HiResFlood-UCI is able to produce spatially distributed, high resolution flow information without compromising the quality of hydrograph simulation at both watershed outlet and interior point already produced by HL-RDHM. These case studies also provide a look at how HiResFlood-UCI can produce high resolution for the entire basin rather than for just a select reach. A unique advantage of HiResFlood-UCI over the current HL-RDHM is that in addition to the flow hydrograph, it offers inundated areas, flow depth, and velocity, which are fundamental to reliable flood warning. The model was also validated for the flooded map using USGS observed water levels available at an interior point. The results show the predicted flood stage error is 0.82m or less.

5) Applying HiResFlood-UCI for flood forecasting using real-time remote sensing precipitation data.

The coupled hydrologic-hydraulic model HiResFlood-UCI was driven by near real-time remote sensing data in an effort to demonstrate flood inundation mapping capabilities of the model in a forecasting framework. Two near real-time precipitation products, PERSIANN-CCS satellite-based product and NEXRAD Stage 2 radar, were used as input for simulating the historic 2008 Iowa flood. The model was run using the a priori hydrologic parameters and hydraulic Manning n values from look-up tables. The model results were evaluated in two aspects: point comparison using USGS streamflow, and areal validation of inundation maps using USDA AWiFS 56m resolution flood extent imagery. The results show the PERSIANN-CCS simulation tends to capture the observed hydrograph shape better than the Stage 2 (minimum correlation of 0.86 for

PERSIANN-CCS and 0.72 for Stage 2 radar); however, at most of the stream gauges, Stage 2 simulation provides more accurate estimates of flood peaks compared to PERSIANN-CCS (49 - 90% bias reduction from PERSIANN-CCS to Stage 2). The simulation in both cases shows a good agreement (0.67 and 0.73 critical success index CSI for Stage 2 and PERSIANN-CCS simulations respectively) with the AWiFS flood extent. Since the PERSIANN-CCS simulation slightly underestimated the discharge, the probability of detection (0.93) is slightly lower than that of the Stage 2 simulation (0.97). As a trade-off, the false alarm ratio for the PERSIANN-CCS simulation (0.23) is better than that of the Stage 2 simulation (0.31).

Through application of the newly developed HiResFlood-UCI model, paired with near real-time, remotely sensed precipitation data, this study demonstrates the ability to recreate detailed flood information (particularly flood extent maps) in a forecast setting. Strong simulation performance for this application is particularly promising, given the fact that the HiResFlood-UCI model was run with *a priori* parameters provided by the NWS. Validation of the event via unique aerial imagery available pre- and post-flood and observed hydrographs reinforces trust in the modeled results.

Largely, results from this work demonstrate the potential benefits for the proposed coupled modeling system, especially in poorly monitored regions with scarce data. Simulation of a data rich basin using information and tools available globally permits the evaluation of the type of results that could be expected in a region where the critical calibration/validation step is nearly impossible.

8.2 Future directions

While initial development and implementation of HiResFlood-UCI has been completed, there are necessary on-going efforts towards validation of the spatial flow information that it provides. Such efforts include utilization of post flood surveys conducted by the USGS in which flood extent was directly measured in many locations of the same basin, and flow depth and velocity were independently determined. Aerial photos of flood events will also aid in the validation of flood extent for HiResFlood-UCI. These pursuits are already underway in an effort to verify the unique spatial information provided by this coupled hydrologic-hydraulic system.

Once HiResFlood-UCI has been tested for some selected catchments in the United States and shown promising results, it will be implemented for global scale using UC Irvine's PERSIANN-CCS real-time high-resolution data and Global Forecast System (GFS) data for flash flood nowcast/forecast purposes. Furthermore, most of the current models used in large scale landslide modeling are empirical (Farahmand & AghaKouchak, 2013). Since HiResFlood-UCI offers high resolution flow velocity and flooded area mapping, it can be applied as a unique global, physically-based model for land slide monitoring and prediction.

The following research directions are recommended for future investigation.

1) Developing automatic techniques to design mesh for the hydraulic component of the model.

Mesh design is a key element of HiResFlood-UCI. New techniques which would extend the proposed approach in this dissertation and automate the steps of mesh design method will further the effectiveness and utility of HiResFlood-UCI. The input is DEM and watershed boundary.

2) Implementing HiResFlood-UCI paired with PERSIANN-CCS and GFS at the global scale for flood warning system.

A global flood warning system consists of a global HL-RDHM at coarse resolution (i.e. 4km) with PERSIANN-CCS and GFS precipitation data and a database of BreZo setup packages for many watersheds, especially for flood-prone regions. HL-RDHM runs permanently in real time mode for the entire globe. An algorithm is necessary to find and activate the hydraulic component to run for specific watersheds subject to potential flooding. Improving the visualization of the information by providing localized details of floods including flood extents, flood depths, and flow velocity will greatly enhance the effectiveness of the HiResFlood-UCI.

This requires a set-up of HL-RDHM for global land with an a priori hydrologic parameter set derived from FAO's global Harmonized World Soil Database of soils, land use, and land cover. Development of a database of BreZo setups for the global flood-prone watersheds using NASA's ASTER Global Digital Elevation Map 30m DEM dataset (http://asterweb.jpl.nasa.gov/gdem.asp) will also greatly enhance the usefulness of the proposed modeling system.

REFERENCES

AghaKouchak A., Behrangi, A., Sorooshian, S. Hsu, K., and E Amitai, 2011. Evaluation of satellite-retrieved extreme precipitation rates across the Central United States. *Journal of Geophysical Research* **116**, D02115, doi:10.1029/2010JD014741.

AghaKouchak A., Mehran, A., Norouzi, H., and Behrangi, A., 2012. Systematic and Random Error Components in Satellite Precipitation Data Sets. *Geophysical Research Letters*, L09406, **39**, doi:10.1029/2012GL051592.

Alsdorf, D.E., Rodriguez, E., and Lettenmaier, D.P., 2007. Measuring surface water from space. *Reviews of Geophysics* **45**, 1-24.

Anderson, E.A., 1973. National Weather Service River Forecast System-Snow Accumulation and Ablation Model. Technical Memo. NOAA, Silver Spring, MD, pp. 217.

Bates, P. D., Horritt, M.S., Fewtrell, T.J., 2010. A simple inertial formulation of the shallow water equations for efficient two dimensional flood inundation modelling. *Journal of Hydrology* **387**, 33–45.

Bates, P.D., Horritt, M.S., Smith, C.N., and D. Mason, 1997. Integrating remote sensing observations of flood hydrology and hydraulic modelling. *Hydrological Processes* **11**, 1777-1795.

Begnudelli, L., Sanders, B.F., 2006. Unstructured Grid Finite-Volume Algorithm for Shallow-Water Flow and Scalar Transport with Wetting and Drying. *Journal of Hydraulic Engineering* **132** (4), 371-384.

Begnudelli, L., Sanders, B.F., 2007. Simulation of the St. Francis Dam-Break Flood. *Journal of Engineering Mechanics* **133** (11), 1200-1212.

Begnudelli, L., Sanders, B.F., and Bradford, S.F., 2008. Adaptive Godunov-based model for Flood simulation. *Journal of Engineering Mechanics* **134** (6), 714-725.

Behrangi A., Khakbaz, B., Jaw, T.C., AghaKouchak, A., Hsu, K., and Sorooshian, S., 2011. Hydrologic evaluation of satellite precipitation products over a mid-size basin, *Journal of Hydrology* **397**, 225-237, doi: 10.1016/j.jhydrol.2010.11.043.

Bergstrom, S., 1995. The HBV model, in: Computer Models of Watershed Hydrology (Ed. Singh, V.P.). Water Resources Publications, 443-476.

Biancamaria, S., Bates, P.D., Boone, A., Mognard, N.M., 2009. Large-scale coupled hydrologic and hydraulic modelling of the Ob river in Siberia. *Journal of Hydrology* **379**, 136-150.

Bjerklie, D.M., Moller, D., Smith, L.C., and Dingman, S.L., 2005. Estimating discharge in rivers using remotely sensed hydraulic information. *Journal of Hydrology* **309**, 191–209.

Bonnifait, L., Delrieua, G., Laya, M. L., Boudevillaina, B., Massonb, A., Belleudya, P., Gaumec, E., Saulnier, G.M., 2009. Distributed hydrologic and hydraulic modelling with radar rainfall input: Reconstruction of the 8–9 September 2002 catastrophic flood event in the Gard region, France. *Advances in Water Resources* **32**, 1077-1089.

Borga, M., Anagnostou, E.N., Blöschl, G., Creutin, J.D., 2010. Flash floods: Observations and analysis of hydro-meteorological controls. *Journal of Hydrology* **394**, 1-3.

Bradford, S.F, Sanders, B.F, 2002. Finite-Volume Model for Shallow-Water Flooding of Arbitrary Topography. *Journal of Hydraulic Engineering* **128** (3), 289-298.

Brakenridge, G.R., Nghiem, S.V., Anderson, E., and Mic, R., 2007. Orbital microwave measurement of river discharge and ice status. *Water Resources Research* **43**, 1-16.

Braud, P.-A. Ayral, C. Bouvier, F. Branger, G. Delrieu, J. Le Coz, G. Nord, J.-P. Vandervaere, S. Anquetin, M. Adamovic, J. Andrieu, C. Batiot, B. Boudevillain, P. Brunet, J. Carreau, A. Confoland, J.-F. Didon-Lescot, J.-M. Domergue, J. Douvinet, G. Dramais, R. Freydier, S. Gérard, J. Huza, E. Leblois, O. Le Bourgeois, R. Le Boursicaud, P. Marchand, P. Martin, L. Nottale, N. Patris, B. Renard, J.-L. Seidel, J.-D. Taupin, O. Vannier, B. Vincendon, and A. Wijbrans. 2014. Multi-scale hydrometeorological observation and modelling for flash-flood understanding. *Hydrology and Earth System Sciences Discussion* **11**, 1871–1945.

Burnash, R.J.C., Ferral, R.L. and McGuire, R.A., 1973. A Generalized Streamflow Simulation System: Conceptual Modeling for Digital Computers. US Department of Commerce. National Weather Service and State of California Department of Water.

Burnash, R.J.C., 1995. The NWS river forecasting-catchment modeling. In: Singh, V.J. (ed.), *Computer Models of Watershed Hydrology*. Water Resources Publication, Highlands Range, Colorado, pp. 311-366.

Chow VT., 1959. Open-channel hydraulics. McGraw-Hill, Book Co., New York, p. 680.

Davis RS. 1998. Detecting time duration of rainfall: a controlling factor of flash flood intensity. In Proceedings of Special Symposium on Hydrology, Phoenix, AZ, pp. 258–263.

Duan, Q.Y., Sorooshian, S., Gupta, V., 1992. Effective and efficient global optimization for conceptual rainfall-runoff models. *Water Resources Research* **28** (4), 1015-1031.

Farahmand A., AghaKouchak A., 2013. A Satellite-Based Global Landslide Model. *Natural Hazards and Earth System Sciences* **13**, 1259-1267, doi:10.5194/nhess-13-1259-2013.

Gesch, B.D., Oimoen, M.J., Evans, G.A., 2014. Accuracy assessment of the U.S. Geological Survey National Elevation Dataset, and comparison with other large-area elevation datasets – SRTM and ASTER., USGS Open-file Report 2014-1008, accessed September 8, 2014.

Gourley, J.J., Erlingis, J.M., Hong, Y., Wells, E., 2012. Evaluation of tools used for monitoring and forecasting flash floods in the United States. *Weather Forecasting* **27**, 158-173.

Hapuarachchi, H. A. P., Wang, Q. J., Pagano, T. C., 2011. A review of advances in flash flood forecasting. *Hydrological Process* **25**, 2771-2784.

Hong, Y., Hsu, K., Gao X., Sorooshian, S., 2004. Precipitation estimation from remotely sensed information using an artificial neural network—cloud classification system. *Journal of Applied Meteorology* **43**, 1834-1852.

Hong, Y., Adler, R.F., Negri, A., and Huffman, G.J., 2007. Flood and landslide applications of near real-time satellite rainfall products. *Natural Hazards* **43**, 285-294.

Hong, Y., Gochis, D., Chen, J.T., Hsu, K., and Sorooshian, S., 2007. Evaluation of PERSIANN-CCS Rainfall Measurement Using the NAME Event Rain Gauge Network. *Journal of Hydrometeorology* **8**(3), 469-482.

Horritt, M.S., Bates, P.D., 2002. Evaluation of 1-D and 2-D numerical models for predicting river flood inundation. *Journal of Hydrology* **268** (1–4), 87–99.

Hossain, F., Siddique-E-Akbor, A.H., Mazumder, L.C., ShahNewaz, S.M., and Biancamaria, S., 2014a. Proof of Concept of an Altimeter-Based River Forecasting System for Transboundary Flow Inside Bangladesh. *IEEE Journal of Selected Topics in Applied Earth Observations and Remote Sensing* **7** (2), 587-601.

Hossain, F., Siddique-E-Akbor, A.H.M., Yigzaw, W., Shah-Newaz, S., Hossain, M., Mazumder, L.C., Ahmed, T., Shum, C.K., Lee, H., Biancamaria, S., Turk, F.J., and Limaye, A., 2014b. Crossing the "Valley of Death": Lessons learned from Implementing an Operational Satellite-Based Flood Forecasting System. *BAMS* **95** (8), 1201-1207.

Hsu, K., Gao, X., Sorooshian, S., Gupta, H.V., 1997. Precipitation Estimation from Remotely Sensed Information Using Artificial Neural Networks. *Journal of Applied Meteorology*, **36**(9), 1176-1190.

Hsu, K., Sellars, S., Nguyen, P., Braithwaite, D., and Chu, W., 2013. G-WADI PERSIANN-CCS GeoServer for extreme precipitation event monitoring. *Sciences in Cold and Arid Regions* **5**(1), 6-15.

Indian National Remote Sensing Agency, 2003. IRS-P6 Data User's Manual. [Available online at http://www.euromap.de/download/P6_data_user_handbook.pdf].

Johnson, D. and Lindsey, M., 2008. AWiFS data: helping reinforce crop acreage statistics within June 2008's flooded areas. FAS/IPAD Semiar, Greenbelt, MD, October 20-21, 2008. [Available online at http://www.nass.usda.gov/Education_and_Outreach/Reports,_Presentations_and_Conferences/Presentations/Johnson_FASSeminar08.pdf].

Kim G, Barros AP. 2001. Quantitative flood forecasting using multisensor data and neural networks. *Journal of Hydrology* **246**, 45–62.

Khakbaz, B., Imam, B., Hsu, K., Sorooshian, S., 2012. From lumped to distributed via semi-distributed: Calibration strategies for semi-distributed hydrologic models. *Journal of Hydrology* **418-419**, 61-77.

Khan, S.I., Hong, Y., Gourley, J.J., Khattak, M.U., and Groeve, T.D., 2014. Multi-Sensor Imaging and Space-Ground Cross-Validation for 2010 Flood along Indus River, Pakistan. *Remote Sensing* **6**, 2393-2407.

Kim, B., Sanders, B.F., Schubert, J.E., Famiglietti, J.S., 2014. Mesh type tradeoffs in 2D hydrodynamic modeling of flooding with a Godunov-based flow solver. *Advances in Water Resources* **68**, 42-61.

Kim, J., Warnock, A., Ivanov, V.Y., Katopodes, N.D., 2012. Coupled modeling of hydrologic and hydrodynamic processes including overland and channel flow. *Advances in Water Resources* **37**, 104-126.

Koren, V., Barrett, C.B., 1995. Satellite based, Distributed monitoring, forecast, and simulation (MFS) system for the Nile River. In: Kite, G.W., Pietroniro, A., Pultz, T.J. (Eds.), *Application of Remote Sensing in Hydrology*, NHRI, Saskatoon, Canada, pp. 187–200.

Koren, V., Smith, M., and Duan, Q., 2003. Use of a priori parameter estimates in the derivation of spatially consistent parameter sets of rainfall–runoff models, Q. Duan, H. Gupta, S. Sorooshian, A. Rousseau, and R. Turcotte, *Calibration of Watershed Models: Water Science and Application Series*, No. 6, American Geophysical Union, 239-254.

Koren, V., Reed, S., Smith, M., Zhang, Z., Seo, D.J., 2004. Hydrology laboratory research modeling system (HL-RMS) of the US National Weather Service. *Journal of Hydrology* **291**, 297–318.

Koren, V., Smith, M., Cui, Z., Cosgrove, B. 2007. Physically-Based Modifications to the Sacramento Soil Moisture Accounting Model: Modeling the Effects of Frozen Ground on the Rainfall-Runoff Process. NOAA Technical Report NWS 52.

Krajewski, W., Seo, B.C., Goska, R., Demir I., and Elsaadani, M., 2013. Precipitation datasets the GPM Iowa Flood Studies (IFLoodS) field experiment. *EGU General Assembly 2013*, Vienna, Austria. [Available online at http://meetingorganizer.copernicus.org/EGU2013/EGU2013-11303.pdf].

Kuzmin, V., Seo, D.J., Koren, V., 2008. Fast and efficient optimization of hydrologic model parameters using a priori estimates and stepwise line search. *Journal of Hydrology* **353**, 109-128.

Liang, X., Lettenmaier, D. P., Wood, E. F., Burges, S. J., 1994. A Simple hydrologically Based Model of Land Surface Water and Energy Fluxes for GSMs. *Journal of Geophysical Research* **99**, 415-428.

Linhart, S. M. and Eash, D.A., 2010. Floods of May 30 to June 15, 2008, in the Iowa River and Cedar River basins, eastern Iowa: U.S. Geological Survey Open-File Report 2010-1190, 99 p. with Appendixes.

Mehran A., AghaKouchak A., 2014. Capabilities of Satellite Precipitation datasets to Estimate Heavy Precipitation Rates at Different Temporal Accumulations. *Hydrological Processes* **28**, 2262-2270, doi: 10.1002/hyp.9779.

Mersel, M.K., Smith, L.C., Andreadis, K.M., Durand, M.T., 2013. Estimation of river depth from remotely sensed hydraulic relationships. *Water Resources Research* **49**, 3165-3179.

Moreda, F., Koren, V., Zhang, Z., Reed, S., Smith, M., 2006. Parameterization of distributed hydrological models: Learning from the experiences of lumped modeling. *Journal of Hydrology* **320**, 218–237.

National Weather Service (NWS), 2011. Hydrology Laboratory-Research Distributed Hydrologic Model (HL-RDHM) User Manual V. 3.2.0.

National Weather Service (NWS), 2012: Summary of Natural Hazard Statistics for 2011 in the United States. [Available online at http://www.nws.noaa.gov/os/hazstats/sum11.pdf].

Neal, J. C., Schumann, G., Bates, P.D., 2012. A subgrid channel model for simulating river hydraulics and floodplain inundation over large and data sparse areas. *Water Resources Research* **48** (11), 16W11506.

Nguyen, P., Sellars, S. Thorstensen, A., Tao, Y., Ashouri, H., Braithwaite, D., Hsu, K., and Sorooshian, S., 2014. Satellites Track Precipitation of Super Typhoon Haiyan. *Eos* **95**, 133&135.

Nguyen, P., Thorstensen, A., Sorooshian, S., Hsu, K., AghaKouchak, A., Sanders, B., Koren, V., Cui, Z., and Smith, M., 2014. A high resolution coupled hydrologic-hydraulic model (HiResFlood-UCI) for flash flood modeling. *Journal of Hydrology*. Under review.

Patro, S., Chatterjee, C., Mohanty, S., Singh, R., Raghuwanshi, N.S., 2009. Flood inundation modeling using MIKE FLOOD and remote sensing data. *Journal of the Indian Society of Remote Sensing* **37**(1), 107-118.

Reed, S., Koren, V., Smith, M., Zhang, Z., Moreda, F., Seo, D.J., 2004. Overall distributed model intercomparison project results. *Journal of Hydrology* **298**(1–4), 27–60.

Reed, S., Schaake, J., Zhang, Z., 2007. A distributed hydrologic model and threshold frequency-based method for flash flood forecasting at ungauged locations. *Journal of Hydrology* **337**, 402–420.

Sanders, B.F., 2007. Evaluation of on-line DEMs for flood inundation modeling. *Advances in Water Resources* **30**, 1821-1843.

Schumann, G.J.P., Neal, J.C., Voisin,N., Andreadis, K.M., Pappenberger, F., Phanthuwongpakdee, N., Hall, A.C., Bates, P.D., 2013. A first large-scale flood inundation forecasting model. *Water Resources Research* **49**, 6248-6257.

Shewchuk, J.R., 1996. Triangle: Engineering a 2D quality mesh generator and Delaunay triangulator. *Lecture Notes Comput. Science* **1148**, 203–222.

Sirdas S, Sen Z., 2007. Determination of flash floods in Western Arabian Peninsula. *Journal of Hydrologic Engineering* **12**, 676–681.

Smith, J.A., Baeck, M.L., Villarini, G., Wright, D.B., and Krajewski, W., 2013. Extreme flood response: The June 2008 Flooding in Iowa. *Journal of Hydrometeorology,* **14** 1810-1825.

Smith, M., Koren, V., Reed, S., Zhang, Z., Zhang, Y., Moreda, F., Cui, Z., Mizukami, N., Anderson, E., Cosgrove, B., 2012a. The distributed model intercomparison project – Phase 2: Motivation and design of the Oklahoma experiments. *Journal of Hydrology* **418–419**, 3-16.

Smith, M., Koren, V., Zhang, Z., Zhang, Y., Reed, S., Cui, Z., Moreda, F., Cosgrove, B., Mizukami, N., Anderson, E., DMIP 2 Participants, 2012b. Results of the DMIP 2 Oklahoma experiments. *Journal of Hydrology* **418–419**, 17-48.

Smith, M., Seo, D., Koren, V., Reed, S., Zhang, Z., Duan, Q., Moreda, F., Cong, S., 2004. The distributed model intercomparison project (DMIP): motivation and experiment design. *Journal of Hydrology* **298**, 4–26.

Sorooshian, S., Gupta, V.K, 1983. Automatic calibration of conceptual rainfall-runoff models: the question of parameter observability and uniqueness. *Water Resources Research* **19** (1), 260-268.

Sorooshian, S., Duan, Q., Gupta, V.K., 1993. Calibration of rainfall-runoff models: application of global optimization to the Sacramento soil moisture accounting model. *Water Resources Research* **29** (4) 1185-1194.

Sorooshian, S., Hsu, K., Gao, X., Gupta, H., Imam, B., and Braithwaite, D., 2000. Evaluation of PERSIANN system satellite-based estimates of tropical rainfall, *Bulletin of the American Meteorology Society* **81**, 2035-2046.

Sorooshian S., AghaKouchak, A., Arkin, P., Eylander, J., Foufoula-Georgiou, E., Harmon, R., Hendrickx, J., Imam, B., Kuligowski, R., Skahill, B., and Skofronick-Jackson, G., 2011. Advanced Concepts on Remote Sensing of Precipitation at Multiple Scales, *Bulletin of the American Meteorological Society* **92** (10), 1353-1357, doi: 10.1175/2011BAMS3158.1.

Sorooshian, S., Nguyen, P., Sellars, S., Braithwaite, D., AghaKouchak A., and Hsu, K., 2014. Satellite-based remote sensing estimation of precipitation for early warning systems. In A. Ismail-Zadeh, J.U. Fucugauchi, A. Kijko, K. Takeuchi and I. Zaliapin (eds), *Extreme Natural Hazards, Disaster Risks and Societal Implication*s, Cambridge University Press, Cambridge, UK.

Strauss, B., Kulp, S., 2014. New Analysis Shows Global Exposure to Sea level Rise. Research Report by Climate Central. Available online at http://www.climatecentral.org/news/new-analysis-global-exposure-to-sea-level-rise-flooding-18066.

Tang, Y., Reed, P., van Werkhoven, K., Wagener, T., 2007. Advancing the identification and evaluation of distributed rainfall-runoff models using global sensitivity analysis. *Water Resources Research* **43**, W06415, doi:10.1029/2006WR005813.

UNESCO, 2012. 2011 Disaster in numbers. International Disaster Database.

Wagener, T., K. van Werkhoven, P. Reed, and Y. Tang, 2009: Multiobjective sensitivity analysis to understand the information content in streamflow observations for distributed watershed modeling, Water Resour. Res., 45, W02501, doi: 10.1029/2008WR007347.

WMO, 2011. Manual on flood forecasting and warning. WMO-No. 1072. [Available online at http://www.wmo.int/pages/prog/hwrp/publications/flood_forecasting_warning/WMO%201072_en.pdf].

Wu, H., Adler, R.F., Tian, Y., Huffman, G.J., Li, H., and Wang, J., 2014. Real-time global flood estimation using satellite-based precipitation and a coupled land surface and routing model, *Water Resources. Research* **50**, 2693-2717.

Yilmaz, K. K., H. V. Gupta, and T. Wagener (2008), A process-based diagnostic approach to model evaluation: Application to the NWS distributed hydrologic model. *Water Resources Research* **44**, W09417, doi:10.1029/2007WR006716.

APPENDICES

Appendix 1: Calibrated coefficients for ELDO2 (provided by NWS)

Parameter	Description	Calibrated Coefficient
sac_PCTIM	Minimum impervious area	0.001
sac_ADIMP	Additional impervious area	0.000
sac_RIVA	Riparian vegetation area	0.025
sac_SIDE	Ratio of non-channel baseflow to channel baseflow	0.000
sac_RSERV	Percent/100 of lower zone free water which cannot be transferred to lower zone tension water	0.300
sac_EFC	Effective forest cover	0.000
sac_UZTWM	Lower zone tension water capacity	-0.753
sac_UZFWM	Upper zone free water capacity	-0.509
sac_UZK	Fractional daily upper zone free	-0.710
sac_ZPERC	Maximum percolation rate	-8.342
sac_REXP	Exponent for the percolation equation	-0.753
sac_LZTWM	Lower zone tension water capacity	-0.628
sac_LZFSM	Lower zone supplemental free water capacity	-1.016
sac_LZFPM	Lower zone primary free water capacity	-1.148
sac_LZSK	Fractional daily supplemental withdrawal rate	-0.569

sac_LZPK	Fractional daily primary withdrawal rate	-0.494
sac_PFREE	Percent/100 of percolated water which always goes directly to lower zone free water storages	-0.357
rutpix_Q0CHN	Specific channel discharge per unit channel cross-section area	-0.900
rutpix_QMCHN	Power value in relationship between discharge and cross-section	-0.980